ornl

ORNL/TM-11645

OAK RIDGE
NATIONAL
LABORATORY

MARTIN MARIETTA

Laboratory Test Results on the Thermal Resistance of Polyisocyanurate Foamboard Insulation Blown with CFC-11 Substitutes—A Cooperative Industry/Government Project

D. L. McElroy
R. S. Graves
D. W. Yarbrough
F. J. Weaver

MANAGED BY
MARTIN MARIETTA ENERGY SYSTEMS, INC.
FOR THE UNITED STATES
DEPARTMENT OF ENERGY

ORNL-TM--11645

DE92 003011

Metals and Ceramics Division

LABORATORY TEST RESULTS ON THE THERMAL RESISTANCE OF POLYISOCYANURATE FOAMBOARD INSULATION BLOWN WITH CFC-11 SUBSTITUTES - A COOPERATIVE INDUSTRY/GOVERNMENT PROJECT

D. L. McElroy, R. S. Graves, D. W. Yarbrough, and F. J. Weaver

Date Published: September 1991

NOTICE: This document contains information of a preliminary nature. It is subject to revision or correction and therefore does not represent a final report.

Prepared for the
U.S. Department of Energy
Office of Buildings Energy Research
EC 01 01 00 0

Prepared by the
OAK RIDGE NATIONAL LABORATORY
Oak Ridge, Tennessee 37831-6092
managed by
MARTIN MARIETTA ENERGY SYSTEMS, INC.
for the
U.S. DEPARTMENT OF ENERGY
under Contract DE-AC05-84OR21400

CONTENTS

LIST OF FIGURES

LIST OF TABLES

EDITOR'S NOTE

Although Oak Ridge National Laboratory has a policy of reporting its work in SI metric units, this report uses English units. The justification is that the insulation industry at present operates completely with English units, and reporting otherwise would lose meaning to the intended readership. To assist the reader in obtaining the SI equivalents, these are listed below for the units occurring in this report.

Property	Unit used	SI equivalent
Dimension	in.	25.4 mm
Dimension	ft	0.3048 m
Density	lb/ft^3	16.02 kg/m^3
Power	Btu/h	0.2929 W
Thermal conductivity	Btu·in./h·ft^2·°F	0.1441 W/m·K
Thermal resistance	h·ft^2·°F/Btu	0.1762 K·m^2/W
Temperature	°F	°C = (5/9)(°F - 32)
Temperature difference	°F	°C = (5/9)°F

LABORATORY TEST RESULTS ON THE THERMAL RESISTANCE OF POLYISOCYANURATE FOAMBOARD INSULATION BLOWN WITH CFC-11 SUBSTITUTES -- A COOPERATIVE INDUSTRY/GOVERNMENT PROJECT*

D. L. McElroy, R. S. Graves, D. W. Yarbrough, and F. J. Weaver

ABSTRACT

The fully halogenated chlorofluorocarbon gases (CFC-11 and CFC-12) are used as blowing agents for foam insulations for building and appliance applications. The thermal resistance per unit thickness of these insulations is greater than that of other commercially available insulations. Mandated reductions in the production of these chemicals may lead to less efficient substitutes and increase U.S. energy consumption by one quad (10^{15} Btu) or more.

This report describes laboratory thermal and aging tests on a set of industry-produced, experimental polyisocyanurate (PIR) laminate boardstock to evaluate the viability of hydrochlorofluorocarbons (HCFCs) as alternative blowing agents to chlorofluorocarbon-11 (CFC-11). All boardstock was produced from the same formulation and was not optimized for thermal performance. The PIR boards were blown with five gases: CFC-11, HCFC-123, HCFC-141b, and 50/50 and 65/35 blends of HCFC-123/HCFC-141b. These HCFC gases have a lower ozone depletion potential than CFC-11 or CFC-12.

Apparent thermal conductivity (k) was determined from 0 to 50°C (30 to 120°F) using techniques that meet ASTM C 1114 (Thin Heater Apparatus) and ASTM C 518 (Heat Flow Meter Apparatus). Results on the laminate boards provide an independent laboratory check on the increase in k observed for field exposure in the Oak Ridge National Laboratory (ORNL) Roof Thermal Research Apparatus (RTRA). The measured laboratory increase in k was between 8 and 11% after a 240-d field exposure in the RTRA.

Results are reported on a thin-specimen, aging procedure to establish the long-term thermal resistance of gas-filled foams. These thin specimens were planed from the industry-produced boardstock foams and aged at 75 and 150°F for up to 300 d. The resulting k-values were correlated with an exponential dependency on (diffusion coefficient × time)$^{1/2}$/thickness and provided diffusion coefficients for air components into, and blowing agent out of, the foam. This aging procedure was used to predict the five-year thermal resistivity of the foams. Aging at 75 and at 150°F showed that the foams blown with alternative blowing agents had a thermal resistivity 3 to 16% (average 9.4%) less than that obtained by CFC-11 under similar conditions.

The thin-specimen aging procedure is supported with calculations by a computer model for aging of foams.

*A Cooperative Industry/Government Research Project sponsored by the Society of the Plastics Industry, Polyisocyanurate Insulation Manufacturers Association, National Roofing Contractors Association, Department of Energy, and Environmental Protection Agency. This research was sponsored by the U.S. Department of Energy, Assistant Secretary for Conservation and Renewable Energy, Office of Buildings Energy Research, Building Systems and Materials Division, under contract DE-AC05-84OR21400 with Martin Marietta Energy Systems, Inc.

1. INTRODUCTION

This report describes apparent thermal conductivity (k) results obtained during FY 1989 and FY 1990 on a set of prototypical, experimental, polyisocyanurate (PIR) laminate boardstock produced to evaluate the viability of alternative hydrochloro-fluorocarbons (HCFCs) as blowing agents. All boardstock was produced from similar formulations that were not optimized for thermal performance. Boardstock made in the future may differ in performance from this set. Thermal resistance values are reported for PIR boards prepared with CFC-11, HCFC-123, HCFC-141b, and two blends of HCFC-123 and HCFC-141b. The primary purpose of the laboratory tests is to answer a key question: will foams produced with alternative blowing agents yield thermal properties that differ from those obtained with CFC-11?

1.1 BACKGROUND

In the mid-1980s, it was recognized that further increases in chlorofluorocarbon (CFC) concentrations in the upper atmosphere would lead to long-term damage to the ozone layer. International recognition of this culminated in the signing of the Montreal Protocol in 1987 by 23 industrialized and developing countries.[1] Currently, there are over 63 nations committed to phasing out CFCs by the year 2000. Domestic legislation[2,3] and the Montreal Protocol address the global impact of CFCs and outline a timetable for reduction of CFC consumption. Table 1 lists the Group I and Group II substances controlled by the Montreal Protocol and the timetable for production decreases. The Montreal Protocol requires periodic assessments to determine whether changes in control provisions are warranted.[4]

The U.S. Environmental Protection Agency (EPA) Regulatory Impact Analysis[3,5] identifies seven specific use areas for CFCs:

1. commercial and residential refrigeration and air conditioning,
2. mobile air conditioning,
3. production of plastic foam and foam insulation products,
4. sterilization of medical equipment and instruments,
5. solvent cleaning of metal and electronic parts,
6. aerosol propellants and other miscellaneous uses, and
7. fire extinguishing.

Table 1. Montreal Protocol controlled substances and timetable

A. Controlled substances

Compound	Formula	Ozone depletion potential (ODP)[a]	Relative greenhouse warming potential[b]
Group I			
CFC-11	$CFCl_3$	1.0	0.4
CFC-12	CF_2Cl_2	1.0	1.0
CFC-113	$C_2F_3Cl_3$	0.8	0.3 - 0.8
CFC-114	$C_2F_4Cl_2$	1.0	0.5 - 1.5
CFC-115	C_2F_5Cl	0.6	1 - 3
Group II			
Halon-1211	CF_2BrCl	3.0	-
Halon-1301	CF_3Br	10.0	-
Halon-2402	$C_2F_4Br_2$	6.0	-

B. Timetable (original Montreal Protocol)

Date	Requirement
July 1, 1989	Freeze CFC production at 1986 levels
July 1, 1993	Limit CFC production to 80% of 1986 levels
July 1, 1998	Limit CFC production to 50% of 1986 levels
July 1, 2000	Eliminate CFC production

C. Timetable (London, Jun 1990)

Date	Requirement
January 1, 1993	Limit CFC production to 80% of 1986 levels (Clean Air Act requires 75%)
January 1, 1995	Limit CFC production to 50% of 1986 levels
January 1, 1997	Limit CFC Production to 15% of 1985 levels
January 1, 2000	Eliminate CFC production
2040 (possibly 2020)	Eliminate HCFC production

[a]Relative to CFC-11 which is assigned the value of 1.00.
[b]Relative to CFC-12 which is assigned the value of 1.00.

The CFCs include most of the best refrigerant fluids available as well as the foaming agents in low-density insulating materials that have improved the energy efficiency of both buildings and appliances. CFCs are used in more than 150 million home appliances, some 90 million vehicular air conditioners, and hundreds of thousands of commercial and industrial cooling and refrigeration systems. Others are solvents and cleaners, described as almost indispensable in the production of energy-conserving electronics and precision mechanical parts.[6]

Area 3 (i.e., production of plastic foam and foam-insulation products) is divided into four subareas:

3.1 molded flexible polyurethane foam,

3.2 slabstock flexible polyurethane foam,

3.3 rigid polyurethane foam, and

3.4 rigid extruded polystyrene foam.

This report focuses on rigid foam insulation.

The CFC issue is enormous. Industry produces over 400,000 metric tons of rigid foamboard insulation annually and, therein, consumes over 60,000 metric tons of CFC-11 and CFC-12. This consumption is equivalent to 6 billion board feet of foam and represents the most effective thermal insulation that is commercially available. If environmentally acceptable alternative gases and foams are not available, the Oak Ridge National Laboratory (ORNL) has estimated an energy impact for building applications to be between 0.65 and 1.5 quad/year.[7]

Industry is pursuing a variety of alternative blowing agents to CFC-11 and CFC-12 for producing rigid-foam-board insulations. Chemicals with low ozone-depletion potential being developed as CFC substitutes are shown in Table 2. In addition, industry is testing blends of Group I chemicals with other chemicals, as a means to reduce CFC usage, but with loss of thermal efficiency of insulations. One goal of the industry search is to obtain a "near drop-in" chemical that requires only a small change in the production process and meets the Montreal Protocol requirements. The other chemicals include H_2O - CO_2, butanes and pentanes, methyl chloride, and ethyl chloride.

Development risks to foam-insulation producers include the commercial availability of the alternative blowing agents and their subsequent acceptance by regulatory agencies. The new products will be less hazardous to the environment but more expensive and less effective as thermal insulations (i.e., lower R/inch values) because the alternative blowing agents have k-values greater than CFC-11 or CFC-12 (see Table 2).

Table 2. Foam-insulation-blowing gas alternatives to chlorofluorocarbons 11 and 12

Chemical	Potential use	Ozone depletion potential[a]	Greenhouse warming potential[b]	Gas thermal conductivity[c] Btu in./h ft^2·°F
HCFC-22	Alone and in blends, for food packaging, fast food freezing, leak-testing of fire extinguisher, refrigeration and air conditioning, and polystyrene foam insulation	0.05	0.07	0.073
HCFC-123	Undergoing toxicity testing for possible use in foam manufacturing, chillers, and solvent cleaning	≤0.03	0.01	0.072
HFC-134a	Undergoing toxicity testing for possible future use in refrigeration, chillers, and mobile air conditioners; and foam manufacturing	0.0	≤0.01	0.094
HCFC-141b	Undergoing toxicity testing for possible use in certain foam, refrigeration, and air-conditioning applications	≤0.1	0.05	0.070
HCFC-142b	For possible use in certain foam, refrigeration, and air-conditioning applications	0.06	<0.2	0.077

[a]Relative to CFC-11 which is assigned a value of 1.00.
[b]Relative to CFC-12 which is assigned a value of 1.00.
[c]The thermal conductivity, Btu in./h ft^2·°F, at 75°F of CFC-11 is 0.057, and CFC-12 is 0.067.

A new rigid, extruded, polystyrene foamboard product foamed with HCFC-142b was announced and became available for buildings application in mid-1989. The new product will reduce the CFC problem because the polystyrene industry provides about 20% of the total rigid-foam tonnage. However, the rigid-polyurethane industry is still developing CFC alternatives.

Prior to the Montreal Protocol agreements to phase out the use of CFCs, two factors influenced foam insulation technology and applications: foam aging and energy regulations. Figure 1 shows that the structure of a typical rigid foam is composed of closed cells that contain blowing agent. Foam aging occurs because the thin plastic cell walls (nominally less than 1 μm thick) are permeable to gas diffusion. The composition of the gas in the cell changes with time after manufacture as air diffuses into the cell and CFC diffuses out of the cell. The gas composition controls the gas thermal conductivity, so the k of foam increases with time after manufacture. Aging decreases the R-value per unit thickness and, hence, the thermal efficiency of the foam.

Many factors affect R/inch values including insulation board facer, foam density, cell size and distribution, cell wall thickness, polymer composition, manufacturing process, foam/facer interface, and exposure environment. There is no such thing as one polyurethane (i.e., polystyrene, polyisocyanurate, or phenolic); they are chemical families with millions of relatives. All such foams tend to show R-value loss with time after manufacture, and this phenomenon appears to be a linear function of log time. Lifetime predictions are often made from data collected 100 to 180 d after manufacture. Field performance rarely equals laboratory values for R/inch.[4]

Models that predict the gas composition of the closed cells as a function of exposure have been developed. These models provide a theoretical basis for predicting aged R-value.[8,9] Laboratory testing of thin sections of foams as a function of time may provide results to validate models that predict R-values for boards as a function of exposure.

A second factor that affected foam insulation technology prior to the Montreal Protocol was the pending energy performance standards for appliances including residential refrigerator/freezers (R/F). These standards affect building equipment applications, but any resulting insulation improvements could change insulations for buildings. In 1987, a typical 16 to 18 ft^3 R/F with automatic defrost and a top-mounted

PHOTO WD32

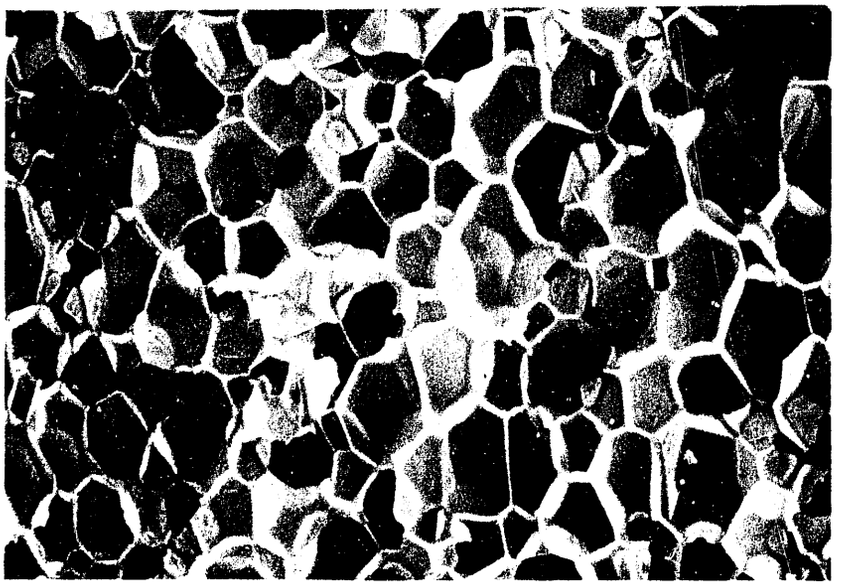

Fig. 1. Microstructure of a typical, closed-cell plastic foam insulation (100X).

freezer used about 1100 kWh/year.[10] California regulations require that a similar unit sold in California after January 1, 1987, use only 978 kWh/year and by 1992 use only 677 kWh/year.[11] Federal regulations require that similar units produced after January 1, 1990, consume only 950 kWh/year.[12] These regulations prompted appliance manufacturers to study improved insulations as a means to achieve energy reduction. At least one R/F manufacturer obtained patents on powder-filled evacuated panels with an R-value per inch of over 20. Current foamed-in-place R/F insulations have an R-value of about 8/inch, and a shift to 20/inch could save as much as 550 kWh/year per R/F unit.[13]

Although the initial application for such panels is in R/Fs, numerous other insulation applications currently met by foam insulations could benefit from such panels if they proved to be economically feasible and were commercially available. In addition, these energy regulations prompted studies on ways to improve existing foam insulations.[14] These studies included (1) decreasing the cell size to the 0.1- to 0.2-mm-diam range to increase the cell strut density and decrease the radiative heat transport and (2) increasing the amount of solid in the cell walls and decreasing the amount in the cell struts to increase the wall resistance to gas diffusion.

1.2 COOPERATIVE PROGRAM

The current effort is a cooperative industry/government program to establish the viability of alternative blowing agents. The research project for CFC alternatives resulted from two workshops that involved participants from industry, government, and academia.[15] At the initial workshop the participants prioritized 29 research projects on a CFC research menu. The second workshop focused on a single cooperative project: the long-term performance of substitute insulations containing HCFC-123 and HCFC-141b for roofing applications. The project is sponsored by the Society of the Plastics Industry (SPI) - Polyurethane Division, the Polyisocyanurate Insulation Manufacturers Association, the National Roofing Contractors Association (NRCA), the U.S. Department of Energy, and the EPA. The project is under the direction of a steering committee with representatives from each of the sponsors and ORNL. The purpose of the project is to determine if the performance of polyisocyanurate roof insulation foam boards blown with alternate agents differs from boards blown with CFC-11.

2. OBJECTIVES

The cooperative project has two field tasks that are supported by two laboratory tasks. One field task is to monitor the field thermal performance of roof test panels of the boardstock installed in the ORNL Roof Thermal Research Apparatus (RTRA) and exposed to seasonal weather cycles. A second field task is to examine the behavior of roof panels for a range of installation conditions used in the ORNL Roof Mechanical Properties and Foundations Research Apparatus (RMPFRA). The objective of the first laboratory task (i.e., Task A) is to establish the thermal conductivity (k) of specimens of boardstock foams produced by industry as a function of temperature from 30 to 120°F prior to installation and as a function of exposure time to field conditions in both the RTRA and the RMPFRA.[16] The objective of the second laboratory task (i.e., Task B) is to establish k at 75°F as a function of aging time at 75 and 150°F for specimens of three thicknesses sliced from the original boardstock. These aging temperatures bound expected exposure conditions.

Task A used two apparatuses that meet American Society for Testing and Materials (ASTM) standards: the ORNL Unguarded Thin-Heater Apparatus (UTHA) [ASTM C 1114][17] and the Advanced R-Matic Apparatus (ASTM C 518).[18] The tests were conducted on rigid boardstock foam specimens that form the test panels to be exposed in the RTRA. The central measurement section of each RTRA panel was nominally 3 in. thick and consisted of two boards (24 × 24 in.), each nominally 1.5 in. thick, with an embedded heat flux transducer (HFT) at the board interface. The embedded HFTs were calibrated in the panels to allow analysis of RTRA data. The tests are in progress, and RTRA results will be reported separately.

For Task B, specimen aging at 75°F was conducted under normal laboratory conditions, and the 150°F aging treatment was conducted by exposing the specimens in an environmental chamber held at 150°F. The Advanced R-Matic Apparatus was used to determine k (75°F) of the specimens as a function of aging time. The goals of Task B are to establish the value of thin-specimen testing as an accelerated aging procedure and to provide a data base to compare to RTRA and RMPFRA results with predictions of an aging model. Specimen characterization tests[19] were an integral part of Task B. Characterizations included cell size, preferred rise dimensions, cell-wall thickness,

fraction solid in the cell wall, and foam permeability to O_2, N_2, and the blowing agent. These properties are needed for a model to predict the increase of k over the life of the rigid foam.[14]

3. EQUIPMENT

3.1 UNGUARDED THIN-HEATER APPARATUS

The thermal conductivity of the RTRA panels and the calibrations of the embedded HFTs (Task A) were determined from 75 to 120°F in the ORNL Unguarded Thin-Heater Apparatus.[17,20,21] Initial tests were performed in a one-sided, heat-flow mode on specimens with GAF black facers (0.025 in. thick) in place, as recommended in ASTM C 1013[22]. The UTHA tests were performed in a two-sided, heat-flow-mode operation for the RMPFRA panels.

The UTHA (Fig. 2) meets the requirements of ASTM C 1114-89.[17] The apparatus is an absolute, longitudinal heat-flow method and consists of an unguarded, electrically heated, flat, large-area nichrome screen-wire heat source sandwiched between two horizontal layers of insulation with flat isothermal bounding surfaces. The screen-wire heat source has a low thermal conductance that reduces unwanted lateral heat flow and minimizes the need for active edge guarding. The heat source provides vertical heat flow in its central region across the subject insulation to two temperature-controlled, water-cooled, copper plates. The screen area (A_o) is large (3 × 5 ft) and is instrumented with 11 thermocouples for temperature measurement and voltage taps for power measurements. A measured direct current passes through the screen, and the heat generated passes through the two layers of insulation of thickness (L). When steady state is reached, commercially available potentiometric equipment is used to measure the thermocouple outputs, the current (I), and the voltage (ΔV). For two-sided heat flow, k is calculated from

$$k = \frac{I \cdot \Delta V}{2} \cdot \frac{L}{A \Delta T}, \qquad (1)$$

where A is the screen meter area defined by its width and the voltage drop lead separation, m^2, and ΔT is the temperature difference between the screen and the plates.

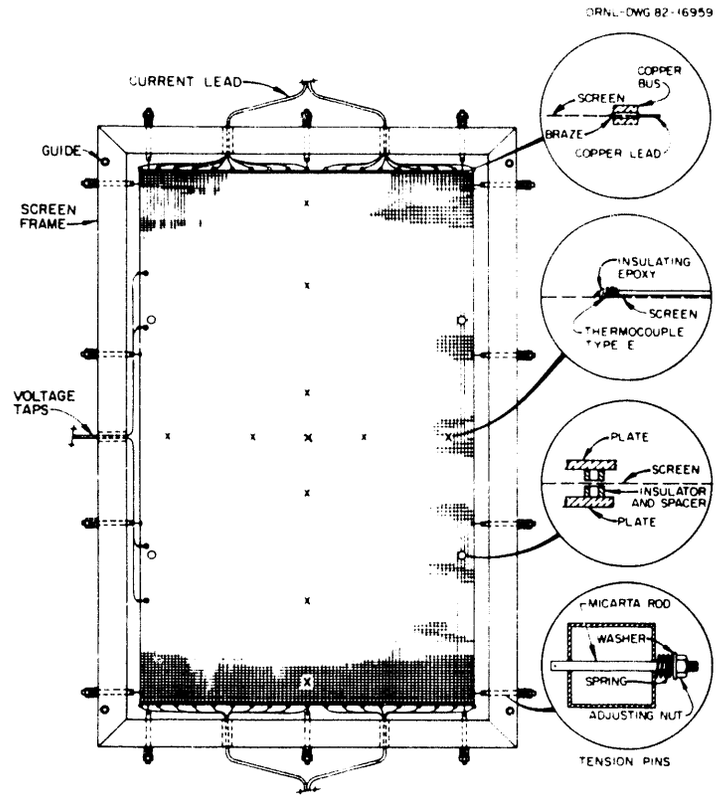

(*a*)

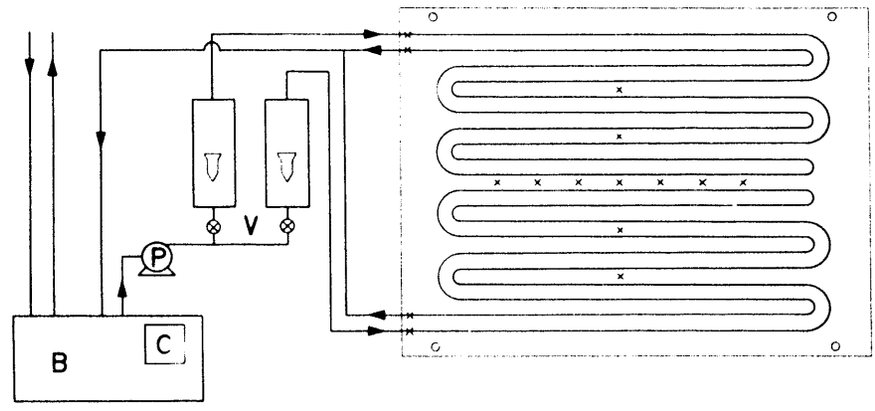

Component	Illustration
Braun Water Bath	B
Controller	C
Booster Pump	P
Balancing Valves	V
Thermocouple	X

(*b*)

Fig. 2. Schematic drawing of (*a*) the instrumented nichrome screen-wire heater and (*b*) the temperature control and plumbing systems for each cold plate of the Unguarded Thin-Heater Apparatus.

For one-sided mode of operation, one plate is controlled to the temperature of the screen-wire heater, and the thermal conductivity of the insulating specimen with an imposed temperature difference (ΔT) is calculated from

$$k = \left\{ I \times V - \frac{k(B) \times \Delta T(B) \times A_o}{L(B)} \right\} \times \frac{L}{A_o \Delta T} . \qquad (2)$$

The B-terms provide a heat-flow correction for the small temperature mismatch between the screen and the guard plate.[23] By changing the screen power and plate temperatures, mean temperatures from 75 to 120°F can be achieved. The measurement errors of the thin-heater apparatus have been assessed. A determinate error analysis of the quantities in a two-sized heat-flow mode of operation predicts a maximum uncertainty of 1.7% if ΔT is 9°F and 0.7% if ΔT is 54°F. The most probable uncertainty is 1.2 and 0.4%, respectively, for these ΔT values. The reproducibility and repeatability of the k measurements have been determined to be ±0.2%.[21] Figure 2 contains a schematic drawing of the instrumented nichrome screen-wire heater and the temperature control and plumbing for the cold plates. Figure 3 shows the assembled UTHA without perimeter insulation.

In 1983, tests were conducted on two standards from the National Institute of Standards and Technology (NIST);[21] with the results shown in Table 3a. The ORNL results on the NIST Certified Transfer Standard were within 0.6% of NIST values at 303 and 313 K (86 and 104°F). ORNL measurements from 72 to 140°F on Standard Reference Material (SRM) 1450b yielded a maximum difference of 0.9% between measurements by the two laboratories at 297.13 K (75°F). These SRMs were retested in the UTHA in 1990 (see Table 3b), and agreement with the NIST values was 0.3% for SRM 1451 and 1.1% for SRM 1450b. The UTHA k-values for the SRMs were fitted to better than 0.3% by a linear function of temperature. Since all of these comparisons are within the most probable uncertainty of 1.2%, the UTHA k-values reported in this paper provide an accurate description of the temperature dependency of k.

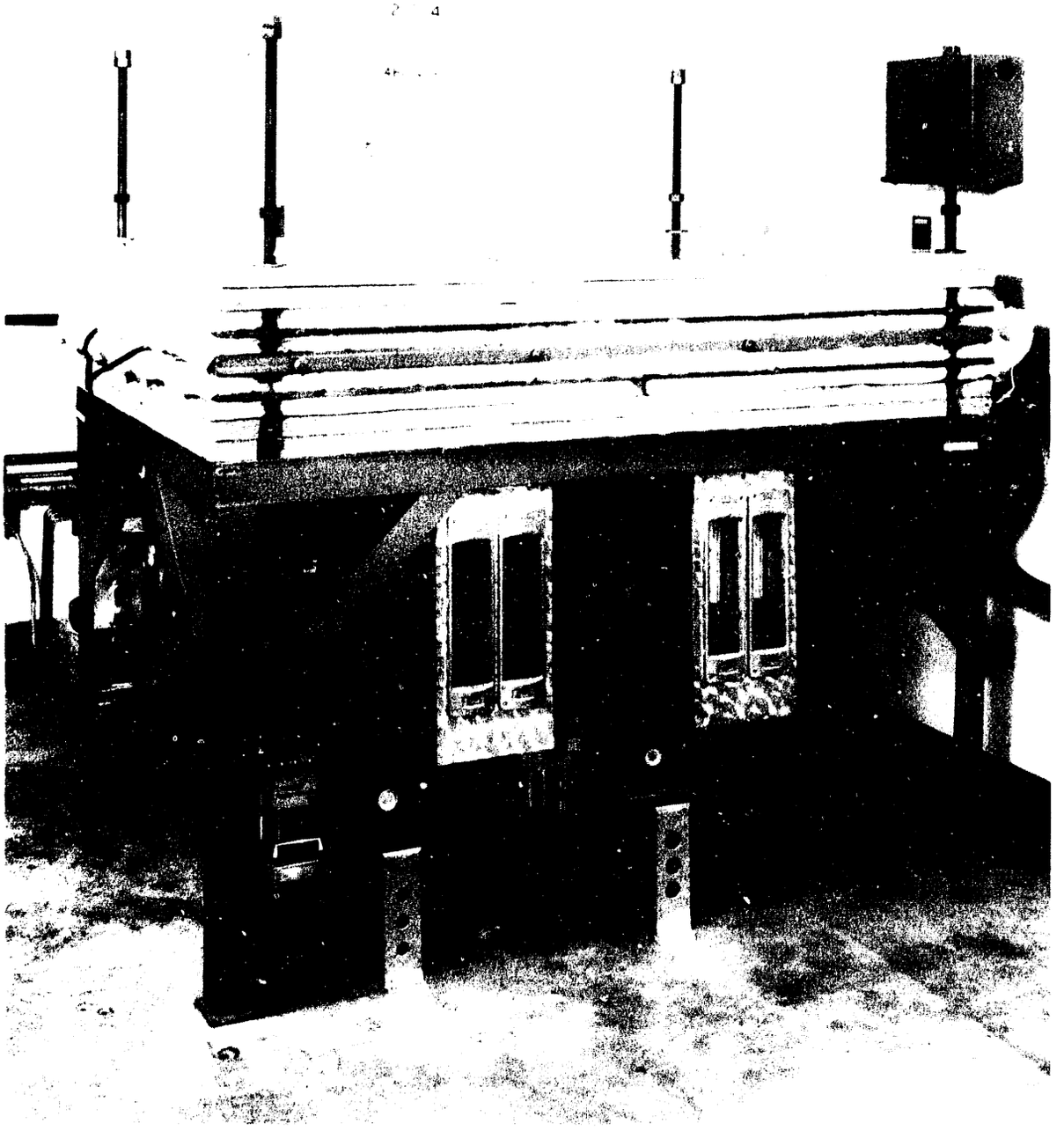

Fig. 3. Assembled Unguarded Thin-Heater Apparatus without perimeter insulation.

Table 3a. A comparison of ORNL UTHA and NIST results (1983)

Specimen	Mean sample temperature (K)	Sample density (kg/m^3)	k-ORNL (W/m·K)	k-NIST (W/m·K)	Difference[a] (%)
Certified Transfer Standard					
Two-sided	303.14	9.255	0.04813	0.04827	-0.29
	313.14	9.270	0.05164	0.05166	-0.04
One-sided	303.23	9.350	0.04811	0.04809	0.04
	303.23	9.340	0.04808	0.04835	-0.56
SRM 1450b					
Two-sided (14 points)	297.13	127.0	0.03454	0.03485	-0.89
(13 points)			0.03466	0.03485	-0.55

[a]100·[(k-ORNL)-(k-NIST)]/(k-NIST).

Table 3b. A comparison of ORNL UTHA and NIST results (1990)

Specimen	Mean sample temperature (K)	Sample density (kg/m^3)	k-ORNL (W/m·K)	k-NIST (W/m·K)	Difference[a] (%)
Certified Transfer Standard, SRM 1451					
Two-sided	303.14	9.255	0.04829	0.04827	0.04
	313.14	9.270	0.05180	0.05166	0.27
SRM 1450b					
Two-sided (4 points)	297.13	127.0	0.03445	0.03485	-1.14

[a]100·[(k-ORNL)-(k-NIST)]/(k-NIST).

3.2 ADVANCED R-MATIC APPARATUS

The thermal conductivity of the RTRA panels (Task A) was determined from 30 to 120° F in the Advanced R-Matic Apparatus.[24] This apparatus was also used to determine k (75° F) of the sliced, aging specimens (Task B). Figure 4 is a photograph of the Advanced R-Matic Apparatus, a comparative heat-flow meter technique[18] designed to meet ASTM C 518, Configuration B: two transducers, both faces. The apparatus is the first commercial unit in a new series of heat-flow-meter apparatuses and includes a dedicated computer for test control, data acquisition, and data analysis. The apparatus has:

1. top and bottom plates (24 × 24 in.) with 10 × 10 in. HFTs in each and independent plate temperature control to allow heat flow up or down;
2. specimen mean temperatures from 20 to 120° F obtained by controlling the hot face between 40 and 140° F and the cold face between 0 and 100° F;
3. a test specimen chamber surrounded on five sides by temperature-conditioned air that accommodates 24 × 24 in. specimens with thicknesses between 0.5 and 7 in.;
4. a dedicated computer allowing test conditions to be programmed to obtain k as a function of temperature for up to five temperatures (the programming features compare the sequential data sets with selected criteria, such as change in k, to decide when thermal equilibrium has been obtained); and
5. circuitry to calibrate HFTs embedded in test specimens.

The current operational mode of the Advanced R-Matic Apparatus uses the output of the 10 × 10 in. HFT on the bottom plate to measure the heat flux (q) [i.e., the time rate of heat flow (Q) through the metering area (A) normal to the heat flow] to obtain the apparent thermal conductivity (k) from Eq. 3:

$$k = \frac{Q}{A}\,\frac{L}{\Delta T}\,. \tag{3}$$

The specimen thickness (L) is obtained by bringing the bottom plate into contact with the specimen; this contacts the fixed top plate with a motor-driven gear train that has a slip clutch to limit the applied force on the system. The thickness is measured by a linear voltage differential transformer that was calibrated with sets of micarta tube

ORNL PHOTO 6593-89

Fig. 4. The Advanced R-Matic Apparatus.

spacers of known thickness. Each plate temperature is measured with a Chromel-Alumel thermocouple with an electronic reference junction. Independent checks of the measured temperatures using calibrated Chromel-Constantan thermocouples attached to the plates show agreement to better than ±0.1°F in the range 50 to 100°F.

As specified by ASTM C 518, the 10 × 10 in. HFT is calibrated with specimens of SRM 1450b and SRM 1451 to establish calibration factors as a function of specimen thickness and temperature prior to a measurement campaign. The apparatus uncertainty has been established to be less than ±5% by tests on identical specimens in the UTHA and in other C 518 apparatuses. Table 4 shows results obtained at 75°F for several materials. Since the UTHA is an absolute apparatus, the percent difference establishes the bias or inaccuracy to be less than 3.7% for 6-in.-thick fiberglass batts. The two standard deviation values (2σ) for the comparison to other C 518 apparatuses shows the imprecision to be between ±2.1 and ±3.4% for polyisocyanurate boards. This apparatus was used to test the RTRA panels as a two-board sandwich and to test the top and bottom boards at mean temperatures of 30, 60, 75, 90, and 120°F (Task A). All tests of RTRA panels were performed on specimens with the GAF facer in place, as recommended in ASTM C 1013.[22]

The apparatus was used to test the thin specimens as a function of aging time at 75 and 150°F (Task B) by using the programming features to achieve a bottom plate temperature of 95°F and a top plate temperature of 55°F; this yielded a specimen mean temperature of 75°F. The temperature-conditioned air was controlled to 75°F, and the thermal equilibrium criteria was set to accept a k-value determination when the change in k-value was less than 0.2% for two sequential data outputs of the ten readings that form a data set. Table 5a is an example of parameters for a test configuration, and Table 5b is an example of the computer printout for this criteria.

4. SPECIMENS

Thermal performance tests were conducted on two types of test specimens produced from the prototypical laminate boardstock manufactured by industry:[25] panels for the RTRA and RMPFRA and thin specimens for aging at 75 and 150°F. The boardstock (blown with CFC-11, HCFC-123, or HCFC-141b) was produced in June 1989, and boardstock blown with 50/50 and 65/35 blends of HCFC-123/HCFC-141b was produced in December 1989. Consequently, more tests were conducted on the former.

Table 4. Comparison of results from the ORNL C 518 apparatus, other C 518 apparatuses, and the ORNL UTHA

Material	C 518 apparatuses				UTHA	Difference (±2σ, %)
	ORNL	TTU	NIST	JWRC		
1. Fiberglass batt $\rho = 0.82$ lb/ft^3	0.2897		-	-	0.2978	+2.8
2. Fiberglass batt $\rho = 0.74$ lb/ft^3	0.2637				0.2734	+3.7
3. Polyisocyanurate boards $\rho = 1.88$ lb/ft^3					0.1408 (0.1382)[a]	+1.2
Board 1	0.1387 0.1406	0.1418	0.1382	0.1400		±2.06
Board 2	0.1391 0.1399	0.1404	0.1376	0.1425		±2.84
Board 1 + 2	0.1360 0.1386	0.1412	0.1381	0.1390		±2.22

[a]Projected from C 518 results.

Table 5a. Advanced R-Matic Apparatus data sheet

R-MATIC DATA SHEET (SINGLE SPECIMEN TEST)

SPECIMEN: OR-C; Heat Flow Down; Bottom HFT; Test #1

DATE: 8-20-90

1. STARTING TIME: 5:05 AM/PM

2. ROOM CONDITIONS: Temperature- 74 °F ; Rel. Hum. - 60 %

3. STARTING DIMENSIONS: THICKNESS - 53.1 mm ; MASS - 640.6 gm

4. DESIRED SETTINGS (deg C)

TOP	BOTTOM	AIR
34.3	12.9	23.9

5. PARAMETERS/LIMITATIONS

Avg Equil	Max Equil	Scan Time	Adj Delay
10 min	14 hrs	2 min	30 min

ST Equil	LT Equil	Upper Bath	Lower Bath
0.1 %	0.1 %	35 °C	35 °C

6. ENDING DIMENSIONS: THICKNESS - 53.1 mm MASS: 640.4 gm

(CHANGES) : 0 mm (0 %) ; -0.2 gm (-0.03 %)

7. COMPLETION TIME: 7:05 AM/PM

8. CALIBRATION FILE USED: SRM 1451 Curve 8/16/90

COMMENTS/MISC:

Table 5b. Computer printout from the ORNL Advanced R-Matic Apparatus

Sample is OR-C; two ½ in. boards encased in XEPS foam from Lawrence Berkeley Laboratory. HFU; BOTT HFT; (Dow Extruded Poly. WT8911).

Setpoints

Upper: 12.9 Lower: 34.2 Air: 23.9

R-Matic Measurement of Thermal Conductivity
now acquiring data at Setpoint 1

Time	Tt	Th	Tc	Tb	Th-Tc	Q	Ratio
15:32:51	11.1	13.0388	34.7880	34.3	-21.7	-945.1	3.1449
15:52:51	11.1	12.9855	34.8918	34.3	-21.9	-866.8	2.8763
16:12:52	11.1	12.9888	34.9211	34.3	-21.9	-864.9	2.8639
16:32:53	11.1	12.9947	34.9380	34.3	-21.9	-862.5	2.8557
16:52:54	11.1	12.9859	34.9271	34.3	-21.9	-862.9	2.8562
17:12:55	11.1	12.9912	34.9310	34.3	-21.9	-862.6	2.8552
17:32:56	11.1	12.9809	34.9175	34.3	-21.9	-862.1	2.8541
17:52:57	11.1	12.9876	34.9251	34.3	-21.9	-863.1	2.8572
18:12:58	11.1	12.9803	34.9237	34.3	-21.9	-863.2	2.8568
18:32:59	11.1	12.9771	34.9246	34.3	-21.9	-863.5	2.8574
18:53:00	11.1	12.9798	34.9223	34.3	-21.9	-863.3	2.8569
19:13:01	11.1	12.9810	34.9358	34.3	-21.9	-864.5	2.8613
19:33:02	11.1	12.9816	34.9368	34.3	-21.9	-862.8	2.8556
19:53:03	11.1	12.9828	34.9198	34.3	-21.9	-864.5	2.8616
20:13:03	11.1	12.9821	34.9236	34.3	-22.0	-865.4	2.8626
20:33:04	11.1	12.9842	34.9224	34.3	-22.0	-863.3	2.8557
20:53:05	11.1	12.9767	34.9343	34.3	-21.9	-864.5	2.8611
21:13:06	11.1	12.9774	34.9286	34.3	-21.9	-865.3	2.8634
21:33:07	11.1	12.9759	34.9296	34.3	-21.9	-864.7	2.8614
21:53:08	11.1	12.9756	34.9285	34.3	-22.0	-864.9	2.8605
22:13:09	11.1	12.9860	34.9286	34.3	-21.9	-863.7	2.8585
22:33:10	11.1	12.9843	34.9296	34.3	-21.9	-863.6	2.8578
22:53:11	11.1	12.9767	34.9285	34.3	-22.0	-864.6	2.8602
23:13:12	11.1	12.9770	34.9276	34.3	-22.0	-863.8	2.8578
23:33:13	11.1	12.9752	34.9232	34.3	-21.9	-864.5	2.8605
23:53:14	11.1	12.9758	34.9225	34.3	-21.9	-865.2	2.8631
00:13:15	11.1	12.9716	34.9201	34.3	-21.9	-865.0	2.8621
00:33:16	11.1	12.9757	34.9242	34.3	-21.9	-865.1	2.8623
00:53:17	11.1	12.9744	34.9262	34.3	-22.0	-864.7	2.8605
01:13:18	11.1	12.9762	34.9278	34.3	-22.0	-865.3	2.8628
01:33:19	11.1	12.9804	34.9326	34.3	-22.0	-864.8	2.8611
01:53:20	11.1	12.9720	34.9239	34.3	-22.0	-864.5	2.8598

Table 5b. (continued)

Time	Tt	Th	Tc	Tb	Th-Tc	Q	Ratio
02:13:21	11.1	12.9720	34.9242	34.3	-21.9	-864.4	2.8601
02:33:22	11.1	12.9758	35.9236	34.3	-21.9	-865.0	2.8619
02:53:23	11.1	12.9741	34.9231	34.3	-22.0	-865.7	2.8637
03:13:24	11.1	12.9707	34.9324	34.3	-22.0	-864.8	2.8606
03:33:24	11.1	12.9766	34.9330	34.3	-21.9	-865.2	2.8628
03:53:25	11.1	12.9842	34.9314	34.3	-21.9	-865.3	2.8632
04:13:26	11.1	12.9828	34.9290	34.3	-22.0	-864.4	2.8595
04:33:27	11.1	12.9752	34.9319	34.3	-22.0	-865.3	2.8619
04:53:28	11.1	12.9750	34.9341	34.3	-22.0	-864.6	2.8601
05:13:29	11.1	12.9802	34.9390	34.3	-21.9	-864.3	2.8597
05:33:30	11.1	12.9812	34.9281	34.3	-21.9	-866.3	2.8663
05:53:31	11.1	12.9790	34.9336	34.3	-22.0	-865.9	2.8645
06:13:32	11.1	12.9804	34.9379	34.3	-22.0	-864.2	2.8587

****

Timeout has occurred on Setpoint 1.
The time has exceeded 15 hours.
The following data may be incorrect.

****

at a temperature of 23.9612 C
with an upper plate temperature of 12.9845 C
and a lower plate temperature of 34.9279 C
and an air temperature of 23.4 C
the calibration constant was .013388 W/m^2/mmV
and the sample thickness was 5.32 cm (0.532 m); 2.0945 in.

Δt = 21.9534 deg
k = 0.02804 W/m·K at 23.9612° C (297.1112K)
0.1944 Btu·in./h·ft^2·° F at 75.1302° F
R = 5.1442 h·ft^2·° F/Btu·in.
R_T = 10.7742 h·ft^2·° F/Btu·in.

4.1 PANELS FOR THE RTRA AND RMPFRA (TASK A)

The Task A test specimens were nominally 24 × 24 × 1.5 in. with GAF black facers (0.025 in. thick) on each face for each type of PIR board-blowing agent. Two of these specimens formed the central area of each 4 × 4 ft panel for the RTRA tests and were picture-framed in similar boards for the UTHA tests. A 2 × 2 × 1/8 in. slot was routed into the lower board to position the embedded HFT at the interface of the two boards.

Thermal performance tests and HFT calibrations were performed in a one-sided mode of operation in the UTHA on panels at mean temperatures of 80, 100, and 120°F. Thermal performance tests were performed in the Advanced R-Matic Apparatus on the panels (consisting of two boards), the top board, and the bottom board at mean temperatures of 30, 60, 75, 90, and 120°F. Table 6 summarizes characteristics of panels produced from the boards to be tested prior to RTRA exposure. Table 6 identifies the blowing agents, the specific board stock used to prepare the specimens with facers, the calculated density of the panel core, and the time elapsed since the boards were manufactured. The GAF black facer had a reported weight of 0.05625 lb/ft^2. The calibration constant, A, is reported for each embedded HFT, and this factor is the term to multiply the millivolt signal from the RTRA test to obtain the heat flux through the specimen. The calibration constant was obtained from three levels of heat flow through the specimen that spanned the range 0.25 to 2.4 Btu/h·ft^2.

Table 6. Characteristics of RTRA panels tested in the UTHA and Advanced R-Matic Apparatus prior to installation in the RTRA

		Density, lb/ft^3			
Blowing gas	Panel numbers	Panel	Core[a]	Age (days)	Calibration constant A (Btu/h·ft^2·MV)
CFC-11	T3B9-1, 2	2.78	2.02	65	0.3826
HCFC-123	T2B7-1, 4	2.78	2.02	71	0.3859
HCFC-141b (black)	T1B8-5, 6	2.72	2.00	76	0.3749
HCFC-141b (white)	T1B8-3, 7	2.72	1.97	82	0.3786
Blend 50/50 123/141b	T1B6-3, 4	2.89	2.15	14	0.3849
Blend 65/35 123/141b	T2B5-1, 2	2.78	2.10	19	0.3682

[a]Core density corrected for GAF facer weight 0.05625 lb/ft^2 and air buoyancy effect (0.0740 lb/ft^3).

Thermal conductivity tests and embedded heat flux transducer calibrations for the first four rigid foamboards (listed in Table 6) prior to RTRA installation were completed on August 25, 1989. The tests on the last two panels were completed in January 1990.

4.2 THIN SPECIMENS FOR AGING AT 75 AND 150°F (TASK B)

Task B required 24 × 24 in. specimens of three thicknesses for each type of blowing agent. Three thicknesses (i.e., nominally 1.3, 0.7, and 0.4 in.) were produced by planing the facer and foam from boardstock to produce one, two, and four specimens, respectively, for aging at 75 and 150°F and for Advanced R-Matic Apparatus tests. The 1.3- and 0.7-in.-thick specimens contained the boardstock centerline, and the 0.4-in.-thick specimen had the boardstock centerline as one face for the CFC-11, HCFC-123, and HCFC-141b boardstock. All of the blend specimens contain the boardstock centerline. Each specimen showed evidence of the production process in that they include planes where the individual foam streams met. Table 7 shows the average specimen thickness produced. The 150°F specimens were aged at 150°F in a 64-ft^3 environmental chamber. The specimen sets were produced by planing at three times: (1) August 29, 1989 - the 75°F specimens blown with CFC-11, HCFC-123 and HCFC-141b; (2) November 16, 1989 - the 150°F specimens blown with CFC-11, HCFC-123, and HCFC-141b; and (3) February 6, 1990 - the 75°F; and February 20, 1990 - 150°F specimens blown with the 50/50 and 65/35 blends. These data were assigned zero time for the subsequent

Table 7. Average specimen thickness (mm) for aging at 75 and 150°F

	CFC-11	HCFC-123	HCFC-141b	50/50 blend	65/35 blend
75°F specimens					
Full thickness (1)[a]	33.0	33.4	33.0	31.7	30.1
Half thickness (2)	19.2	18.8	19.1	17.25	17.1
Quarter thickness (4)	10.1	10.1	10.0	9.6	9.6
150°F specimens					
Full thickness (1)	32.2	32.2	32.1	31.7	32.2
Half thickness (2)	16.5	16.4	16.35	17.35	17.45
Quarter thickness (4)	8.7	8.5	8.7	10.7	10.75

[a]Number of boards tested.

aging treatments because the planing operation removed original boardstock material that had undergone some aging. It is believed that the resulting core specimens had not aged due to gas diffusion.

Table 8 contains structural results obtained on the three boardstock foams produced in June 1989. The cells are elongated in the direction of boardstock production, cell wall thicknesses are between 0.3 and 0.5 μm, and the fraction solid in the cell wall is greater for the HCFC gases. Previous studies on foams blown with HCFC-123 and HCFC-141b show a similar increase in the fraction solid in the cell wall.[19] Determinations of the structural features of boardstock blown with the 50/50 and 65/35 blends are in progress.

Table 8. Structural features of boardstock blown with CFC-11, HCFC-123, or HCFC-141b

	CFC-11	HCFC-123	HCFC-141b
Average distance between cell walls, mm			
Parallel to facer	0.24	0.20	0.27
Perpendicular to facer	0.16	0.15	0.16
Cell wall thickness, μm	0.30	0.40	0.53
Percent solid in cell wall	17	30	38

5. RESULTS

5.1 RTRA PANELS AND RMPFRA PANELS

Table 9 contains the k results obtained as a function of temperature in the UTHA for six panels prior to installation in the RTRA. Duplicate RTRA panels of HCFC-141b were tested for field exposure under black and white EPDM membranes. All of the k-values increase with temperature, and the linear equations given in Table 9 describe the results with an average percent deviation of less than ±0.23%.

Appendix A, Table A1 contains the k results obtained on the RTRA panels as a function of temperature from 30 to 120° F in the Advanced R-Matic Apparatus. This table contains equations that describe the UTHA and Advanced R-Matic Apparatus data

Table 9. UTHA k results on panels prior to RTRA installation

Specimen: age	Mean temperature (°F)	k (Btu·in./h·ft^2·°F)
PIR CFC-11: 61 d		
	76.99	0.1288
	100.13	0.1422
	121.60	0.1533
$k = 0.0867 + 5.4958 \times 10^{-4} T$, ±0.22%[a]		
PIR HCFC-123: 68 d		
	80.03	0.1385
	99.91	0.1486
	121.44	0.1609
$k = 0.09496 + 5.4126 \times 10^{-4} T$, ±0.19%[a]		
PIR HCFC-141b: 71 d T1B8-5, 6 (Black)		
	80.39	0.1475
	99.91	0.1570
	121.17	0.1683
$k = 0.10631 + 5.1044 \times 10^{-4} T$, ±0.13%[a]		
PIR HCFC-141b: 77 d T1B8-3, 7 (White)		
	80.00	0.1472
	100.03	0.1579
	121.16	0.1703
$k = 0.1022 + 5.6133 \times 10^{-4} T$, ±0.15%[a]		
PIR 50/50 blend: 15 d		
	79.75	0.1371
	99.34	0.1454
	121.34	0.1564
$k = 0.0995 + 4.6702 \times 10^{-4} T$, ±0.23%[a]		
PIR 65/35 blend: 19 d		
	79.92	0.1378
	100.14	0.1474
	121.49	0.1566
$k = 0.10183 + 4.5205 \times 10^{-4} T$, ±0.14%[a]		

[a]Average percent deviation.

as a function of temperature. Figures A1 through A6 show the temperature dependency of k (panels) as measured in the UTHA and the Advanced R-Matic Apparatus.

Figure 5 shows the temperature dependency of k as measured in the UTHA and the Advanced R-Matic Apparatus for the Task A specimen blown with CFC-11. The panels for the other blowing agents showed a similar temperature dependency for k (i.e., a minimum k below 60° F, a nearly linear temperature dependency above 80° F, but a displacement in k that depended on blowing agent and age at the time of testing). The k-values determined with the UTHA are lower than the k-values determined with the Advanced R-Matic Apparatus in the temperature range of overlap but are within the experimental uncertainties expected for the two apparatuses. Because the UTHA is more accurate, our data analysis is weighted toward the UTHA k-values. A least-squares fit was produced for both data sets. The curve fit to the Advanced R-Matic Apparatus data showed a minimum, and a constant was subtracted from this fit to produce agreement with the UTHA data from 80 to 120° F and to maintain the minimum. The resulting curve is shown in Fig. 5. Table 10 contains the equation and the equation k-values (including the facers) as a function of temperature.

The results shown in Table 10 describe the thermal performance of the panels blown with CFC-11, HCFC-123, and HCFC-141b. The panels blown with the blends were installed in the RTRA in February 1990. Results on RTRA panels show that for an age of 14 to 19 d, the panels blown with the blends had nearly equal k (75° F) values.

Results for the other panels at an age of about 75 d show:

$$k(\text{CFC-11}) < k\ (\text{HCFC-123}) < k\ (\text{HCFC-141b})\ .$$

The first set of RTRA panels was removed in March 1990 after an RTRA exposure of 241 d and tested in the UTHA and the Advanced R-Matic Apparatus. Table 11 contains the results and shows that the k (R-Matic) was 5 to 8% larger than k (UTHA) noted earlier. The k (75° F) after 241 d is given in Table 10. The HFT calibration constants changed less than 0.75%.

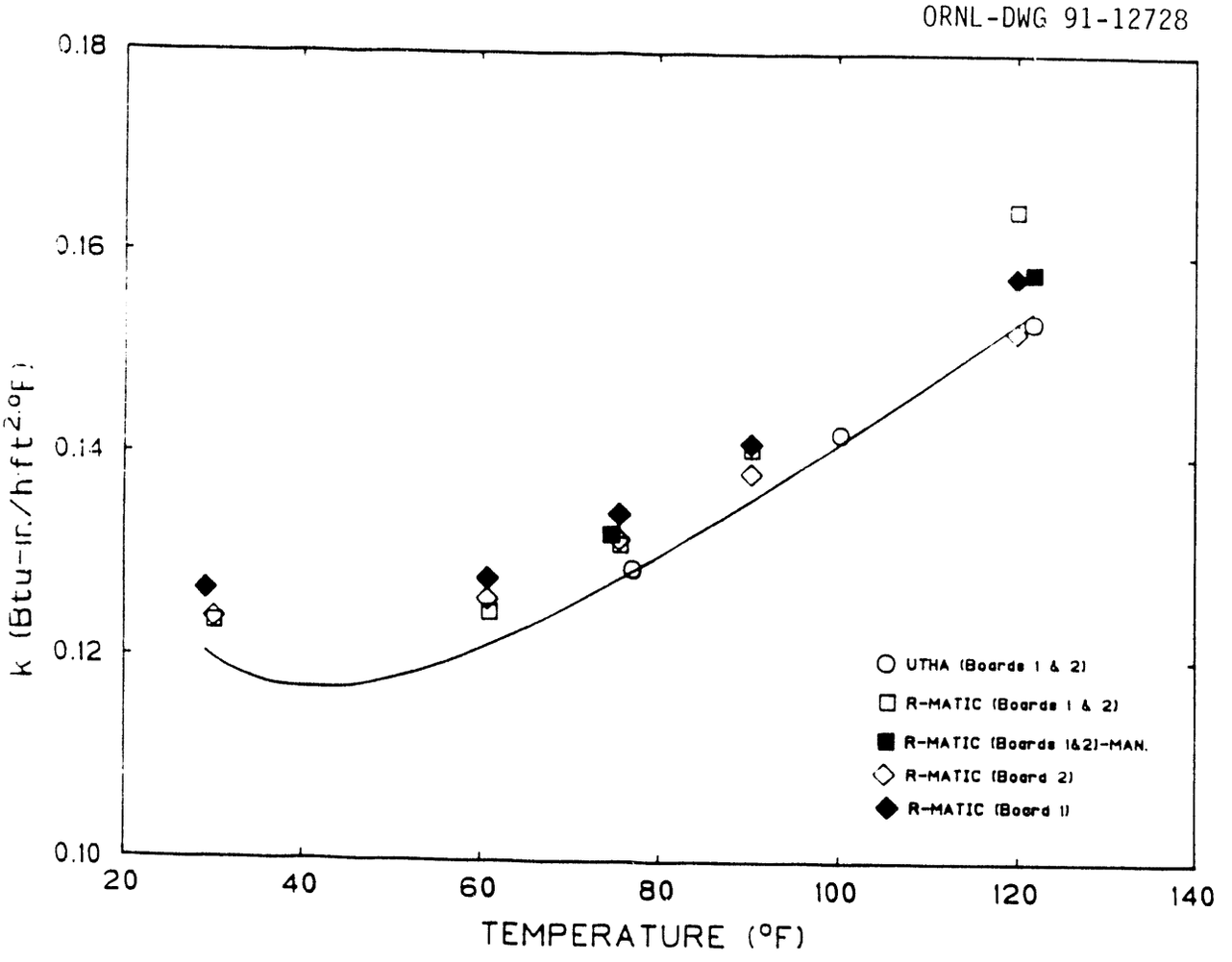

Fig. 5. The temperature dependency of the thermal conductivity of boardstock blown with CFC-11.

Table 10. The thermal conductivity[a] of RTRA and RMPFRA panels blown with CFC-11, HCFC-123, HCFC-141b, and two blends (50/50 and 65/35) of HCFC-123/HCFC-141b

1. Before RTRA exposure

Temperature	Thermal conductivity (Btu·in./h·ft^2·°F)				
°F	CFC-11	HCFC-123	HCFC-141b	50/50	65/35
Age, days[b]	65	71	78	14	19
30[b]	0.120	0.128	0.140	-	-
45[b]	0.117	0.125	0.134	-	-
60[b]	0.121	0.129	0.137	-	-
75[b]	0.128	0.135	0.143	0.135	0.136
90[b]	0.136	0.143	0.151	0.142	0.142
120[b]	0.153	0.161	0.169	0.156	0.156
$k = A + B\,T + C\,T^{-1}$, 30 to 120°F					
A	0.0585	0.0672	0.0679	0.0995	0.1018
B	7.067×10^{-4}	6.955×10^{-4}	7.4×10^{-4}	4.670×10^{-4}	4.521×10^{-4}
C	1.204	1.1935	1.495	-	-
2. After 241 d of RTRA exposure					
Days[c]	334	336	340	-	-
75[c]	0.139	0.150	0.156	-	-
Increase, %	8.6	11.1	9		
3. RMPFRA panels after being stored at ORNL for 1 year					
75[a]	0.154	0.152	0.165		
Increase, %	20.3	12.6	15.4		
4. After 430 d of RTRA Exposure				After 295 d of RTRA Exposure	
Days[c]	529	533	527	309	314
75[c]	0.156	0.163	0.170	0.163	0.164
Increase, %	21.9	20.7	18.9	20.7	20.6

[a]Includes GAF facer.
[b]Time since production when tested prior to installation in the RTRA.
[c]Includes 241 d of exposure in RTRA under black EPDM membranes.

Table 11. The k of RTRA panels after 241 d of exposure in the RTRA

Blowing agent	Mean temperature (°F)	k (Btu·in./h·ft²·°F)	A
CFC-11[a]	76.91 120.73	0.1405 0.1676	0.3800 (0.3826)[b]
$k = 0.0929 + 6.1849 \times 10^{-4} T$ k (75): 0.1393			
R-Matic 1, 2 334 d, 2 1	75.57 75.67 75.53	0.1524 0.1509 0.1502	
HCFC-123[a]	79.18 120.38	0.1527 0.1746	0.3840 (0.3849)
$k = 0.1106 + 5.3155 \times 10^{-4} T$ k (75): 0.1505			
R-Matic 1, 4 (333 d), 1 4	75.39 75.39 75.57	0.1597 0.1613 0.1550	
HCFC-141b[a] (Black)	79.27 121.06	0.1584 0.1841	0.3721 (0.3749)
$k = 0.1096 + 6.150 \times 10^{-4} T$ k (75): 0.1558			
R-Matic 5, 6 342 d, 5 6	75.35 75.42 75.42	0.1662 0.1672 0.1665	
HCFC-141b[a] (White)	79.08 120.99	0.1604 0.1852	0.3772 (0.3768)
$k = 0.1136 + 5.918 \times 10^{-4} T$ k (75): 0.1580			
R-Matic 3, 7 342 d, 3 7	75.52 75.52 75.52	0.1654 0.1651 0.1638	

[a]UTHA results.
[b]Pre RTRA calibration factor A.

In June 1990, tests were conducted on panels to be installed in the RMPFRA. These panels were produced from boardstock that had been stored at ORNL since June 1989 and were just over 1 year old at the time of the tests. Table 12 contains the results of two-sided heat-flow UTHA tests on these panels that contained embedded heat flux transducers. The k (75°F) values are given in Table 10 and Table 12. The k-values after one year of storage are greater than those of the prior set by 12 to 20%.

Table 12. Thermal conductivity of RMPFRA panels produced from boardstock stored since June 1989

Blowing agent	Mean temperature	k (Btu·in./h·ft²·°F)	A	
CFC-11	83.84	0.1570	(1, 2)	0.4138
	120.87	0.1690	(3, 4)	0.4085
	129.10	0.1744		
$k = 0.1261 + 3.660 \times 10^{-4}\ T,\ \pm 0.51\%$ $k\ (75) = 0.1535$				
HCFC-123	83.86	0.1561	(3, 2)	0.3765
	119.75	0.1741	(1, 4)	0.4110
$k = 0.1126 + 5.1828 \times 10^{-4}\ T$ $k\ (75) = 0.1515$				
HCFC-141b	83.58	0.1707	(1, 2)	0.4147
	110.05	0.1934	(3, 4)	0.4162
$k = 0.1172 + 6.400 \times 10^{-4}\ T$ $k\ (75) = 0.1652$				

In November 1990, the set of six RTRA panels was removed for testing in the UTHA and the Advanced R-Matic Apparatus. The results of these tests are given in Appendix A and are summarized in Table 10. The k (75) values given in Table 10 after 430 d of exposure show that the k of each panel has increased about 20% and that the order (i.e., ranking) of k is

$$k\ (\text{CFC-11}) < k\ (\text{HCFC-123}) < k\ (\text{HCFC-141b})\ .$$

The k-values for the panels blown with two blends are very similar to the panel blown with HCFC-123. Data in Appendix A show that the k-values for the HCFC-141b blown panels exposed under black-and-white EPDM are similar to each other. Appendix A provides data for the HFT calibration constant (this has changed less than 1% during the RTRA tests for the six HFTs).

5.2 THIN SPECIMENS AGING AT 75 AND 150°F

The Advanced R-Matic Apparatus was used to obtain k (75°F) values for planed specimens of three thicknesses being aged at 75 and 150°F. Table 13 indicates the time when the tests were conducted on stacks of one, two, or four specimens and when the specimens were planed (i.e., zero time).

Table 13. Time at temperature when k (75°F) tests were conducted on planed specimens (days measured from time of planing)

Task B specimens	75°F aging test times	150°F aging test times
CFC-11, HCFC-123, and HCFC-141b	3, 17, 51.5, 106.5, 190, 290 (0: August 29, 1989)	1.5, 13.5, 43, 114.5, 185 (0: November 16, 1989)
Blends if 50/50 and 65/35 HCFC-123/141b	2, 42.5, 74.5, 127 (0: February 6, 1990)	1.5, 29.5, 62.5, 118.5 (0: February 20, 1990)

Tables 14 and 15 contain the k (75) values obtained at these test times. The intent of this test procedure is to establish the value of thin-specimen aging as a means to measure the diffusion process that causes foams with permeable facers or no facing to slowly lose their insulating power as a function of time. Without a barrier, air components diffuse into the foam cells, and the blowing agent diffuses out of the foam cells. This process changes the cell gas composition, which changes the cell gas thermal conductivity, and this changes the product thermal resistance. The thinner specimens show a more rapid change in thermal conductivity because of the shorter diffusion distance to the specimen centerline.

Table 14a. k (75) values for planed specimens aging at 75°F

		Thermal conductivity (Btu·in./h·ft²·°F)		
Age, d	Boards	CFC-11	HCFC-123	HCFC-141b
3	1	0.1268	0.1371	0.1423
	2	0.1206	0.1342	0.1406
	4	0.1322	0.1411	0.1509
17	1	0.1239	0.1374	0.1452
	2	0.1286	0.1437	0.1534
	4	0.1390	0.1515	0.1580
51.5	1	0.1315	0.1423	0.1512
	2	0.1396	0.1536	0.1641
	4	0.1502	0.1622	0.1695
106.5	1	0.1322	0.1464	0.1540
	2	0.1476	0.1644	0.1697
	4	0.1560	0.1681	0.1734
190	1	0.1418	0.1522	0.1606
	2	0.1540	0.1721	0.1729
	4	0.1592	0.1709	0.1767
290	1	0.1440	0.1556	0.1625
	2	0.1602	0.1713	0.1788
	4	0.1628	0.1762	0.1816

Table 14b. k (75) values for planed specimens aging at 75°F

		Thermal conductivity (Btu·in./h·ft²·°F)	
Age, d	Boards	50/50	65/35
2	1	0.1370	0.1381
	2	0.1360	0.1352
	4	0.1468	0.1452
42.5	1	0.1454	0.1486
	2	0.1596	0.1579
	4	0.1758	0.1755
74.5	1	0.1522	0.1578
	2	0.1712	0.1708
	4	0.1812	0.1804
127	1	0.1507	0.1569
	2	0.1750	0.1707
	4	0.1848	0.1811

Table 15a. k (75) values for planed specimens aging at 150° F

		Thermal conductivity (Btu·in./h·ft^2·° F)		
Age, d	Board	CFC-11	HCFC-123	HCFC-141b
1.5	1	0.1333	0.1442	0.1527
	2	0.1305	0.1398	0.1532
	4	0.1473	0.1556	0.1630
13.5	1	0.1409	0.1520	0.1586
	2	0.1574	0.1630	0.1793
	4	0.1616	0.1707	0.1743
43	1	0.1511	0.1598	0.1682
	2	0.1631	0.1701	0.1836
	4	0.1641	0.1737	0.1789
114.5	1	0.1579	0.1665	0.1769
	2	0.1680	0.1737	0.1913
	4	0.1698	0.1813	0.1850
185	1	0.1556	0.1606	0.1696
	2	0.1688	0.1755	0.1850
	4	0.1784	0.1859	0.1958

Table 15b. k (75) values for planed specimens aging at 150° F

		Thermal conductivity (Btu·in./h·ft^2·° F)	
Age, d	Boards	50/50	65/35
1.5	1	0.1360	0.1417
	2	0.1397	0.1388
	4	0.1458	0.1499
29.5	1	0.1533	0.1577
	2	0.1723	0.1717
	4	0.1870	0.1862
62.5	1	0.1632	0.1690
	2	0.1850	0.1833
	4	0.1952	0.1986
118.5	1	0.1591	0.1590
	2	0.1732	0.1721
	4	0.1904	0.1893

The results given in Tables 14 and 15 confirm the premise of the test procedure. For example, the 54 k-values for the 75°F aging study (three materials, three thicknesses, and six test times) show that for each thickness and time the order of the material k-values is

$$k\ (\text{CFC-11}) < k\ (\text{HCFC-123}) < k\ (\text{HCFC-141b})\ ,$$

and for each material and time it is

$$k\ (33\ \text{mm}) < k\ (19\ \text{mm}) < k\ (10\ \text{mm})\ .$$

The material order is the same as that observed for the tests on the RTRA panels. These 54 k-values are smooth, monotonic functions of time divided by thickness squared (i.e., t/h^2), and this fact is shown in Fig. 6 for the specimens with the blowing agents, CFC-11, HCFC-123, and HCFC-141b. Appendix B contains the specific values for the quantity t/h^2 in d/mm^2 and $\sqrt{t}/h$ in $d^{1/2}/mm$ for the test results given in Tables 14 and 15.

The k-values for three materials plotted in Fig. 6 show a nonlinear dependence on t/h^2 for values of t/h^2 up to 2.7 d/mm^2 at 75°F. Figure 7 is a similar plot for the 50/50 and 65/35 blends and includes the results for the CFC-11 specimens. The 24 k-values for the two blends show the same trends noted for the other material, but the aged k is greater than that for the specimens blown with HCFC-141b. The k-values for the two blends are very similar in value. Figures 8 and 9 show the nonlinear dependence on t/h^2 for aging at 150°F.

6. DISCUSSION OF RESULTS OF AGING THIN SPECIMENS

6.1 EFFECTIVE DIFFUSION COEFFICIENTS

The nonlinear behavior of the increase in k with time/(thickness)^2 can be described by two linear regions if one plots ℓn k vs (time)$^{1/2}$/thickness. If one empirically assumes that k can be described by an exponential dependence on diffusion coefficient (D), time (t), and thickness (h):

$$k = k_0 \exp\{(Dt)^{1/2}/h\}\ , \qquad (4)$$

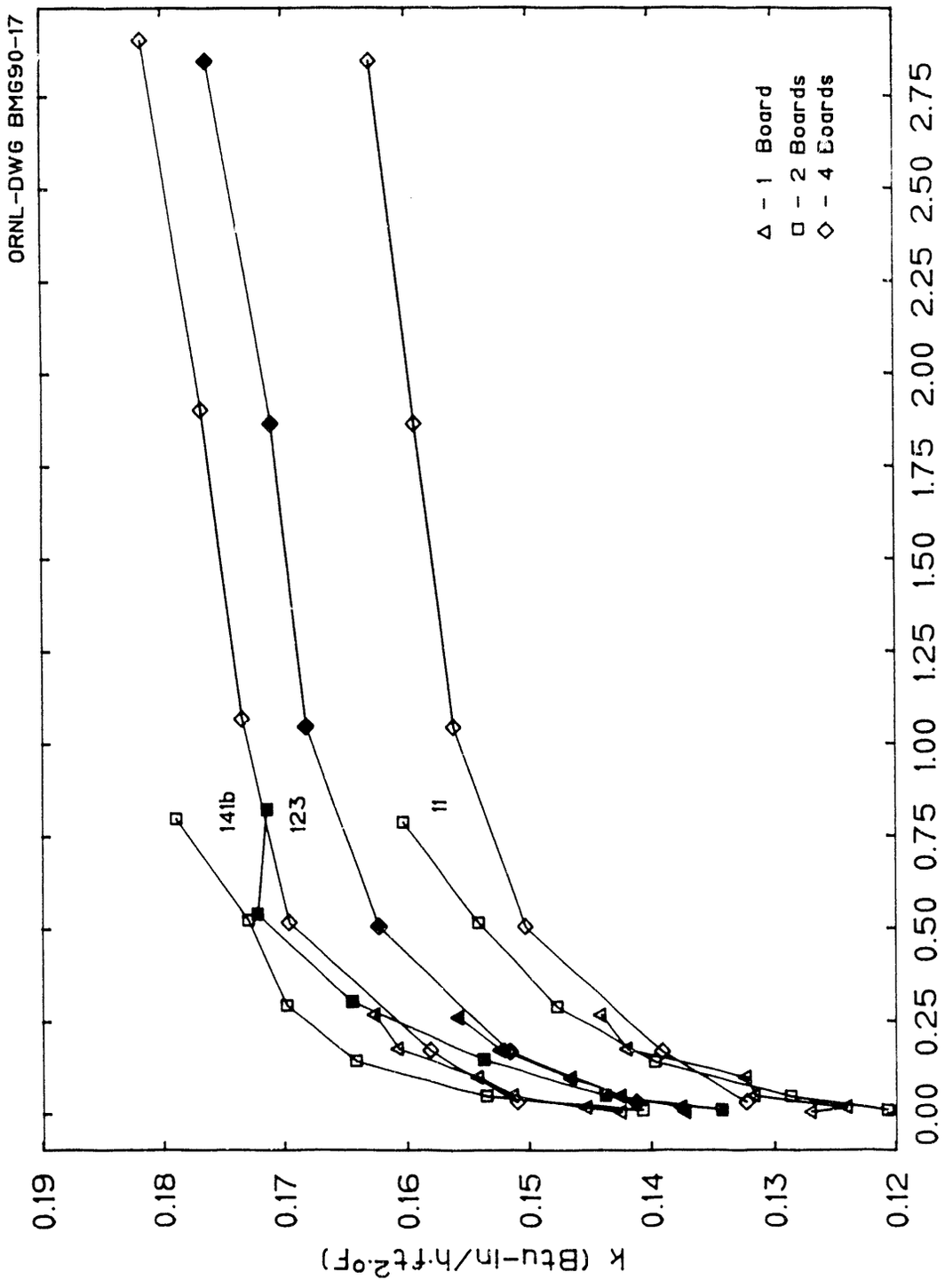

Fig. 6. Thermal conductivity at 75°F for thin specimens aging at 75°F as a function of time/(thickness)^2 in d/mm^2.

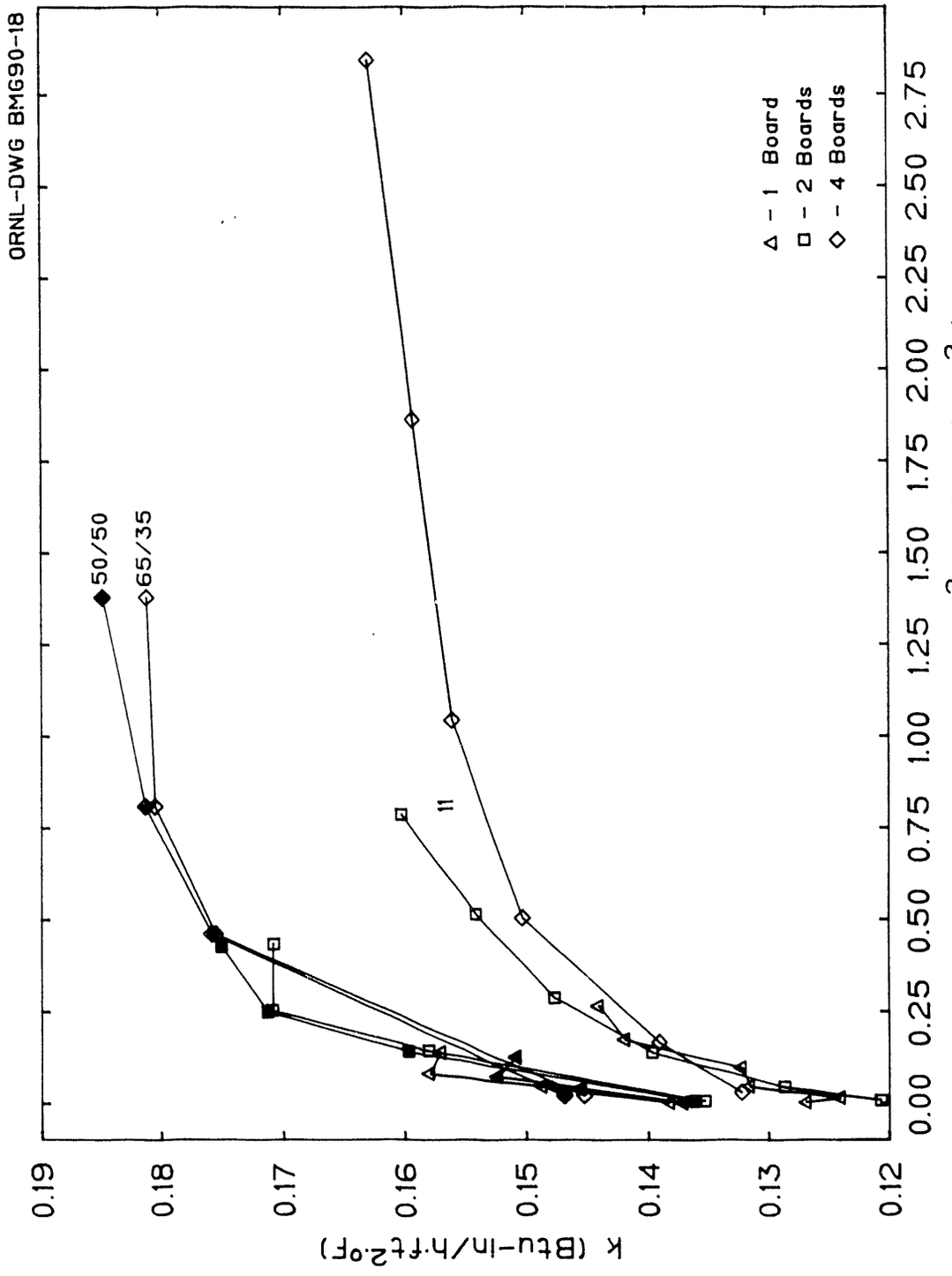

Fig. 7. Thermal conductivity at 75°F for thin specimens aging at 75°F as a function of time/(thickness)^2 in d/mm^2.

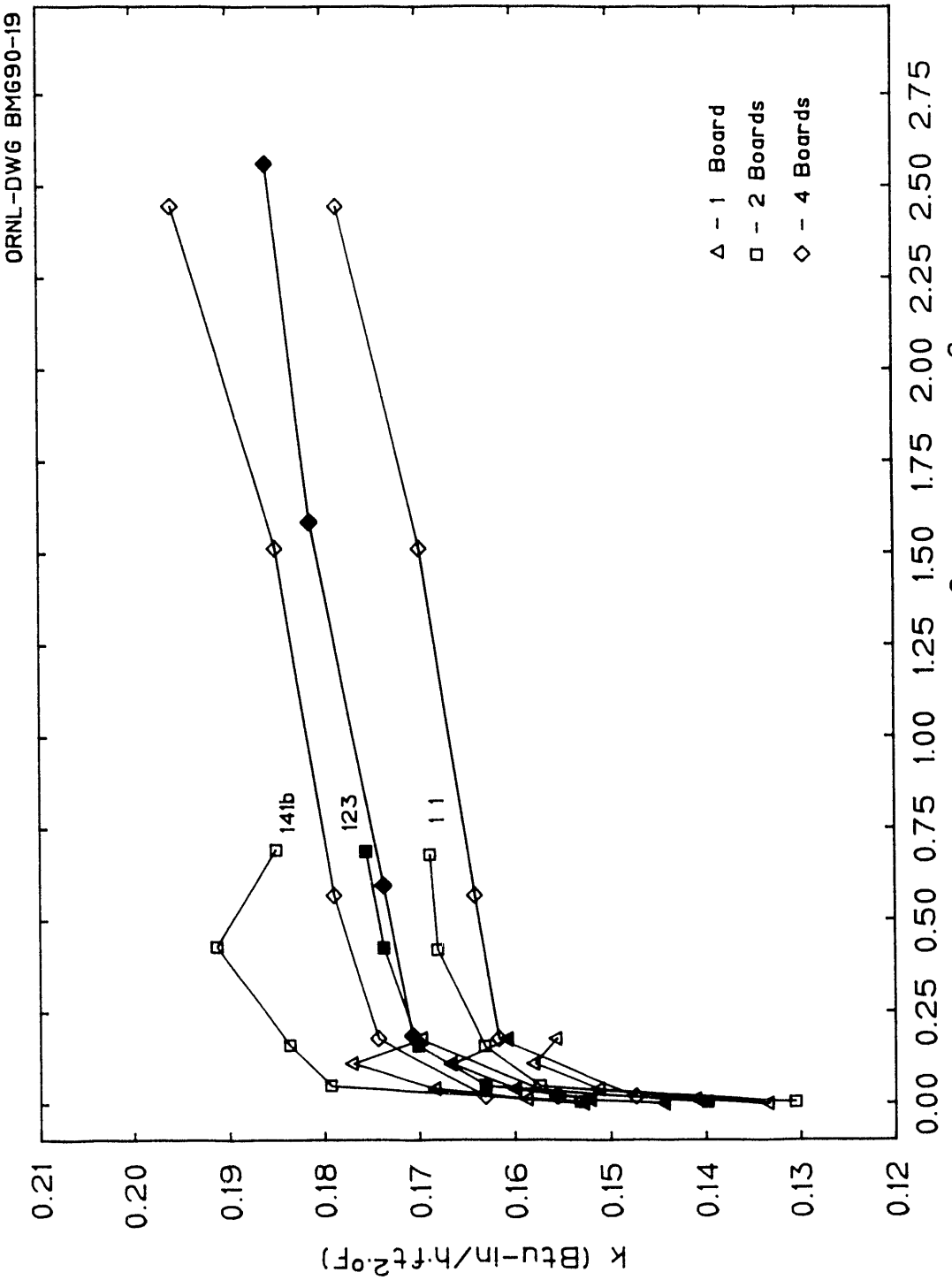

Fig. 8. Thermal conductivity at 75°F for thin specimens aging at 150°F as a function of time/(thickness)^2 in d/mm^2.

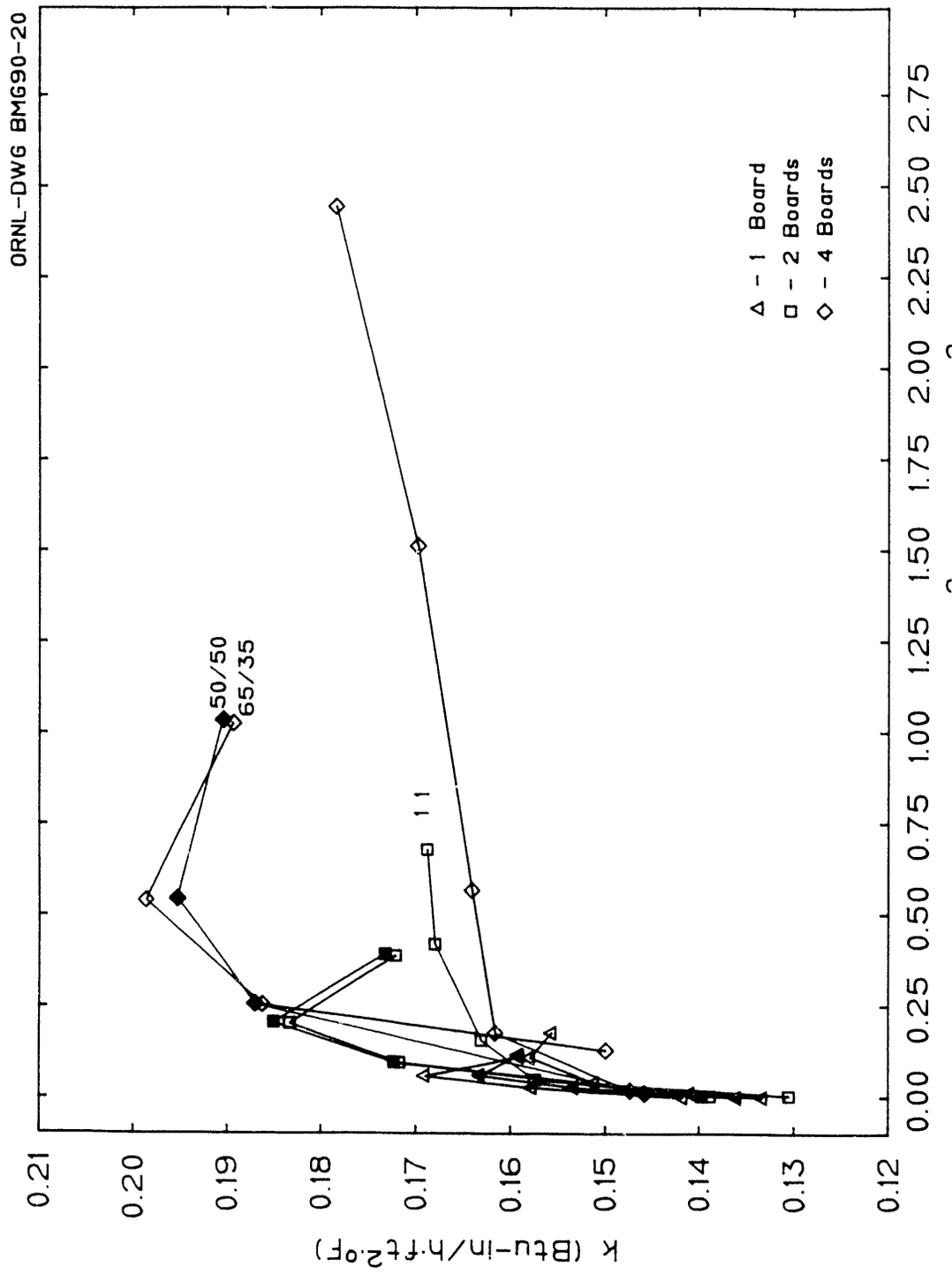

Fig. 9. Thermal conductivity at 75°F for thin specimens aging at 150°F as a function of time/(thickness)^2 in d/mm^2.

where k_o is the initial thermal conductivity, then one observes

$$\ln k = \ln k_o + (Dt)^{1/2}/h , \tag{5}$$

$$Y = A + B X , \tag{6}$$

where

$$A = \ln k_o ,$$

$$Y = \ln k ,$$

$$X = t^{1/2}/h , \text{ and}$$

$$B = D^{1/2} .$$

Thus, if one measures the k of a foam product of thickness (h) as a function of aging time (t), then a plot of Y versus X should yield a straight line with slope B. A least-squares fitting of the data to the straight line represented by Eq. 6 yields an intercept of $\ln k_o$ and a slope of $D^{1/2}$.

Figure 10 shows the increase of k (75°F) (plotted as $\ln 100\ k$ for convenience) as a function of time$^{1/2}$/thickness, ($d^{1/2}$/mm) for specimens of three thicknesses of foam blown with CFC-11 and aged at 75°F. The test data for the specimens of three thicknesses describe two distinct linear regions of behavior with an intermediate transition zone. The thin specimen has reached larger values of $t^{1/2}/h$ than the thick specimen. The first linear region should be associated with the increase in k due to the influx of air components; the second, lower slope, linear region should be associated with the loss of CFC-11 from the foam. The results of five tests up to 290 d after planing are similar to the Massachusetts Institute of Technology (MIT) model predictions[9,26] for 50.8-mm-thick specimens aged for 5400 d ($t^{1/2}/h$ of 1.45) and 5.08-mm-thick specimens aged for 15 d ($t^{1/2}/h$ of 0.76) at 75°F (see Table B5). The predictions are higher in k owing to the model assumptions (see Sect. 7), but the behavior of k with $t^{1/2}/h$ is supportive of the test results. Figure 11 includes the model predictions and the test data on three thicknesses of foam blown with CFC-11 aged at 150°F. The two-linear-region behavior occurs for aging at 150°F with larger values of k (75°F) that are closer to the model predictions. For example, at 150°F the linear-region extrapolations intersect near a value of $t^{1/2}/h$ of 0.25 $d^{1/2}$/mm, but at 75°F this intersection is near 0.55 $d^{1/2}$/mm. This result shows that,

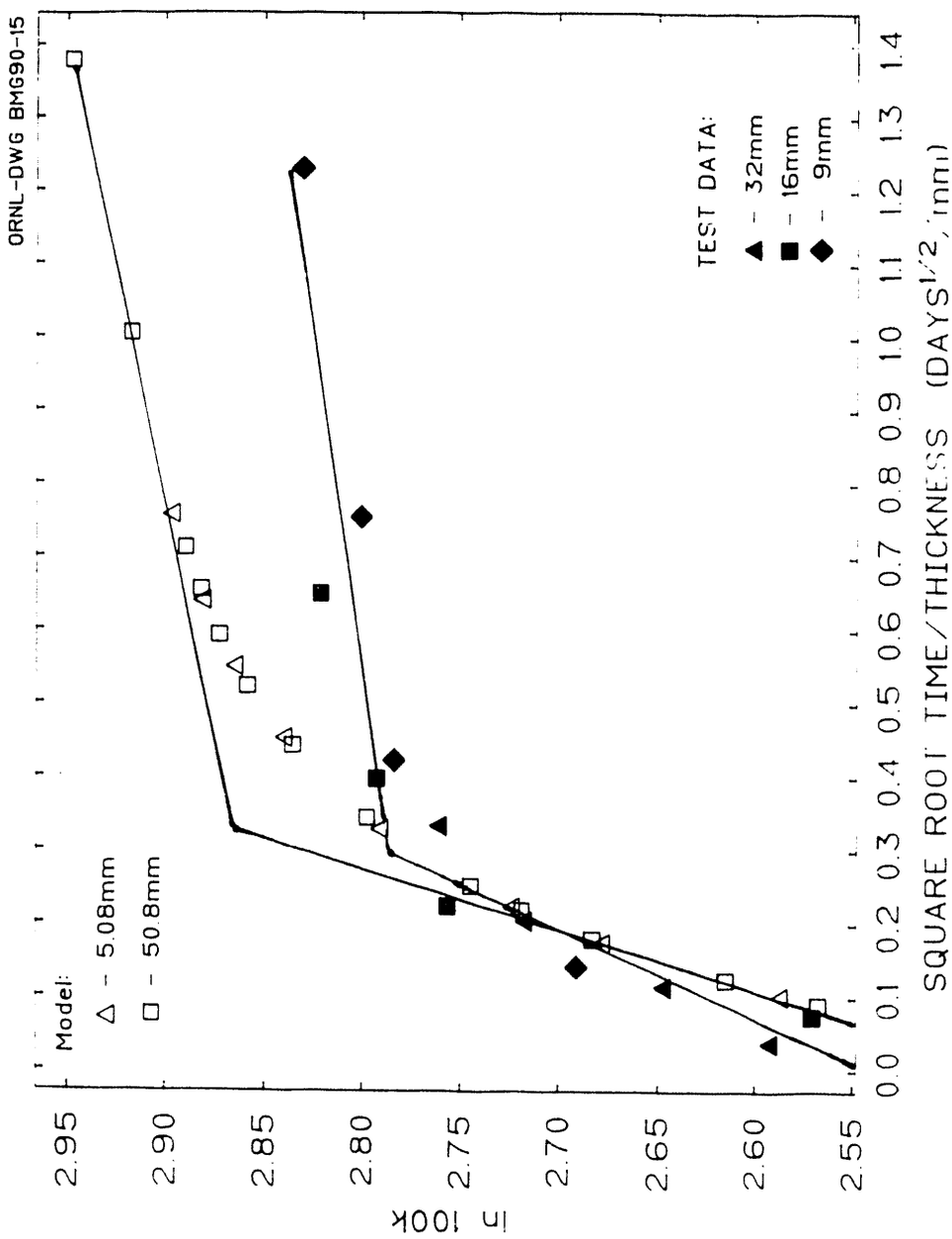

Fig. 10. Increase in k (75°F) for thin specimens of rigid board foamed with CFC-11 aging at 75°F compared with Massachusetts Institute of Technology model predictions.

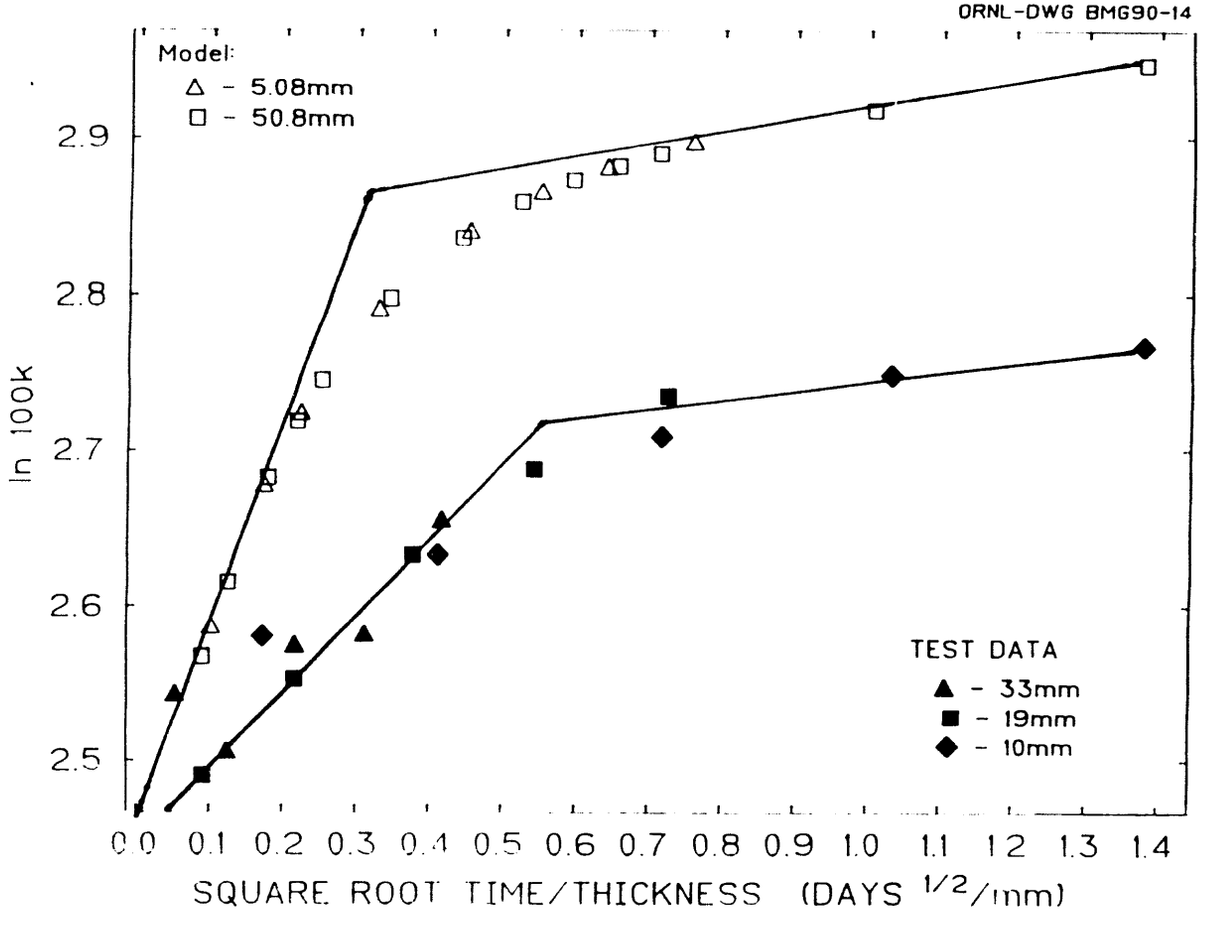

Fig. 11. Increase in k (75°F) for thin specimens of rigid board foamed with CFC-11 aging at 150°F compared with Massachusetts Institute of Technology model predictions.

as expected, the diffusion of air components into the foam is faster at 150° F (339 K) than at 75° F (297 K).

We treated the model predictions for 75° F aging and the available test data for the foams blown with five gases aging at 75 and 150° F, as suggested by Eqs. 5 and 6. The specific equations used were

$$\ell n\ k\ (\text{Region 1, air}) = \ell n\ k_1 + (D_1\ t)^{1/2}/h\ , \tag{7}$$

and

$$\ell n\ k\ (\text{Region 2, Blowing agent}) = \ell n\ k_2 + (D_2\ t)^{1/2}/h\ , \tag{8}$$

where k_1 is the projected initial k of the foam (Region 1), k_2 is the intercept for Region 2, D_1 is the effective diffusion coefficient for air components into the foam, cm^2/s, and D_2 is the effective diffusion coefficient of the blowing agent out of the foam, cm^2/s.

The k-value results given in Tables 14 and 15 are plotted as ℓn 100 k vs the square root of time divided by thickness in $s^{1/2}/cm$ in Figs. 12 through 16 for thin specimens aging at 75° F, and in Figs. 17 through 21 for thin specimens aging at 150° F. Each of these figures includes the k results for three specimens and indicates two straight lines that were fitted by a least-squares method to the k-values.

Table 16 is a summary of the data fits obtained by a least-squares method. The average percent deviation is less than 1% for all of the results, but is 2% for that of the blends in Region 2 and aging at 150° F. This scatter is evident in Figs. 20 and 21. The low average percent deviation is shown in Figs. 12 through 21 for Region 1 and Region 2.

The square root of the B coefficients for the data fits provides the effective diffusion coefficients for Region 1 and Region 2. The resulting values for D_1, D_2, and the ratio, D_1/D_2, are given in Table 17. The effective diffusion coefficients derived from the aging tests are of the expected order of magnitude and appear to be reasonable values. The results for aging at 75° F show D_1 values near 1.5×10^{-8} cm^2/s for the foams blown with individual gases and near 2.5×10^{-8} cm^2/s for the foams blown with the blends. The D_1 values for aging at 150° F are 3 to 7 times larger than the D_1 (75° F aging) as would be expected for temperature dependent diffusion processes. The results

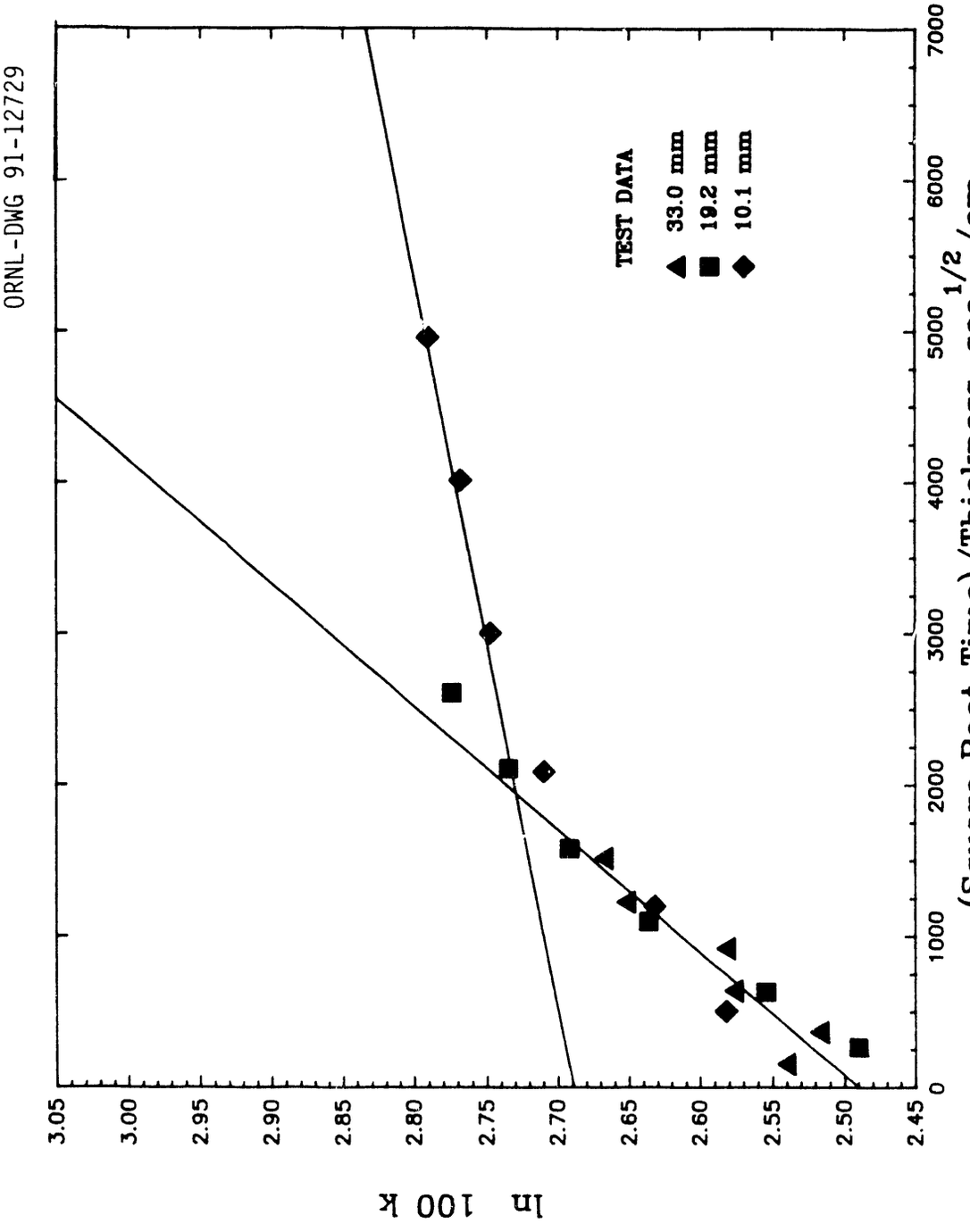

Fig. 12. Increase in k (75°F) for thin specimens of rigid board foamed with CFC-11 aging at 75°F.

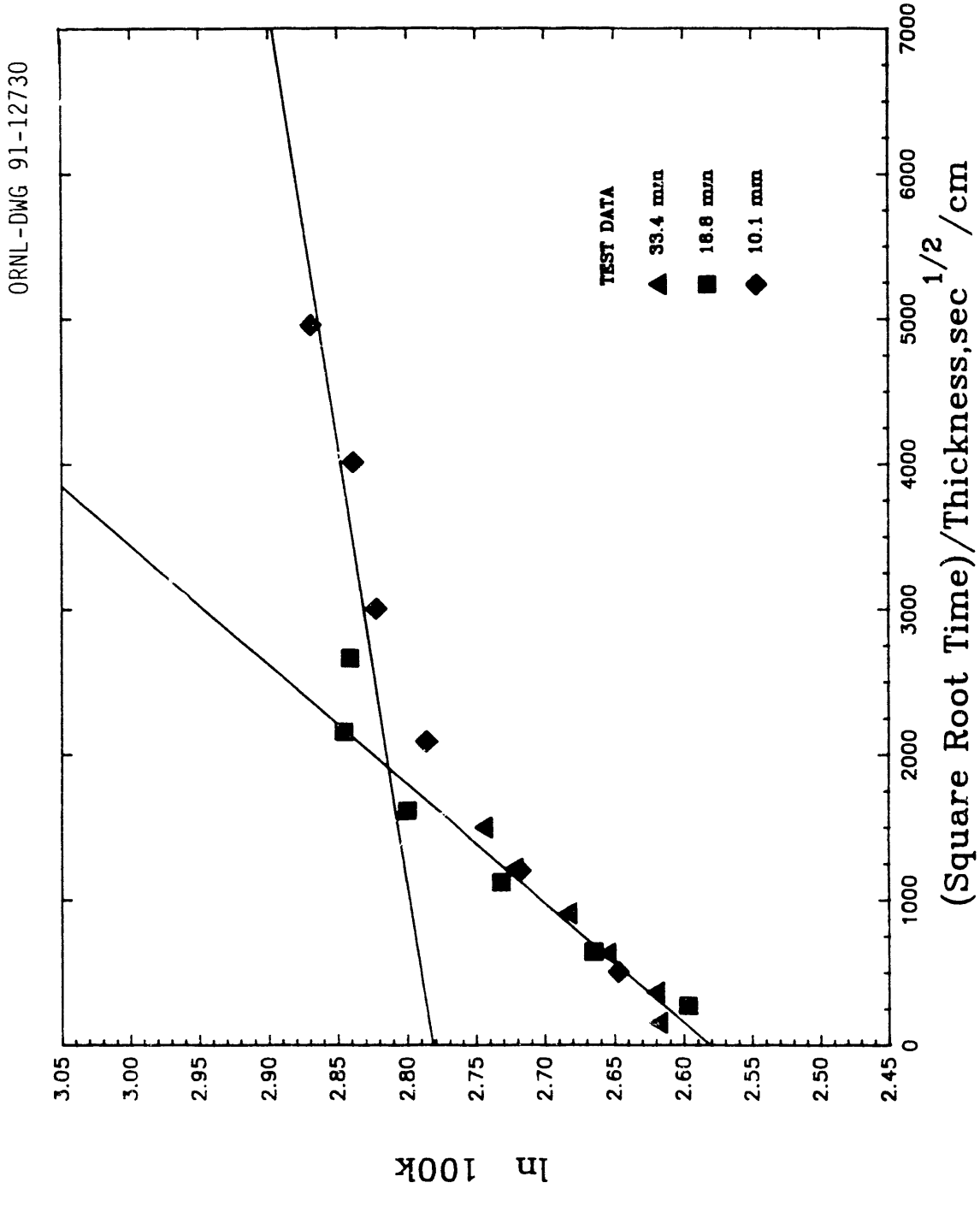

Fig. 13. Increase in k (75°F) for thin specimens of rigid board foamed with HCFC-123 aging at 75°F.

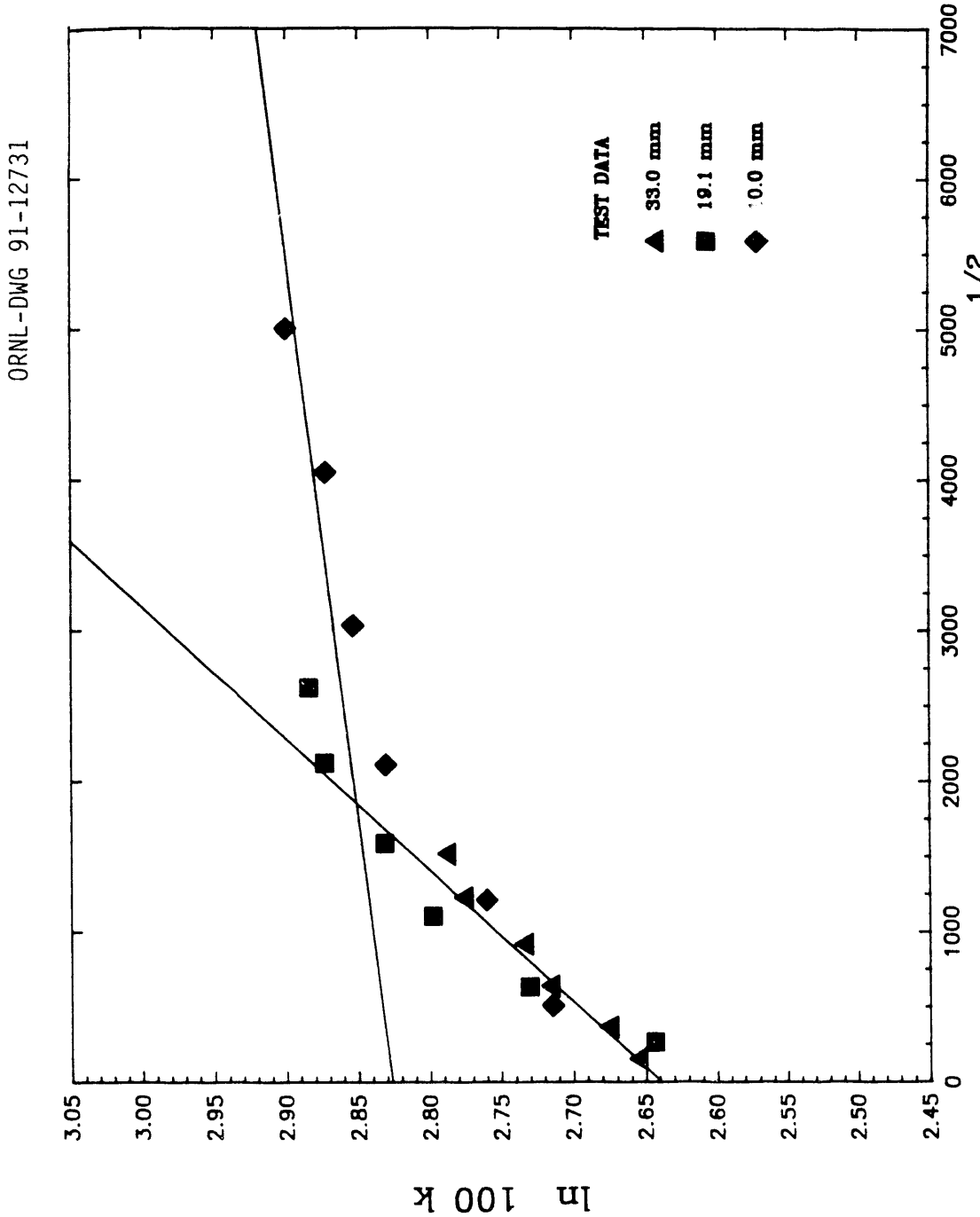

Fig. 14. Increase in k (75°F) for thin specimens of rigid board foamed with HCFC-141b aging at 75°F.

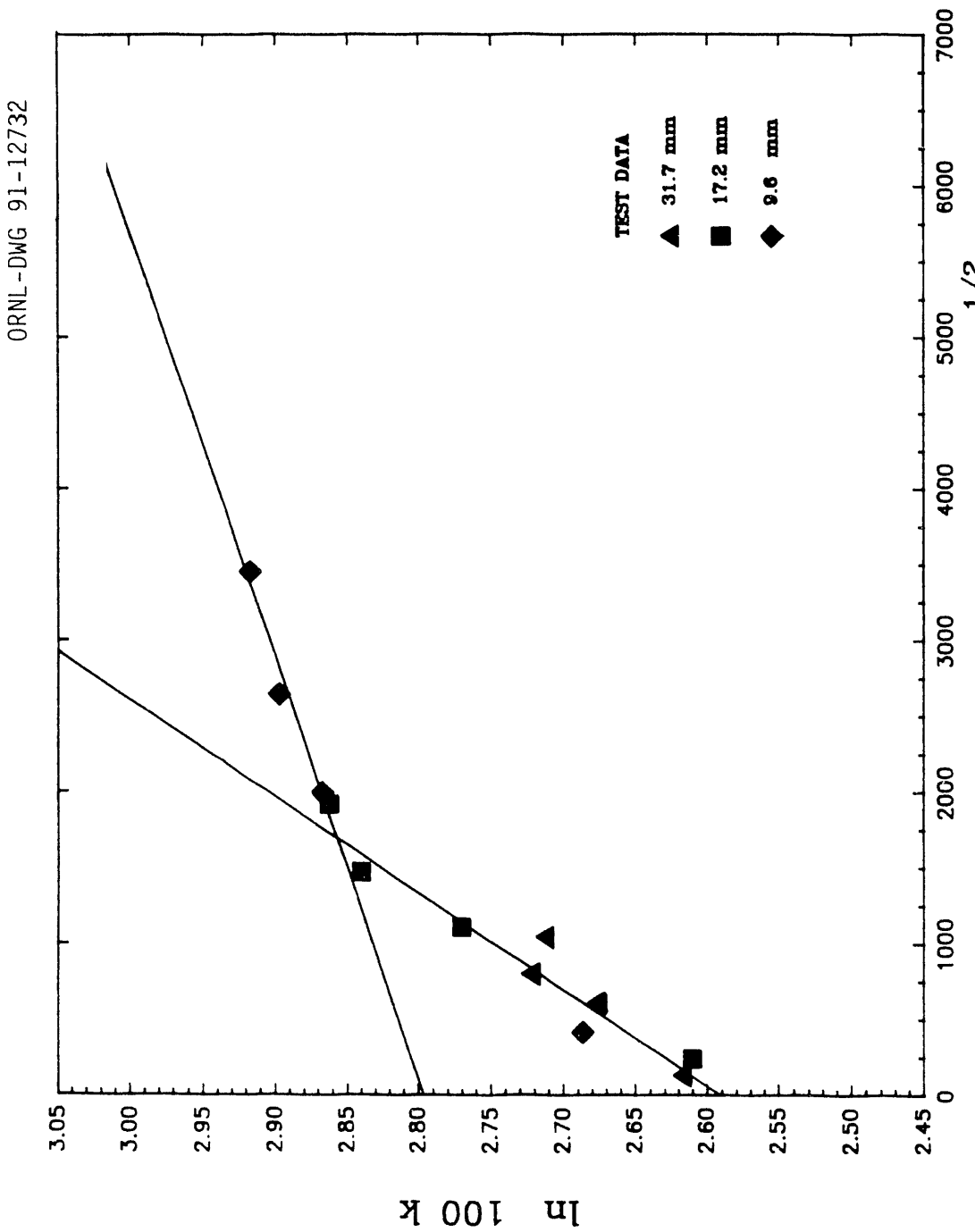

Fig. 15. Increase in k (75°F) for thin specimens of rigid board foamed with a 50/50 blend aging at 75°F.

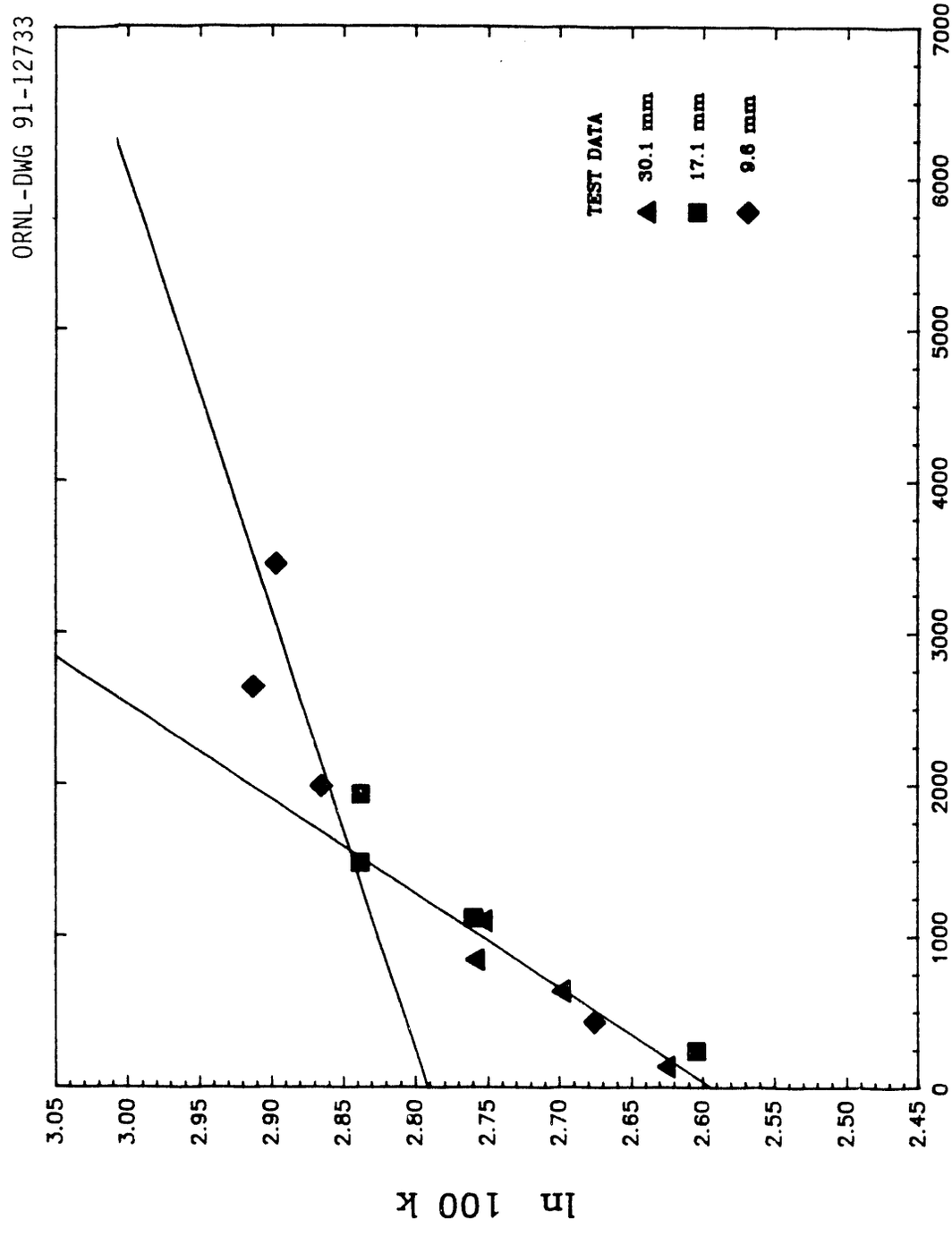

Fig. 16. Increase in k (75°F) for thin specimens of rigid board foamed with a 65/35 blend aging at 75°F.

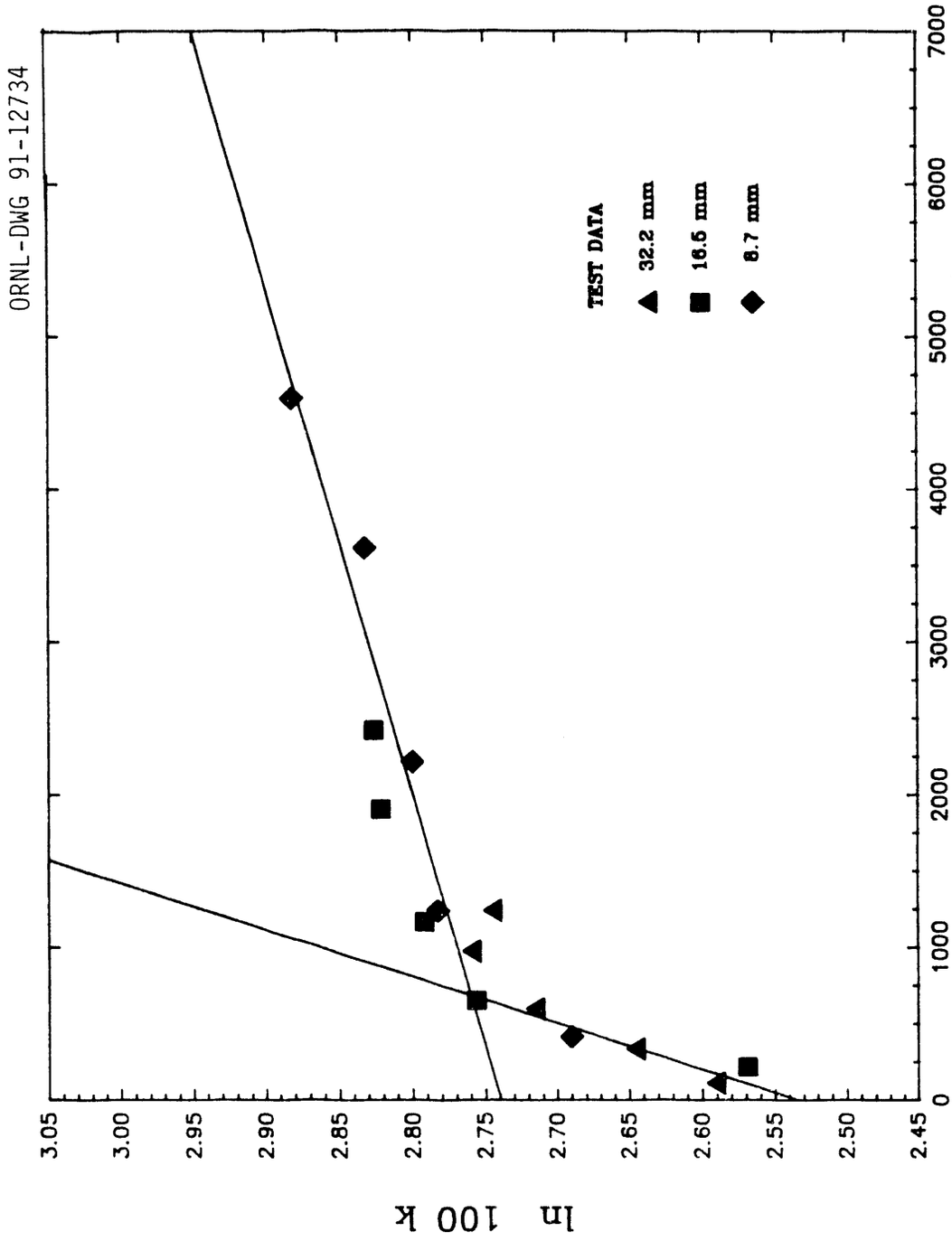

Fig. 17. Increase in k (75°F) for thin specimens of rigid board ic ..ed with CFC-11 blend aging at 150°F.

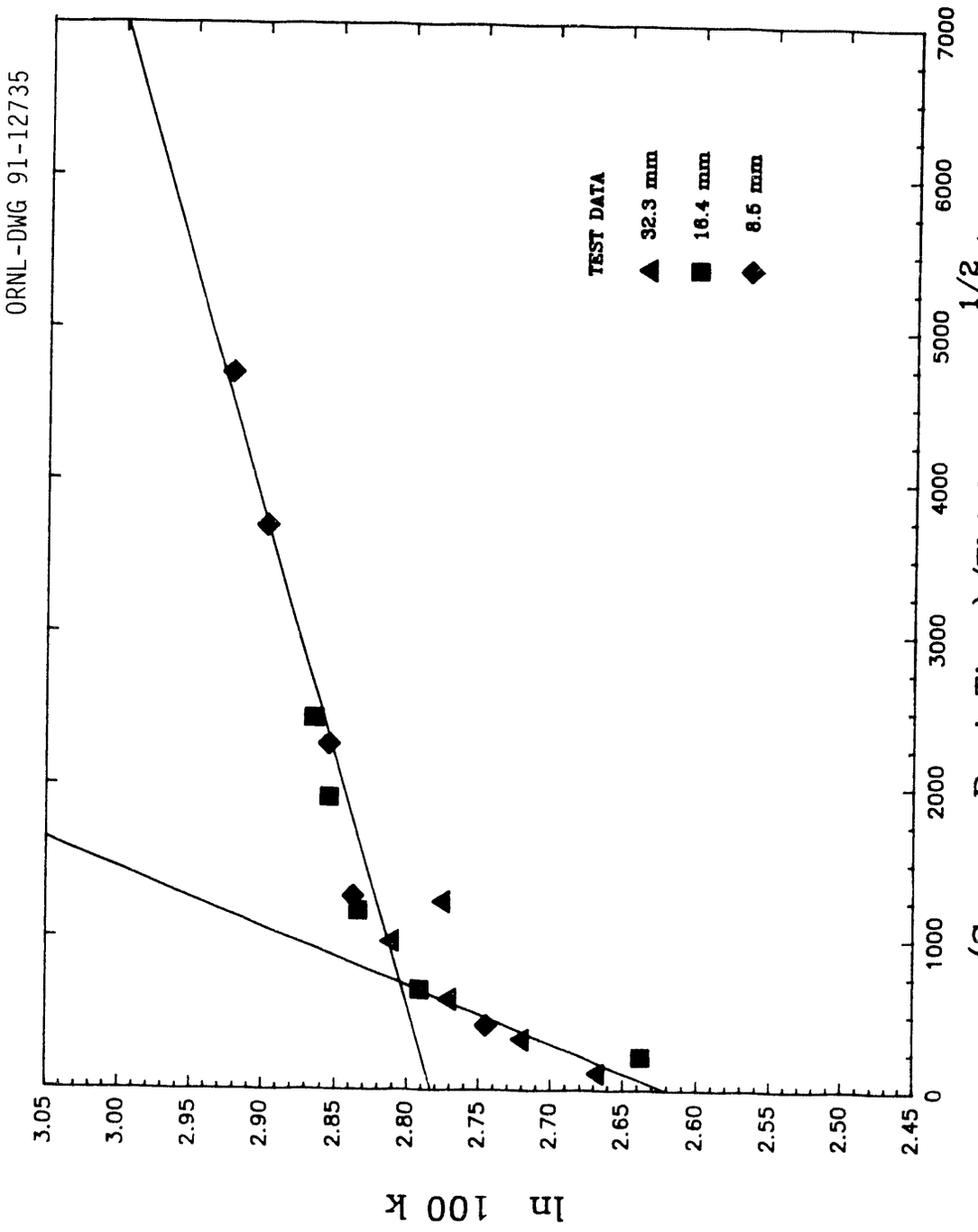

Fig. 18. Increase in k (75°F) for thin specimens of rigid board foamed with HCFC-123 aging at 150°F.

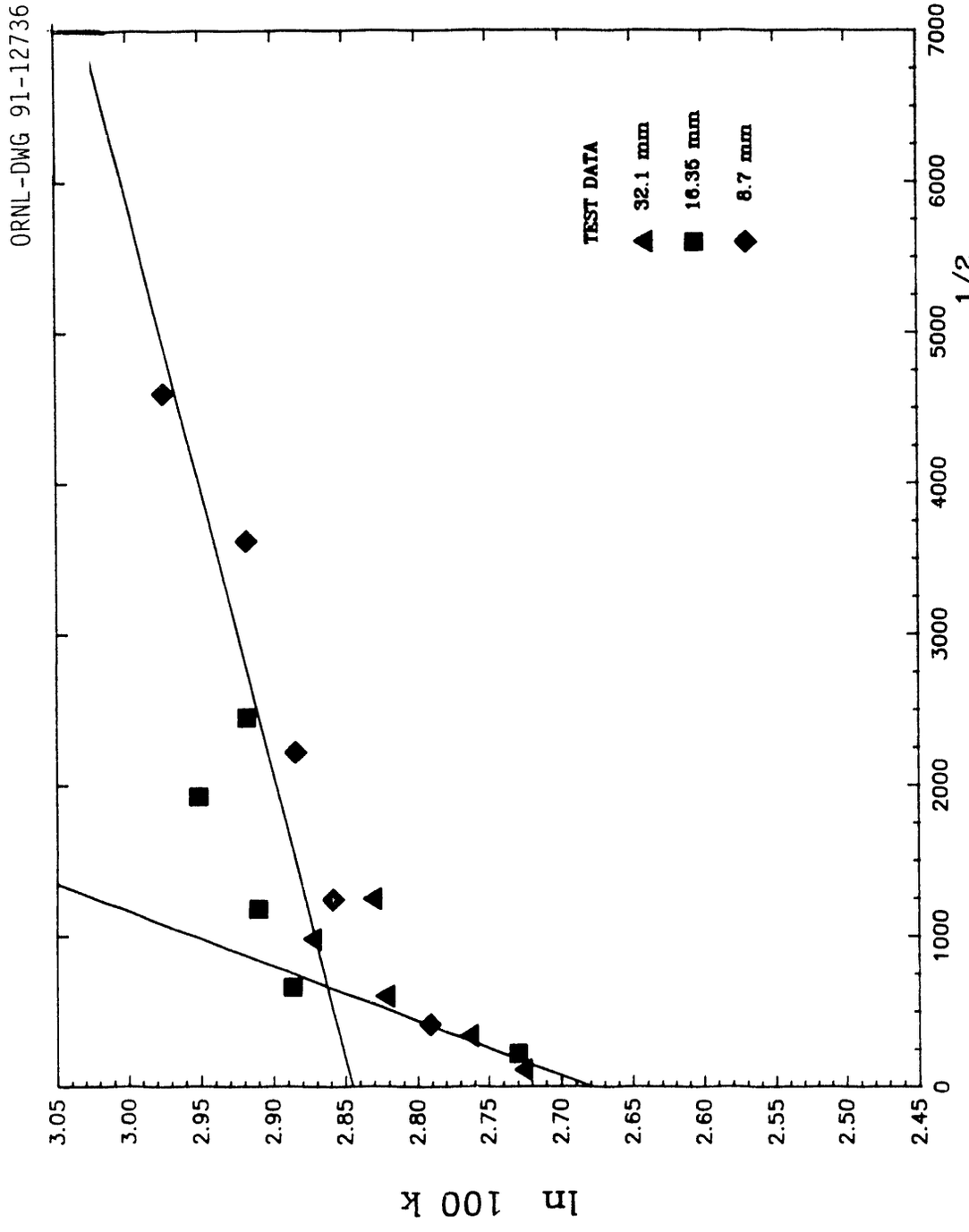

Fig. 19. Increase in k (75°F) for thin specimens of rigid board foamed with HCFC-141b aging at 150°F.

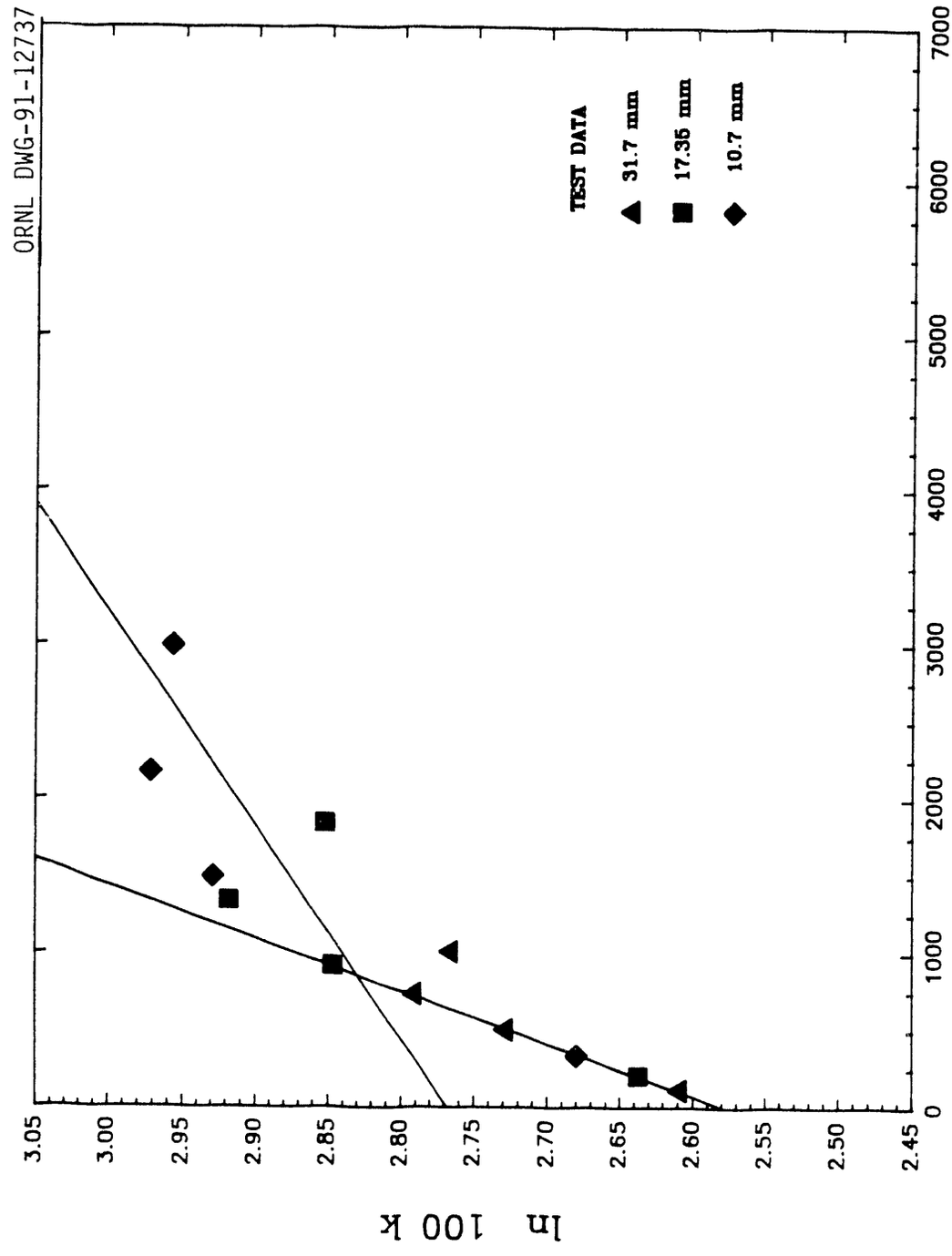

Fig. 20. Increase in k (75°F) for thin specimens of rigid board foamed with a 50/50 blend aging at 150°F.

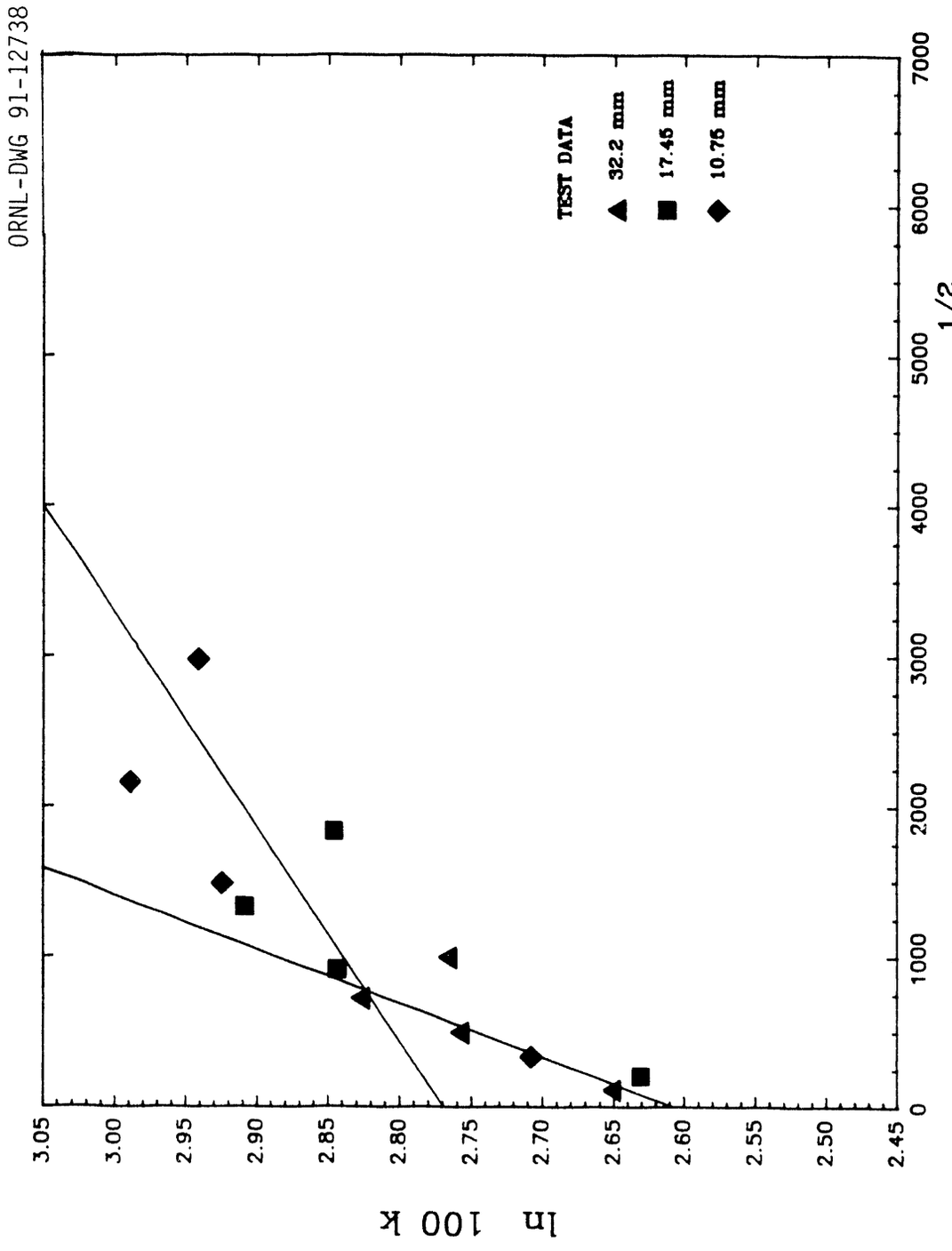

Fig. 21. Increase in k (75°F) for thin specimens of rigid board foamed with a 65/35 blend aging at 150°F.

Table 16. Summary of data fits by a least-squares method

Blowing agent	Region	A	B × 10^4	Number of data points	Average deviation (%)	Intercept k (Btu in./h ft^2·°F)
Specimens aging at 75°F						
CFC-11	1	2.4897	1.230	12	0.65	0.1206
	2	2.6892	0.2063	6	0.39	0.1472
HCFC-123	1	2.5808	1.218	12	0.41	0.1321
	2	2.7820	0.1643	6	0.57	0.1615
HCFC-141b	1	2.6386	1.1437	12	0.52	0.1399
	2	2.8266	0.1329	6	0.54	0.1689
50/50 Blend	1	2.5905	1.5692	8	0.63	0.1344
	2	2.796	0.3582	4	0.11	0.1638
65/35 Blend	1	2.5936	1.6070	8	0.56	0.1338
	2	2.7911	0.3462	4	0.60	0.1630
Specimens aging at 150°F						
CFC-11	1	2.5334	3.2829	6	0.64	0.1260
	2	2.7394	0.3015	9	0.51	0.1547
HCFC-123	1	2.6205	2.6102	6	0.57	0.1374
	2	2.7829	0.3087	6	0.40	0.1616
HCFC-141b	1	2.6789	2.7556	6	0.49	0.1457
	2	2.8449	0.2641	9	0.83	0.1720
50/50 Blend	1	2.5784	2.9327	6	0.08	0.1317
	2	2.7680	0.7231	6	1.75	0.1593
65/35 Blend	1	2.6067	2.7907	6	0.64	0.1355
	2	2.7696	0.7013	6	1.88	0.1595

Table 17. Effective diffusion coefficients derived from aging tests (cm^2/s): D_1 (air components), D_2 (blowing gas)

	$D_1 \times 10^8$	$D_2 \times 10^{10}$	D_1/D_2	D_1 (150)/D_1 (75)	D^2 (150)/D_2 (75)
MIT model (CFC-11)	18.78	9.23	203.5		
75°F					
CFC-11	1.51	4.26	35.4	7.1	2.1
HCFC-123	1.48	2.70	54.8	4.6	3.5
HCFC-141b	1.31	1.77	74	5.8	3.9
50/50	2.46	12.83	19.2	3.5	4.1
65/35	2.48	11.99	21.5	3.0	4.1
150°F					
CFC-11	10.78	9.09	118		
HCFC-123	6.81	9.53	71		
HCFC-141b	7.59	6.98	109		
50/50	8.60	52.3	16.4		
65/35	7.79	49.2	15.8		

for aging at 75° F show D_2 values significantly lower than the D_1 values. The D_2 values range from 1.8 to 4.3 × 10^{-10} cm^2/s for the individual gases and are above 12 × 10^{-10} cm^2/s for the blends. The D_2 values for aging at 150° F are 2 to 4 times larger than the D_2 values for aging at 75° F. Some evidence exists that the D_2 values for the foams aging at 75° F are lower for the more complex alternative blowing agents [i.e., D_2 (HCFC-123 and HCFC-141b) < D_2 (CFC-11)]. The ratio of the D_1 to D_2 values ranges from 20 to 75 at 75° F and from 15 to 100 at 150° F. The blends have the lower D_1/D_2 values at both temperatures. The D_1 values appear to be relatively firm, and as aging proceeds, more tests will help define D_2 values better. The D values are a clear reflection of the foam structural properties and the diffusing species and may be a guide to optimizing boardstock. The D_1 values at 75° F do decrease with increasing cell wall thickness.

Figure 22 is a plot of the D_1 and D_2 values obtained at 75° F (297 K) and 150° F (338.6 K) as a function of 1/T (K). This is an Arrhenius plot used to obtain the activation energy ΔH for chemical processes such as gaseous diffusion, using

$$D = D_o \exp - \Delta H/RT , \qquad (9)$$

where D_o is a jump frequency, cm^2/s, R is the gas constant, 1.987 cal/mol K, ΔH is the activation energy, cal/mol, and T is the absolute temperature, K.

Table 18 gives the activation energy values and D_o values for Region 1 and Region 2 processes.

Table 18. Activation energies for Region 1 and Region 2 derived from effective diffusion coefficients

Region 1	Activation energy (cal/mol)	Jump frequency (jumps/s × 10^4)
CFC-11	9434	1321
HCFC-123	7326	36
HCFC-141b	8432	210
50/50 blend	6007	6.5
65/35 blend	5304	2.0
Region 2		
CFC-11	3638	0.002
HCFC-123	6054	0.007
HCFC-141b	6586	0.12
50/50 blend	6745	1.18
65/35 blend	6777	1.16

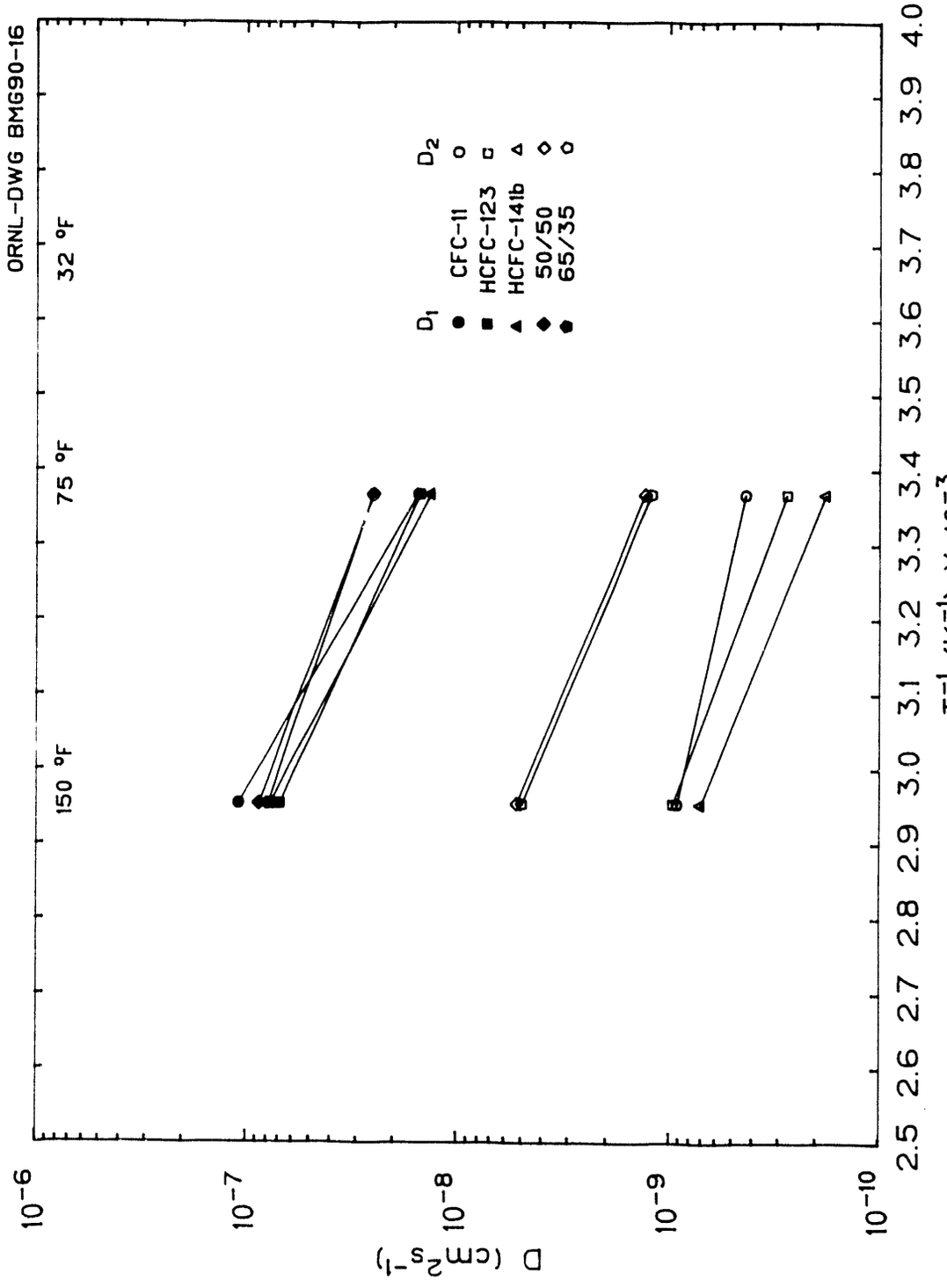

Fig. 22. Effective diffusion coefficients as a function of absolute temperature.

The ΔH values for Region 1 are near 8 k cal/mol and for Region 2 are near 6 k cal/mol. The jump frequency for Region 1 is greater than for Region 2.

6.2 EFFECTIVE k-VALUES OF FOAMS

The constants, A, given in Table 16 can be used to obtain the intercept values k_1 and k_2 for Regions 1 and 2. These values are given in Table 16. The values of k_1, the initial k of the foam, can be used to compare the impact of the blowing agents before any aging occurred. The 75° F aging results show that the order of k_1 values from low to high are CFC-11, HCFC-123 (9%), 50/50 (11%), 65/35 (11%), and HCFC-141b (15%), where the value in parentheses is the percent increase in k over that of the foam blown with CFC-11. The 150° F aging results suggest a slightly different order (i.e., the blends are lower in k than the HCFC-123). Both data sets suggest that the blends have very similar k-values.

It has been suggested[14,27] that the k of a 2-lb/ft^3 fresh (unaged) foam can be calculated by adding the blowing gas k and a constant term, 0.073 Btu·in./h·ft^2·° F, to represent the solid and radiation conduction contribution to k. Table 19 shows that this calculation overestimates k_1, but the percent difference between k (calculated) and k_1 is less than 10%. An alternative calculation is to subtract k(gas) from k_1 and associate the difference with k(solid) + k(radiation). Table 19 shows that the result of doing so yields an average value of 0.064 for the prototypical foams being tested in this project.

Table 19. Calculated k (75) for unaged foams for various gases

Gas	Gas k	k calculated	Difference[a] (%)	k_1-k(g)	E (ft^{-1})
CFC-11	0.057	0.130	-7.8	0.064	523
HCFC-123	0.072	0.145	-9.8	0.060	558
HCFC-141b	0.070	0.143	-2.2	0.070	480
50/50	0.071	0.144	-7.9	0.062	540
65/35	0.0713	0.144	-6.9	0.063	532
				0.064	527

[a] $100 \times [k_1 - k \text{ (calculated)}]/k_1$.

If half of this contribution is assigned to the radiation contribution,[14] and if this is described by the Rosseland approximation,[28,29]

$$k(rad) = \frac{16}{3} \times \frac{\sigma n^2 T^3}{E} , \qquad (8)$$

where σ is the Stefan-Boltzmann constant, n is the index of refraction and a value of 1 was used, and E is the extinction coefficient, ft^{-1}, then the E-values in Table 19 can be computed from Eq. 8. The average E-value is 527 ft^{-1}. Theory predicts a value of about 900 ft^{-1} for a foam density of 1.95 lb/ft^3 and a cell size of 0.2 mm.[26] This E-value would be obtained if 30% of k(radiation) + k(solid) had been associated with k(radiation) instead of 50%, as suggested for polystyrene.[30]

The accelerated aging test results from this study can be used to predict the thermal resistivity (r, where r = 1/k) at 75°F as a function of aging time at 75 or 150°F for 1.5-in.-thick unfaced prototypical foamboards. Table 20 shows initial and predicted r-values for 1, 2, and 5 years; these correspond to values of $t^{1/2}/h$, $(d)^{1/2}/mm$, of 0.50, 0.71, and 1.12, respectively, for a 38.1-mm thickness. The predicted r-values decrease with time at 75°F but exceed 5.7 $h \cdot ft^2 \cdot °F/Btu \cdot in.$ for the individual gas-blowing agents tested. This value exceeds the minimum stabilized r-value of 5.6 for unfaced polyurethane (PUR) or PIR foams stated by the SPI Industry assessment.[31] The blends reach an r-value of 5.4 at 5 years. The predicted 75°F r-values decrease with time at 150°F and reach lower r-values than when aged at 75°F. All of the values reported in Table 20 are within the existing accelerated aging data set (i.e., these are interpolated values). As Table 13 shows, the longest exposure time is 290 d for the initially produced boardstock. Additional thin-specimen test data will allow Table 20 to be completed for longer times. The results given in Table 20 show that thin-specimen aging is a promising accelerated aging procedure and provides a positive response to the key question of this program: the blowing agents tested in these prototypical experimental boards exhibit a long-term thermal performance at 75°F that is within 7 to 15% (average 11.6%) of that obtained by CFC-11 under similar conditions.

Table 20. Predicted thermal resistivity at 75°F for unfaced 1.5-in.-thick prototypical foamboards aged at 75 and at 150°F

	Initial		Aging time (years)		
Blowing agent at 75°F	k_1	r[a]	1 r(1)[b]	2 r(2)	5 r(5)
At 75°F					
CFC-11	0.121	8.29	6.90	6.51	6.35
HCFC-123	0.132	7.58	6.31	5.98	5.87
HCFC-141b	0.140	7.14	6.02	5.76	5.67
50/50	0.133	7.52	5.93	5.67	5.43
65/35	0.134	7.46	5.87	5.71	5.47
At 150°F					
CFC-11	0.126	7.94	6.18	6.07	5.85
HCFC-123	0.137	7.30	5.91	5.80	5.59
HCFC-141b	0.146	6.85	5.89	5.50	5.33
50/50	0.132	7.58	5.63	5.40	4.95
65/35	0.136	7.35	5.64	5.42	4.98

[a] $h \cdot ft^2 \cdot °F/Btu \cdot in.$
[b] Number in parentheses indicates years.

7. MODELING OF AGING PHENOMENA IN FOAMBOARD INSULATIONS

7.1 BACKGROUND

The reduction in the thermal resistance with time of foamboard insulations produced with a gas other than air is primarily a result of changes in cell-gas composition caused by the inward diffusion of oxygen and nitrogen and the outward diffusion of the low-conductivity gas used to produce the foamboard. The gas used to produce foamboard insulations is selected for low thermal conductivity, favorable handling characteristics, flammability, toxicity, and corrosiveness. The inward and outward diffusion of gases changes the cell-gas composition with the result that the gas-phase thermal conductivity increases with time. The cell-gas eventually becomes air, and the limiting thermal resistance for a foamboard insulation with permeable surfaces is that of an air-filled foam.

During the aging process the cell-gas composition at any time, t, is a function of position, C (x, y, z, t). Since the thermal conductivity of a gas mixture, k_g, can be calculated from pure component properties, the k_g of the cell-gas is a function of spatial coordinates (x, y, z) and time (t). A primary objective, therefore, of the foam-modeling effort is to obtain C (x, y, z, t) from which k_g (x, y, z, t) is derived. The k_g is added to the solid-phase conductivity, k_s, and a radiative term, k_r, to obtain the apparent thermal conductivity of the foam, k. This final quantity can then be compared with experimental measurements of k.

The apparent thermal conductivity of a foamboard, k, is approximated by the sum of the major contributors to the total heat flux (i.e., gas-phase conduction, solid-phase conduction, and diffusive radiation):

$$k = k_g + k_s + k_r \tag{9}$$

Convective transport is neglected because the cell dimensions are usually of the order of fractions of millimeters. "Shine-through" radiative transport is neglected, since there are generally a large number of cell walls and struts between any two parallel surfaces, and direct radiation is highly attenuated even though the cell-wall transmission may be high. The solid-phase contribution to the total heat flux depends on the thermal conductivity of the solid polymer, k_p, making up the cell walls and struts, the arrangement of walls and struts, and dimensions. The assumption that k_s is constant is reasonable although a possibility exists that k_s changes because of exposure to the environment and that cell dimension changes or material distribution changes because of thermal or mechanical stresses. The solid-phase thermal conductivity has been related to k_p by Glicksman.[32] The radiative term, k_r, is also taken to be constant although it can change for the same reasons as k_s. The k_r depends on the radiative properties of the foam and the arrangement of material in the direction of heat flow. Glicksman[32] has proposed the Rosseland expression[29] for k_r with an experimentally determined extinction coefficient, E. An important input for the foam modeling effort is reliable data for k_p and E so that representative k_s and k_r can be calculated. An alternative approach is to take the sum

$k_s + k_r$ to be an adjustable parameter equal to $k - k_g$. Since k can be measured and k_g can be determined from a model, the approximation $k_s + k_r$ equal a constant can be tested.

There are at least two approaches to obtaining C (x, y, z, t). The first is to treat the foamboard as a continuum and solve Eq. (10) subject to appropriate initial and boundary conditions for each of the diffusing species:

$$\frac{\partial c}{\partial t} = \frac{\partial}{\partial x}\left(D_x \frac{\partial c}{\partial x}\right) + \frac{\partial}{\partial y}\left(D_y \frac{\partial c}{\partial y}\right) + \frac{\partial}{\partial z}\left(D_z \frac{\partial c}{\partial z}\right) . \tag{10}$$

The pressures and temperatures generally encountered in foams are such that ideal gas behavior can be assumed. If, in addition, the temperature variation is small and directional effects are absent, then Eq. (10) is reduced to Eq. (11), and concentration can be replaced by partial pressure:

$$\frac{\partial c_i}{\partial t} = D_i \nabla^2 C_i \quad or \quad \frac{\partial P_i}{\partial t} = D_i \nabla^2 P_i . \tag{11}$$

Equation (11) forms the basis for the "DOW" model[33] and a model programmed by Destephen.[34]

A solution of Eq. (11) is obtained for each gas species present in the foamboard on the assumption that the diffusing species do not interact in the solid phase. The P_i are used to calculate mole fractions that, in turn, are used to calculate k_g (x, y, z, t). The use of a continuum model is justified if the largest cell dimension is much smaller than the least foamboard dimension. When this is the case, the discrete diffusions across cell walls can be "smeared" to a continuum much like the diffusive approximation for radiative transport. Important practical steps in this process involve obtaining D from permeability data, Pe_i, and obtaining k_g from pure component data.

Equation (11) can be solved by separation of variables and a Fourier series description of the spacial part of the solution. The treatise by Carslaw and Jaeger[35] contains numerous solutions for the one-dimensional form of Eq. (11) that can be used to obtain solutions for the three-dimensional form of the equation using the principle of superposition. This approach has been used by Sheffield[33] and Destephen.[34]

Equation (11) can also be solved by finite difference methods,[36] but this method seems to be unnecessary for the geometries and boundary conditions being considered. The evaluation of the infinite series expressions that are part of the analytical solutions can be performed more economically than the finite difference calculations in many cases.

The second approach to obtaining C (x, y, z, t) is to model gas transport between cells in series. This approach tends to retain the discrete nature of the diffusion process. Ostrogorsky[9] has used this approach to develop a solution in one-dimension, C (x, t). The use of the one-dimensional model is applied to relatively thin foamboards that do not have diffusion barriers on the surface. The diffusion of gases from the edges of the foamboard are neglected in this model. In this case the gas-phase partial pressures can be described by an implicit numerical method that results in a tridiagonal matrix that can be inverted using the Thomas Algorithm[37] to obtain P_i (x, t). The numerical solutions for P_i are combined to calculate C_i and k_g. This approach has been programmed[9] in Fortran and adapted for use at ORNL. The program is not generally executed to obtain gas compositions in individual cells but rather divides the foamboard into a specified number of regions that are treated as cells (pseudo-cells). The numerical solutions for C (x, t) are used to calculate k (x, t) by use of mixture equations.[38,39] The Lindsey-Bromley equation is recommended.[32,40] The Lindsey-Bromley equation requires viscosity data for the components in the mixture as well as thermal conductivities, and these data are not always available. The minimum input required for a k_g calculation is pure component thermal conductivities and chemical composition.

Appendix C contains a Fortran code, KMIX. FOR, for calculating the thermal conductivity of gaseous mixtures from the thermal conductivity of the components, the molecular weight of the components, and the composition.[39] KMIX gives the result that the thermal conductivity of a gas mixture falls below a value that would be predicted from a "rule of mixtures" type calculation. This is shown in Fig. 23, in which the thermal conductivities at 75° F of air + CFC-11, air + CFC-12, air + HCFC-141B, and air + HCFC-123 are shown as functions of the mole fraction of air. The curves were calculated for mixtures of N_2, O_2, and the indicated gas. Table 21 contains the numerical output used to establish the curves in Fig. 23. At present, the program KMIX is

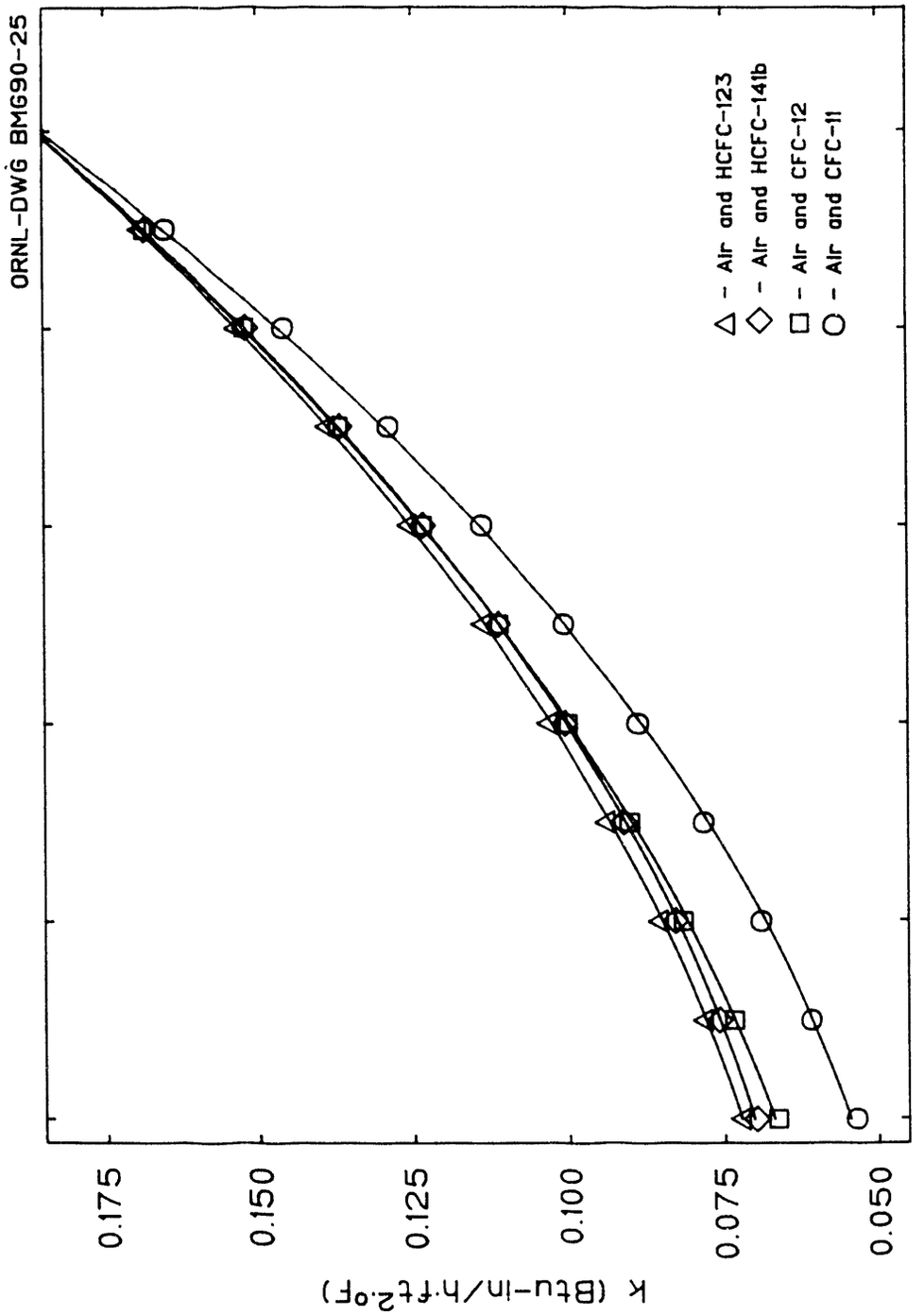

Fig. 23. The k for air-CFC/HCFC mixtures at 75°F calculated using KMIX.FOR.

Table 21. Values for k of gas mixtures containing air and refrigerant at 75°F calculated with KMIX.FOR

	k W/mK (Btu in./ft^2 h °F)			
Mole fraction air	With CFC-11	With CFC-12	With HCFC-123	With HCFC-141b
0.0	0.00775 (0.0537)[a]	0.00958 (0.0664)	0.01038 (0.0720)	0.01008 (0.06988)
0.1	0.00879 (0.0609)	0.01058 (0.0734)	0.01125 (0.0780)	0.01093 (0.07578)
0.2	0.00997 (0.0691)	0.01171 (0.0816)	0.01229 (0.0852)	0.01194 (0.08285)
0.3	0.01130 (0.0783)	0.01299 (0.0901)	0.01348 (0.0935)	0.01313 (0.09103)
0.4	0.01281 (0.0888)	0.01443 (0.1000)	0.01484 (0.1029)	0.01450 (0.1005)
0.5	0.01452 (0.1007)	0.01603 (0.1111)	0.01638 (0.1136)	0.01605 (0.1113)
0.6	0.01644 (0.1140)	0.01780 (0.1234)	0.01809 (0.1254)	0.01779 (0.1233)
0.7	0.01860 (0.1290)	0.01976 (0.1370)	0.01999 (0.1386)	0.01973 (0.1368)
0.8	0.02104 (0.1459)	0.02192 (0.1520)	0.02208 (0.1531)	0.02189 (0.1518)
0.9	0.02379 (0.1649)	0.02430 (0.1685)	0.02438 (0.1690)	0.02428 (0.1683)
1.0	0.02691 (0.1866)	0.02691 (0.1866)	0.02691 (0.1866)	0.02691 (0.1866)

[a]Ref. 41.

configured for the calculation of thermal conductivities for gas mixtures containing any combination of the gases: He, Ar, Kr, Xe, H_2, N_2, O_2, CO_2, CFC-11, HCFC-123, HCFC-141B, CFC-12, and R-22.

A Fortran program for calculating the thermal conductivity of gas mixtures using the Lindsay-Bromley correlation, LB.FOR, is listed in Appendix D. The program as listed in Appendix D is for the calculation of mixtures of CO_2, O_2, N_2, and HCFC-22 at temperatures from 40 to 100°F. Input property data for LB.FOR consists of pure component thermal conductivities, normal boiling points, viscosity coefficients, and gas-mixture composition. Table 22 contains calculated k at 75°F for a three-component gas mixture containing N_2, O_2, and HCFC-22. Thermal conductivities calculated using KMIX.FOR are shown in the table for comparison. The differences between the calculated values for k_{mix} are greatest for air and air-rich mixtures. The thermal conductivity for air at 75°F calculated with LB.FOR is 0.02583 W/mK, while that obtained with KMIX.FOR is 0.02691. In both cases air was taken to be an O_2 - N_2 mixture with mole fraction O_2 of 0.21. The ASHRAE handbook[41] lists 0.02588 W/mK for the thermal conductivity of air at 75°F. The Lindsey-Bromley expression provides a slightly better result than the KMIX correlation for the thermal conductivity of air at 75°F (297.04 K).

Let us assume that k_g (x, y, z, t) or k_g (x, t) is available. The subsequent requirement is to obtain an average k_g that characterizes the gas-phase heat transport and can be substituted into Eq. (9) for k. At least three approaches can be used. The first is to integrate the expression for C (x, t) over the spatial coordinate to obtain an average composition from which k_g can be calculated. The second is to integrate k (x, t) over the spatial coordinate to obtain an average k_g, and the last is to consider individual cells or pseudo-cells as resistances in series. Sheffield[33] and Destephen[34] have used average C values, while Ostrogorsky[9] has used cell resistances in series to calculate the foamboard k. The adoption of methods for calculating k_g combined with expressions for k_s and k_r yields k (t) and thermal resistance R (t).

The programs generated by Destephen and Ostrogorsky have been configured to run on the ORNL computing system. Appendix E contains the program for Destephen's model, while Appendix F contains the Ostrogorsky model. Initial steps to implement the Dow model on the ORNL computer have been taken, and a copy of the Dow code has

Table 22. Calculated thermal conductivities at 297.04 K for gas mixtures containing N_2, O_2, and HCFC-22

Mole fraction air	(a) k (W/mk) using LB.FOR	(b) k (W/mK) using KMIX.FOR	(b)/(a)
0	0.01082	0.01086	1.0037
0.1	0.01199	0.01191	0.9933
0.2	0.01322	0.01307	0.9887
0.3	0.01452	0.01435	0.9883
0.4	0.01588	0.01574	0.9912
0.5	0.01732	0.01726	0.9965
0.6	0.01883	0.01890	1.0037
0.7	0.02044	0.02068	1.0117
0.8	0.02213	0.02261	1.0217
0.9	0.02393	0.02468	1.0313
1.0	0.02583	0.02691	1.0418

been requested. Destephen's code has been used to calculate k for a foamboard containing HCFC-22.[30,42] The "MIT" model[9] has been used to calculate k (t) for a number of cases. Results obtained with these two models will be discussed in the following paragraphs. The MIT model as modified for use at ORNL has been filed as MITB.FOR. The code MITB can be used to study the effect on k (t) of changing properties or conditions. The code has been used to simulate experimental results to test data treatment strategies. Simulated k (t) can be used to examine ways of labeling thermal performance, testing foamboard products, or changing the manufacturing process.

One important objective of the modeling effort is to provide meaningful thermal performance criteria for the consumer. The current practice[22] involves a thermal resistance evaluation 180 d after production. This approach may not be adequate because the product will normally be in use for many years. The use of a time-average k_d or time-average r-value is one alternate to the 180-d value that is in use at present. The time-average values can be determined from simulated k (t) or an empirically derived k (t):

$$k_d = k_d(t^*) = (1/t^*)\int_o^{t^*} k\,(t)\,dt \quad . \tag{12}$$

The t^* in Eq. (12) is the lifetime of the insulation that must be assigned to fix k_d. The result for k_d depends on the value selected for t^*. An empirical expression for k (t), Eq. (13), for a foamboard produced with HCFC-22 was used to calculate $k_d\,(t^*)/k\,(1/2)$ as a function of t^*.[30] The term k (1/2) is the apparent thermal conductivity obtained from the correlation at 180 d:

$$k(t) = k^{\infty} + (k^o - k^{\infty})\,e^{-\beta t} \quad . \tag{13}$$

Table 23 contains a few values for the ratio $k_d\,(t^*)/k\,(1/2)$ for the developmental product containing HCFC-22. The ratios in Table 23 indicate that the r-value of the foamboard is overstated by the 180-d values by as much as 10%.

Table 23. $k\,(t^*)/k\,(1/2)$ for an unfaced foamboard product initially containing HCFC-22

t* (years)	$k_d\,(t^*)/k\,(1/2)$
5	1.074
10	1.088
20	1.095
∞	1.103

Ratios were computed using $k^{\infty} = 0.2521$, $k^o = 0.1694$, $\beta = 2.557$ year^{-1}, and $k\,(1/2) = 0.2286$. The constant, β, is related to the time required for 50% of the product aging to take place ($t_{1/2}$) by the expression $t\,(1/2) = \beta^{-1}\,\ell n\,2$ (ref. 30).

Variation of the parameters in Eq. (13) shows that the ratio $k_d\,(t^*)/k\,(1/2)$ can exceed the value 1.10, as shown in Table 23. Calculated ratios as high as 1.219 indicate r-value overstatements as high as 21.9% in Table 24.

Table 24. Calculated values for the overstatement of r-value by the 180-d criteria

			$\{[k_d(t^*)/k(½)] - 1\} \times 100^a$	
k^∞	k^o	β (years^{-1})	$t^* = 5$	$t^* = 50$ (years)
0.15	0.10	2.0	10.2%	13.0%
		5.0	1.4	2.7
0.20	0.10	2.0	16.4	21.9
		5.0	2.2	4.1
0.20	0.14	2.0	9.1	12.1
		5.0	1.3	2.4

[a]The calculation assumes Eq. (13).

Figure 24 shows a result obtained with Destephen's model using k_r as an adjustable parameter.[30] The solid-phase contribution, k_s, was calculated in this case using a procedure suggested by Batty et al.[43] The calculated thermal resistivities indicated by solid curves in Fig. 24 were computed on the assumption that the diffusion coefficient for HCFC-22 equals that of CFC-12. The points in Fig. 24 represent measurements over time on foamboard specimens that were stored and repeatedly measured.

7.2 CALCULATIONS WITH THE MITB PROGRAM

The program MITB has been run for a variety of conditions to show the effect of specific properties on k (t). In all of the cases to be discussed, k_s and k_r were fixed at 0.019204 Btu·in./ft^2·hr·°F and 0.044371 Btu·in./ft^2·hr·°F, respectively. The permeability data were taken from Ostrogorsky,[9] and a uniform temperature of 76.7°F was assumed. The permeabilities from Ostrogorsky will be referred to as the "standard" values.* Figures 25 and 26 show calculated values for ℓn [100 k (t)] as a function of $\sqrt{t}/x$. This particular representation is shown because of the data analysis discussed

*D (O_2) = 46.79 × 10^{-8} cm^2/s; D (N_2) = 7.60 × 10^{-8} cm^2/s; and D (CFC-11) = 19.8 × 10^{-10} cm^2/s.

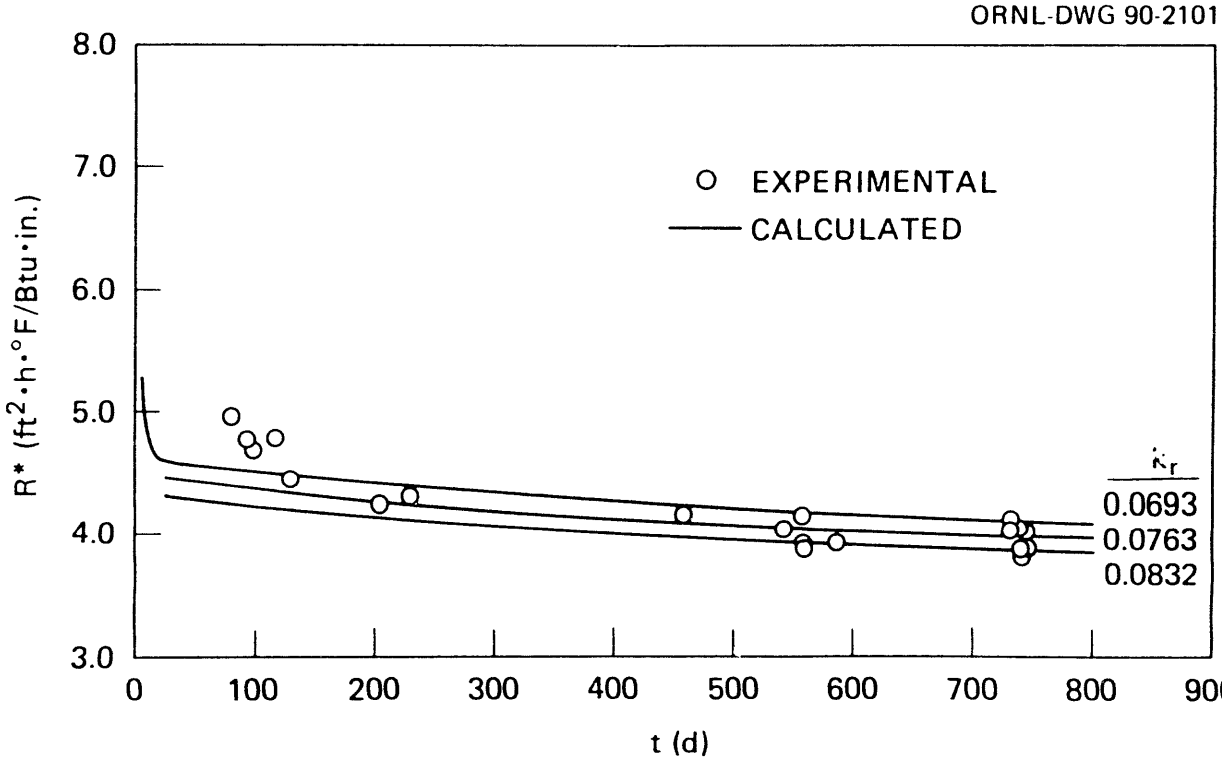

Fig. 24. R^* (t) for a closed-cell foamboard produced with HCFC-22 (k_r has units Btu·in./ft²·hr·°F).

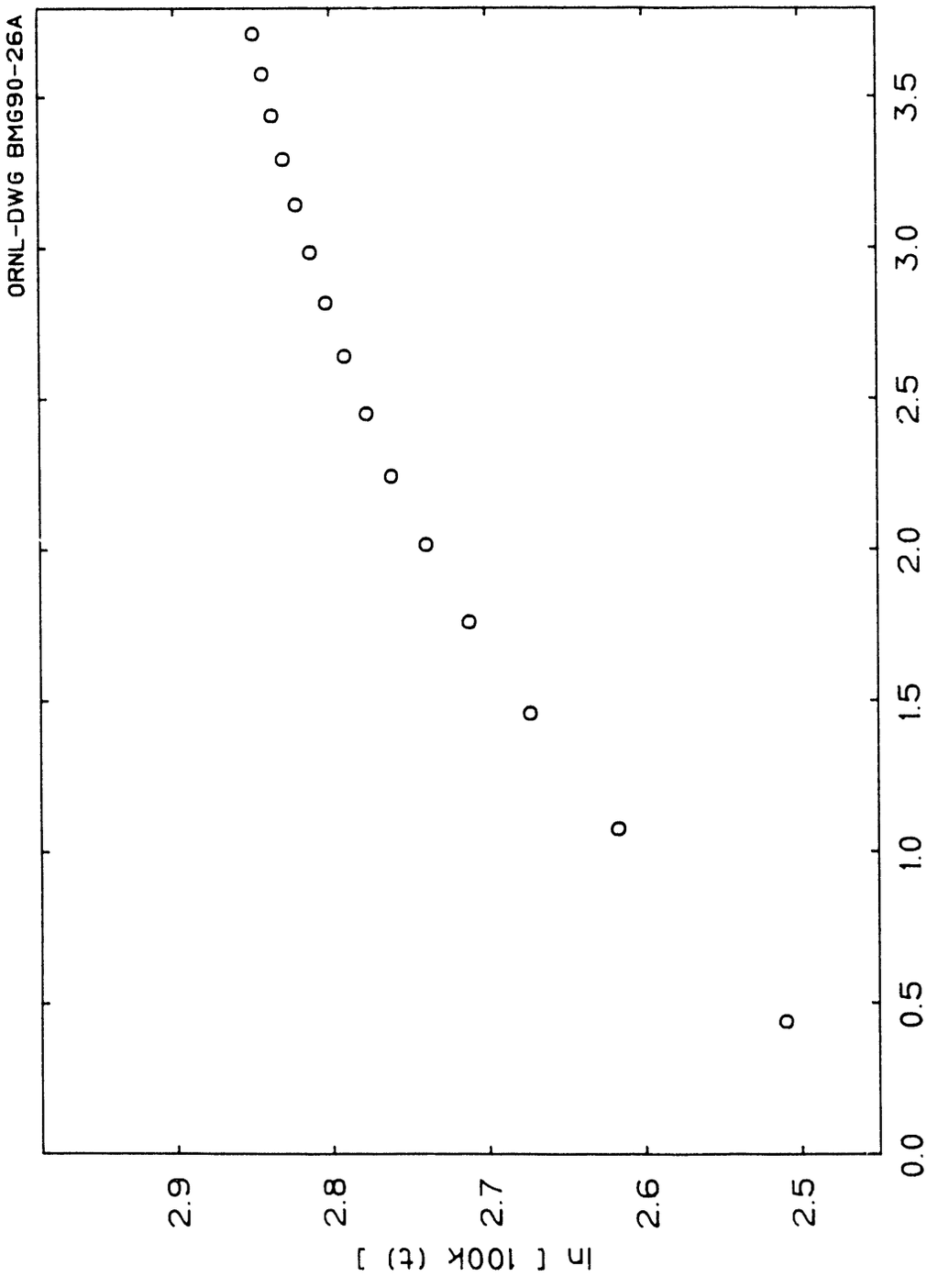

Fig. 25. The thermal conductivity as a function of time calculated with MITB for a 5.08-cm-thick foamboard produced with CFC-11. The initial aging period is shown.

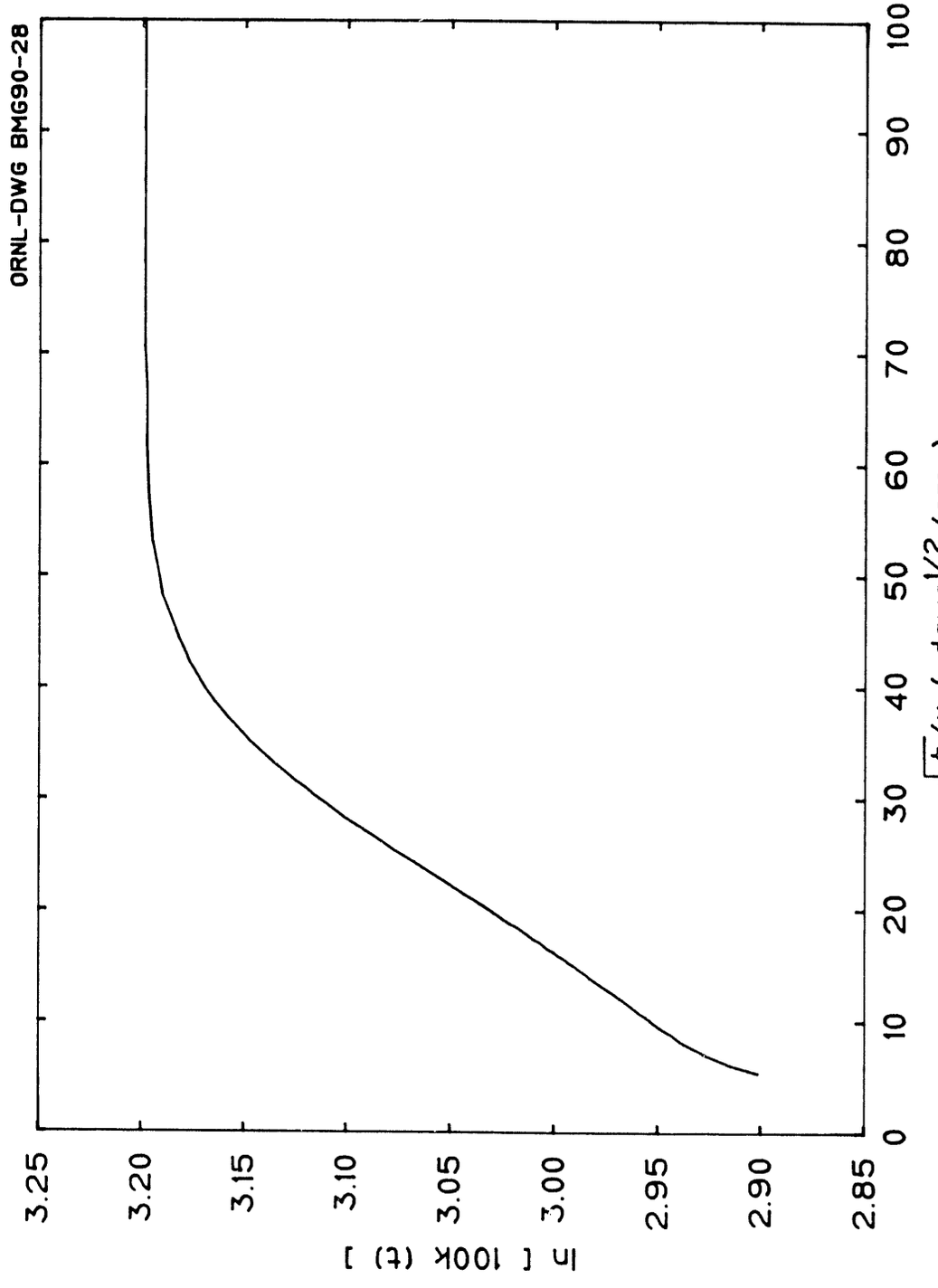

Fig. 26. The thermal conductivity as a function of time calculated with MITB for a 5.08-cm-thick foamboard produced with CFC-11. The long-term aging period is shown.

elsewhere in this report. The curves shown in Figs. 25 and 26 were computed using MITB with standard permeability data, CFC-11 as the foam gas, and 5.08 cm (2.0 in.) as the foamboard thickness. Figure 25 shows ℓn [100 k_a (t)] for $\sqrt{t/x}$ up to about 400 d. The 180-d value for $\sqrt{t/x}$ is 2.64, and k is 0.164. The calculated curve clearly shows that k (t) or ℓn [100 k (t)] has not attained a steady value at 180 d. Figure 26 extends the curve for k to $\sqrt{t/x}$ of 100. This calculation indicates a changing thermal resistance over long time periods. The horizontal scales in Figs. 25 and 26 differ by a factor of 10. The calculated results, however, show that the aging process extends over a long period of time even for the relatively thin specimen being modeled.

The calculated k shown in Figs. 25 and 26 was used to calculate diffusion coefficients by assuming that d [ℓn 100 k (t)]/d$\sqrt{t/x}$ equals D. The calculated values for ℓn [100 k (t)] for $\sqrt{t/x}$ for 1.078 (approximately 30 d) to 2.641 (approximately 180 d) were fit to a linear expression in $\sqrt{t/x}$ by the method of least squares. The slope of the line that was obtained was used to calculate a D of 14.17×10^{-8} cm^2/s, and this value was taken to be an average value for air. The diffusion coefficient data used to generate the curve were 46.79×10^{-8} cm^2/s for O_2 and 7.60×10^{-8} cm^2/s for N_2. If the composition of air is taken to be 0.21 mol fraction O_2 and 0.79 mol fraction N_2, then the average value for air based on mol fractions was 15.83×10^{-8} cm^2/s, a number that is about 12% greater than the value obtained by analysis of the calculated results. An application of the same procedure to calculate D_2 from k_a for $\sqrt{t/x}$ from 6.469 (about 3 years) to 25.06 $d^{1/2}/cm$ (about 44 years) was not as successful. The input value for the diffusion coefficient of CFC-11 was 19.83×10^{-10} cm^2/s, while the analysis of the calculated results gave 7.65×10^{-10} cm^2/s. Unfortunately, the D obtained from analyses of the calculated results is sensitive to the data set input to the least-squares calculation. A positive observation, however, is that the order-of-magnitude predicted for the D's is correct and that agreement may be sufficient for many purposes.

The output from MITB includes cell-gas pressures as a function of time. In the case of the "standard" data set and an unfaced foamboard thickness of 5.08 cm, the O_2 diffusion is essentially complete at about 200 d, while the N_2 diffusion continues for at least 350 d. This timing would suggest that the previous result for $t < 180$ d be interpreted as an air result. As with any such model, the program MITB can be used to study the effect on calculated quantities of changing input parameters. Figure 27 shows

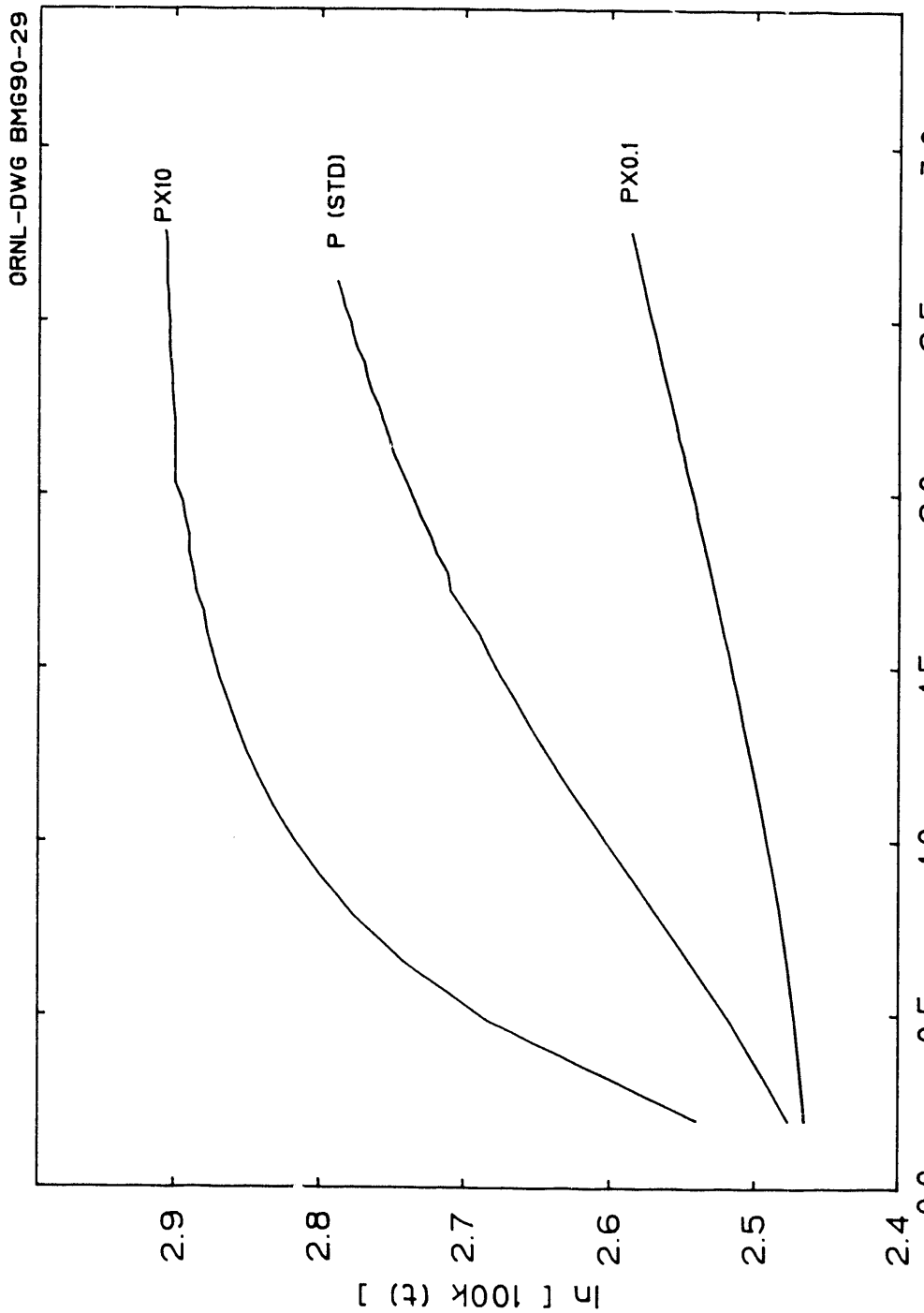

Fig. 27. Calculated values for ln [100 k (t)] for three air permeabilities.

early-time values for ℓn [100 k (t)] for three values of the permeability of O_2 and N_2. The permeability for the foaming gas, CFC-11, is the same for the three curves in Fig. 27, while the air component diffusion coefficients were increased and decreased by a factor of 10, P × 10 and P × 0.1. The three curves show the relatively large change that would occur in k measured at 180 d after manufacture ($\sqrt{t}/x = 2.64$) and, more importantly, they show that for a fast diffuser (P × 10) the 180-d value would be a more appropriate measure of thermal performance than for a slow diffuser (P × 0.1).

Figure 28 shows calculated k for relatively long times for a range of values for the permeability of the foaming gas. Air properties were held constant for the four curves shown in Fig. 28. The curve extends to $\sqrt{t}/x = 20$, which is about 28 years for x = 5.08. The curves are labeled to indicate the multiplier for the foam-gas permeability, P. A definite break in the slope of the curves indicates a change in the primary diffusing species. All four curves would eventually reach the same limiting value but, as shown by the figure, the time required is different. The average k for a finite age such as 20 years is significantly different, although the 180-d values for k are not significantly different. The curves converge at small time values because the dominant diffusing species is air, and the air permeability was the same for all four calculations.

An interesting observation results from running MITB for a sequence of thicknesses ranging from 2.54 cm (1 in.) to 30.48 cm (12 in.). Figure 29 shows k as a function of t for five foamboard thicknesses obtained using standard parameters. These results were used to calculate k(20) and κ(20)/k(1/2). Table 25 shows calculated results for the five thicknesses. The second entry in the table for 30.48 cm shows the effect of increasing the number of pseudo-cells used in the calculation from 11 to 21.

The ratios k(20)/k(1/2) shown in Table 25 exceed 1.24 and indicate a relative maximum for thicknesses near 30.48 cm. This maximum can be rationalized by examining the curves in Fig. 30. The lower curve, k(1/2), approaches a low-constant value for large thicknesses, since the fraction of a large specimen that is penetrated by air at 180 d is small. The upper curve, representing k(20), decreases for all thicknesses, as shown in Fig. 30. The two curves have the same value at thickness zero and thickness ∞, so a relative extrema in the difference between the two curves follows from Rolle's Theorem.

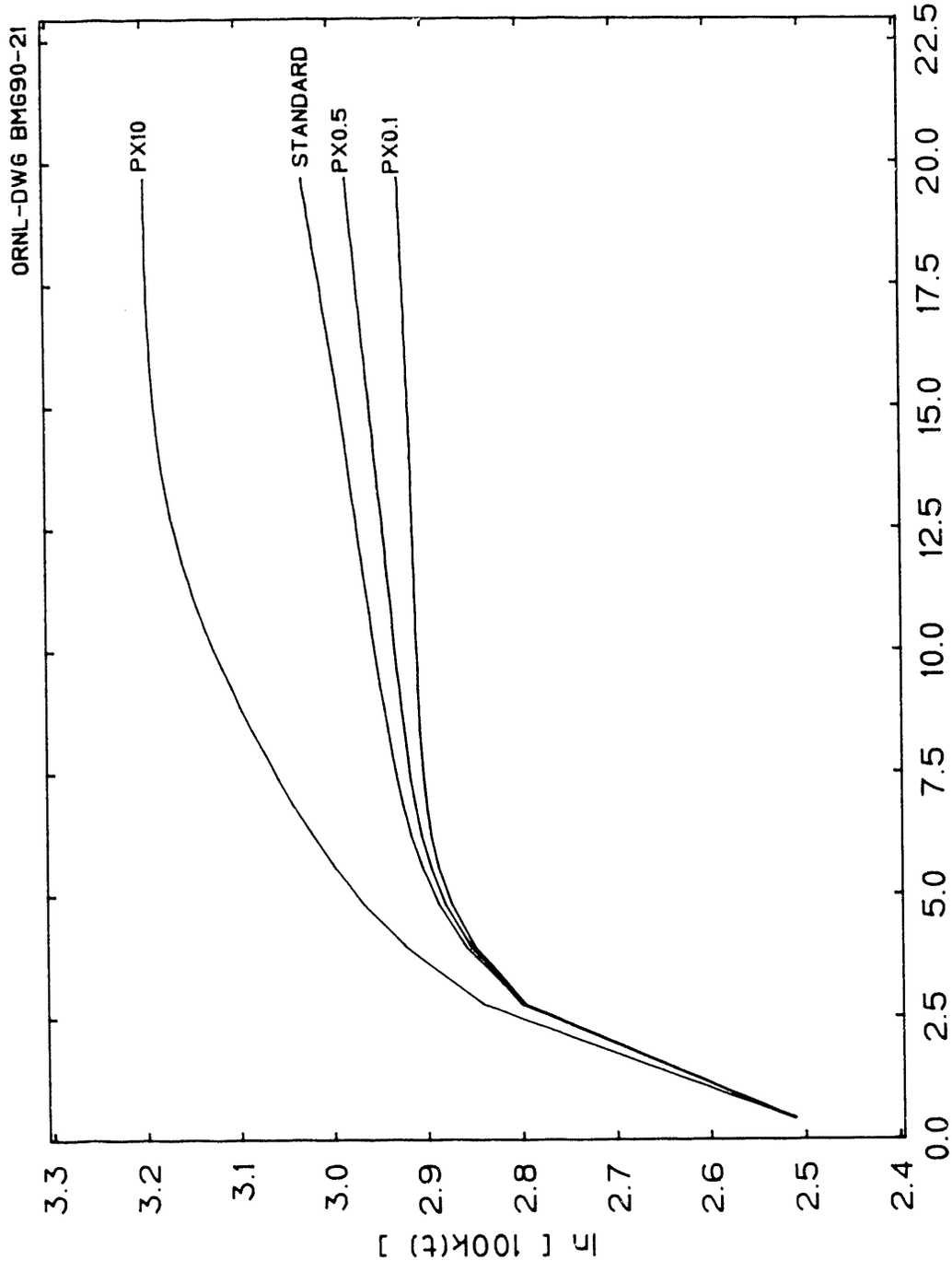

Fig. 28. Calculated values for ln [100 k (t)] for four values of the diffusion coefficient for CFC-11.

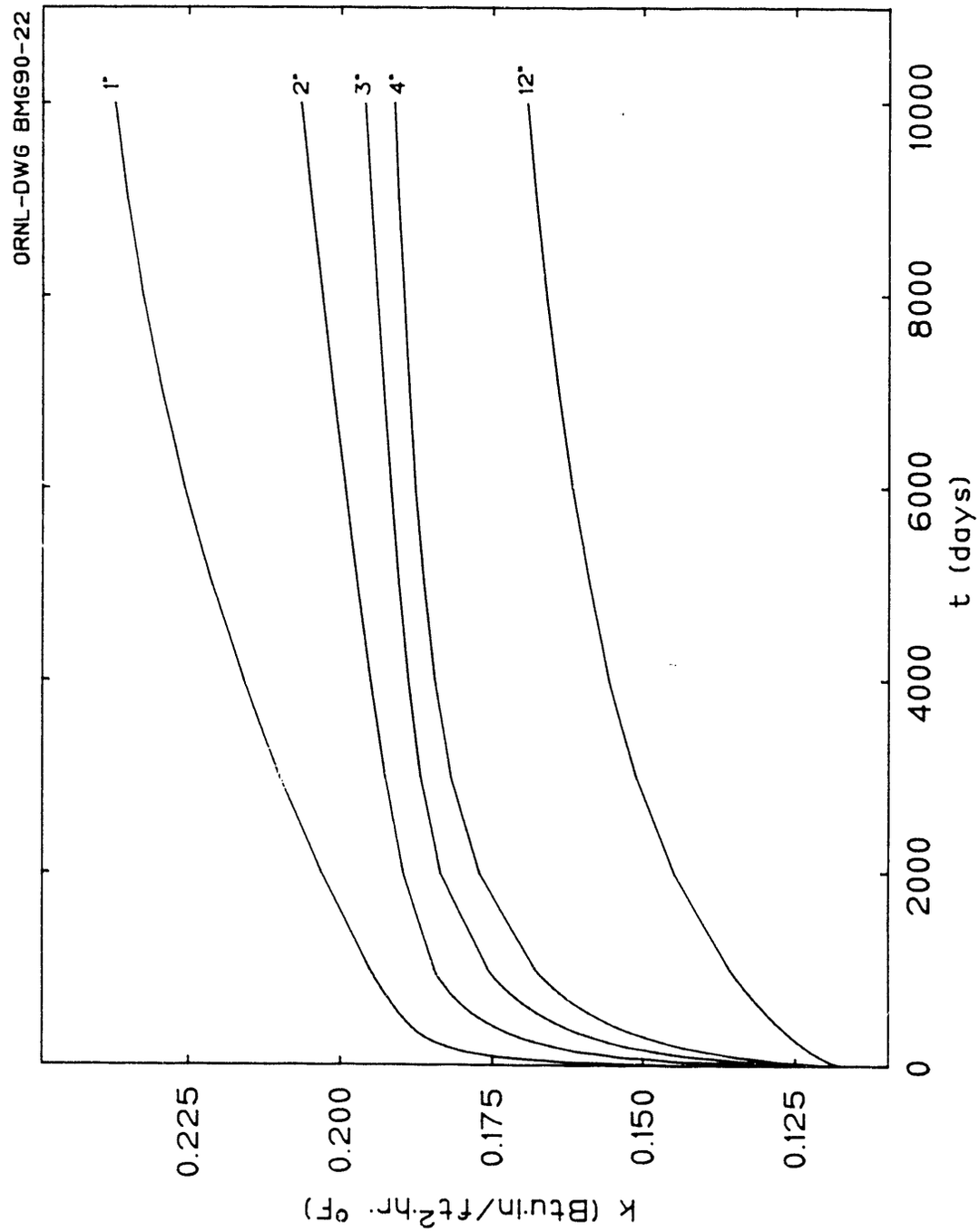

Fig. 29. Calculated k (t) for a foamboard insulation as a function of thickness.

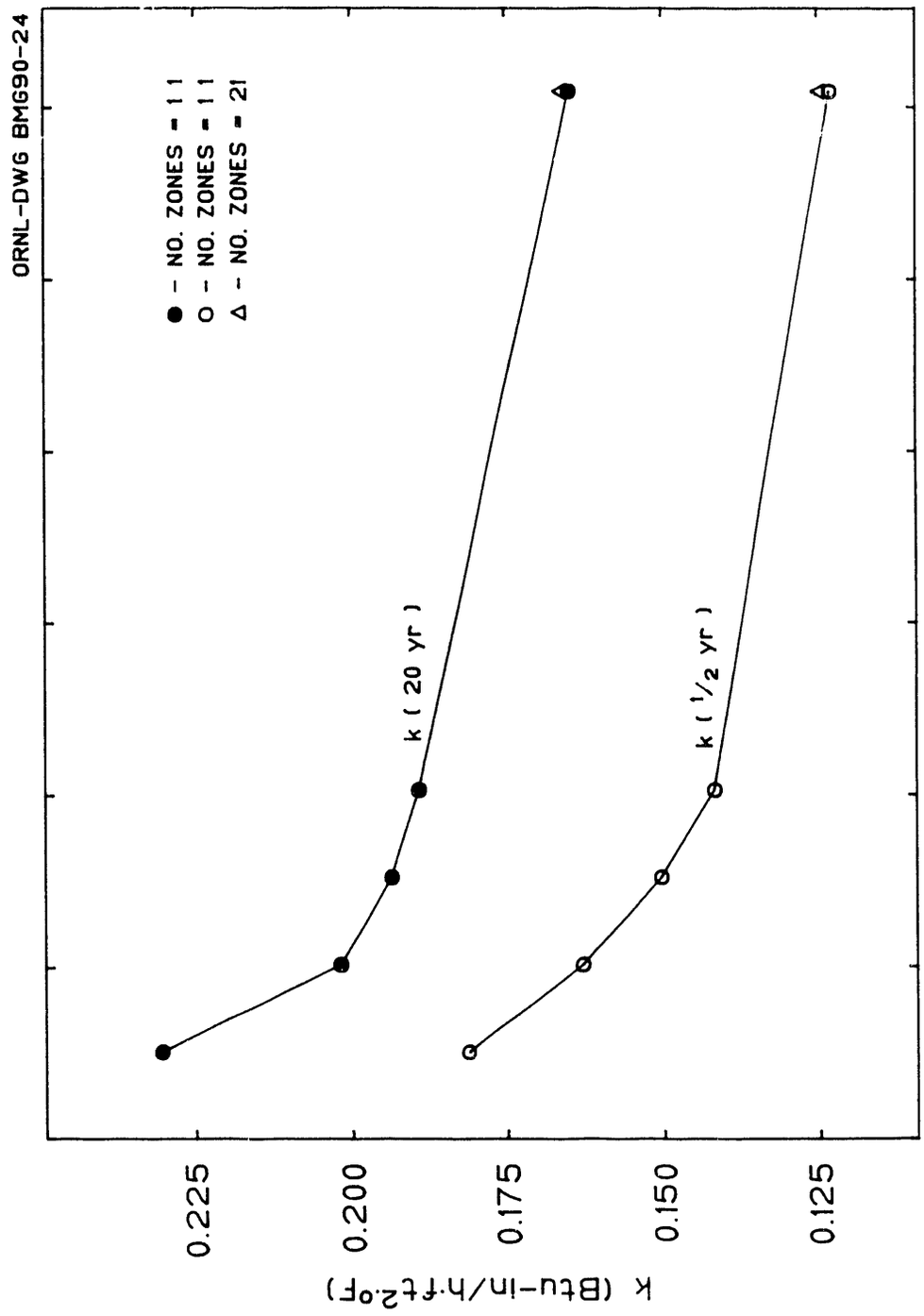

Fig. 30. Calculated foamboard thermal conductivities at 180 d and 20 years as a function of foamboard thickness.

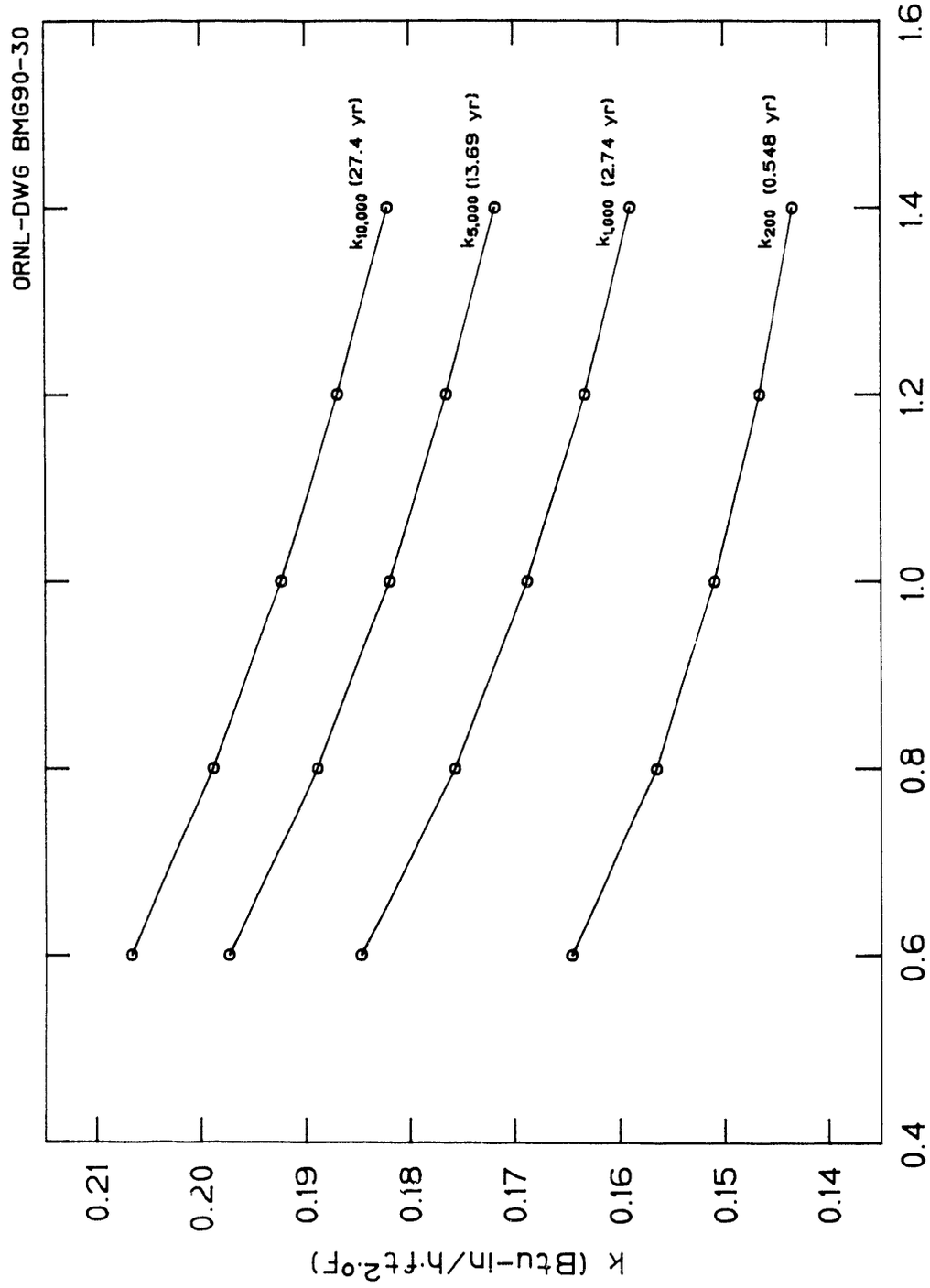

Fig. 31. Calculated foamboard thermal conductivities as a function of time and initial cell-gas pressure.

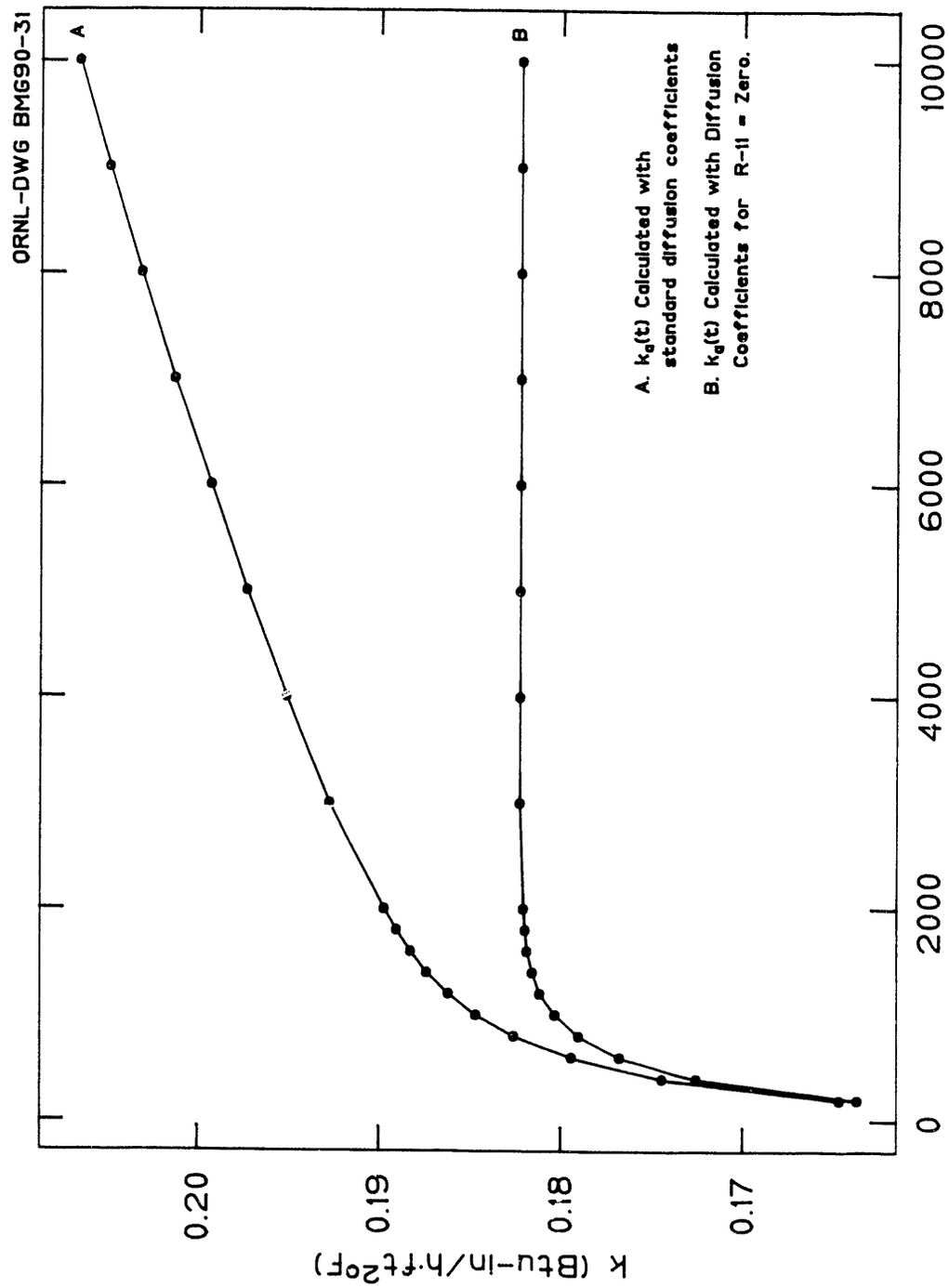

Fig. 32. Calculated foamboard thermal conductivities with standard CFC-11 diffusion coefficient and the CFC-11 diffusion coefficient set equal to zero.

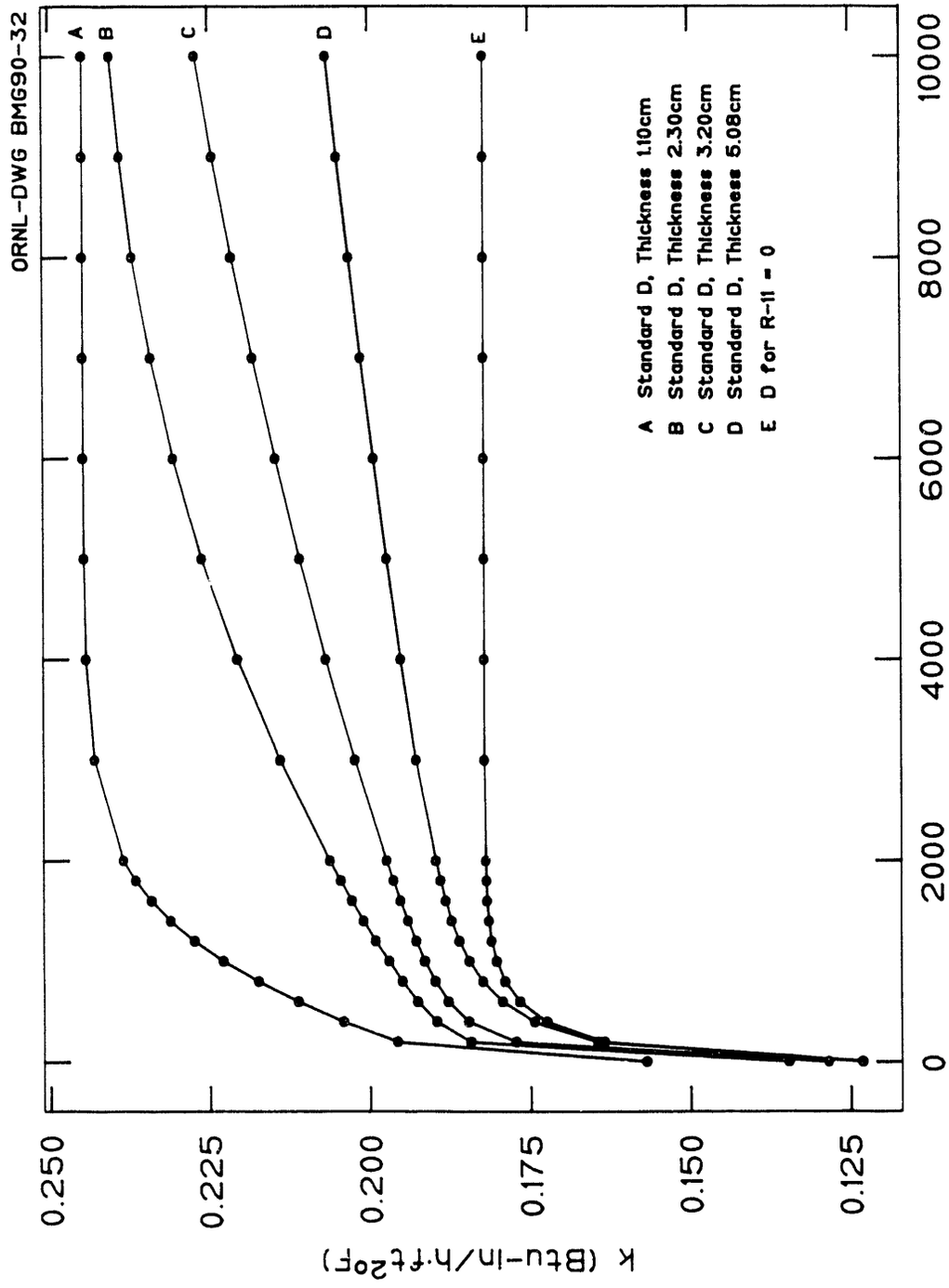

Fig. 33. Calculated foamboard thermal conductivities as a function of thickness.

Table 25. The ratio k(20)/k(1/2) from simulator results at five thicknesses

Thickness [cm (in.)]	k(1/2)[a] (Btu·in./ft²·hr·°F)	k(20)[b] (Btu·in./ft²·hr·°F)	k(20)/k(1/2)
2.54 (1.0)	0.1813	0.2306	1.272
5.08 (2.0)	0.1628	0.2018	1.240
7.62 (3.0)	0.1503	0.1934	1.287
10.16 (4.0)	0.1418	0.1891	1.334
30.48 (12.0)	0.1230	0.1647	1.339
30.48 (12.0)	0.1245	0.1660	1.333

[a]1/2 = 180 d.
[b]20 years.

The apparent thermal conductivity of a foamboard has a strong dependence on the cell-gas composition. The cell-gas composition is, in turn, dependent on the initial pressure of the blowing gas. Figure 31 shows calculated apparent thermal conductivities for foams with initial cell-gas pressures from 0.6 to 1.4 atmospheres. The four curves in the figure show k at 200 d, 1000 d, 5000 d, and 10,000 d. These curves predict that the effect of the initial pressure persists for the life of the foam.

The curves in Fig. 32 were obtained with MITB executed with "standard" diffusion coefficient data, Curve A, and with the diffusion coefficient for the blowing gas, CFC-11, set equal to zero, Curve B. Curves A and B are nearly identical for the first 400 d, but diverge for larger times as CFC-11 is lost from the foamboard. Curve B becomes constant at k = 0.1822 Btu·in./ft²·hr·°F for t > 2500 d (6.8 years), while Curve A continues to increase slowly at t = 10,000 d (27.4 years). The k on Curve A is 13.4% greater than the k on Curve B at t = 10,000 d. Figure 33 shows calculated k for four foamboard thicknesses obtained with standard diffusion coefficients for N_2, O_2, and CFC-11. Curve E in Fig. 33 was generated with the diffusion coefficient for CFC-11 set equal to zero.

7.3 A PENETRATION MODEL

The previously discussed observation that d [ℓn 100 k (t)]/d($\sqrt{t}$/x) is approximately linear in certain time intervals is supported by a "penetration" model that will be described. The basic idea is that gas diffusing into a foam creates a region in which the gas composition has changed, a penetrated region, and a region that has not been disturbed. The depth of

the penetration region increases with $\sqrt{t}$ until the center of the foamboard is disturbed. The penetrated region and the undisturbed region are taken as resistances in series to obtain an expression for $\ell n\ [k(t)]$ that is approximately linear with respect to $\sqrt{t}$ with a slope that is proportional to $\sqrt{D}$.

The starting assumptions for the "penetration" model are additivity of the heat transfer modes k_s, k_g, and k_r and treatment of the foamboard as a semi-infinite medium for limited time periods. A step-change in the concentration occurs at the surface of the foamboard at $t = 0$ and persists for $t > 0$. A solution for C (x, t) can be adapted from the corresponding heat conduction problem:[35]

$$(C/C_o)_i = C_i(X_i\ ,\ t)/C_i(o,t) = 1 - erf\ (X/2\sqrt{D_i t}\ )\ . \tag{14}$$

Equation (14) can be used to define a depth, x_p, where (C/C_o) equals 0.01. This depth is referred to as the penetration depth and forms a region in which the cell-gas composition has been changed:

$$(X_p)_i = 3.6\sqrt{D_i t}\ . \tag{15}$$

The penetration concept provides the following representation for $C\ (x, t)_i$:

$$\begin{aligned} (C/C_o)_i &= 1 - ERF(X/2\sqrt{D_i t}) \qquad 0 < X < 3.6\sqrt{D_i t} \\ &= 0 \qquad\qquad\qquad\qquad X > 3.6\sqrt{D_i t}\ . \end{aligned} \tag{16}$$

The average concentration of species i at time $t = Z$ and x between 0 and X_p is given by

$$\overline{(C/C_o)_i} = \frac{1}{X_p} \int_o^{X_p} \left\{1 - erf\left(\frac{X}{2\ (D_i\ Z)^{1/2}}\right)\right\} dx\ . \tag{17}$$

A change in the variable of integration yields the result that C_i is a constant that is independent of x or time. The penetration depth, however, is proportional to $\sqrt{t}$. If the penetrated region is identified as having $k_g = k_g^{\ s} + \Delta k_g$, then,

$$k_1 = k_s + k_r + k_g^s + \Delta k_g$$

and

$$k_2 = k_s + k_2 + k_g^s$$

The quantities k_1 and k_2 are constants, but the sizes of the regions for which they are valid vary as $\sqrt{t}$. Region 1 with apparent thermal conductivity k_1 is valid for x in $[0, 3.6\ (Dt)^{1/2}]$, while Region 2 with apparent thermal conductivity k_2 is valid for x in $[3.6\ (Dt)^{1/2}, L/2]$, where L is the thickness of the foamboard.

The apparent thermal conductivity for the foamboard, k (t), with diffusing species "one" is

$$k(t) = \frac{L}{R(t)} = 7.2\sqrt{D_1 t}\left\{\frac{1}{k_s + k_r + k_g^s + \Delta k_g} - \frac{1}{k_s + k_r + k_g^s}\right\} + \frac{L}{k_s + k_r + k_g^s} . \qquad (18)$$

Differentiation of Eq. (18) yields

$$d\ \ln k(t)/d\sqrt{t} = \frac{7.2\sqrt{D_1}}{L}\left\{\frac{k(t)}{k_s + k_r + k_g^s} - 1\right\} \qquad (19)$$

or

$$\frac{d\ \ln[100\ k(t)]}{d\ \ln(\sqrt{t}/L)} = 7.2\sqrt{D_1}\left\{\frac{k(t)}{k_s + k_r + k_g^s} - 1\right\} . \qquad (20)$$

The term in brackets on the right-hand side of Eq. (20) is expected to be in the range 0.15 to 0.25, and this suggests that D predicted from the square of the derivative in Eq. (20) should be multiplied by a factor in the range 0.85 to 0.31 to get D_1.

A derivation similar to the one summarized above leads to an expression for k (t) after the specimen is saturated with air and the outward diffusing gas has created a region of changing cell-gas composition near the surface. The apparent thermal conductivity for this second diffusion period is labeled k′(t) and

$$\frac{d\ \ell n[100\ k'(t)]}{d(\sqrt{t}/L)} = 7.2\ \sqrt{D_2}\left\{\frac{k'(t)}{k_s + k_g^* + k_r} - 1\right\}, \qquad (21)$$

where D_2 is the diffusion coefficient for the slow diffusing species and k_g^* is the gas phase conductivity after the air diffusion is complete. As in the case of the fast diffusing species, the bracketed term on the right side of Eq. (21) is expected to be in the range 0.15 to 0.25, and D_2 is 0.31 to 0.85 times the square of d ℓn [100 k(t)]/d($\sqrt{t}$/L).

The need and usefulness of foam-aging models has been demonstrated. Existing models show that the 180-d criteria for characterizing the thermal performance of foamboard insulations containing a gas other than air substantially overstates the lifetime performance of the product. The existing models can be used to study factors such as thickness and initial gas pressures on lifetime thermal performance. A two-region penetration model has been proposed and used to partially justify the identification of diffusion coefficients with the square of the experimentally determined derivative d (ℓn [100 k_a (t)]/d ($\sqrt{t}$/L).

A continued effort is needed to extend the existing models to three dimensions and to incorporate a variety of surface conditions into the calculations. The existing code, MITB, should be extended to three dimensions and used to justify new criteria for labeling foamboard products. Improved models can be used to guide the development of new foamboard products since k (t) can be predicted from property data. Refinement of the penetration model could be useful in providing alternate ways to analyze transient heat flow data.

8. CONCLUSIONS

This report presents k-values on a set of industry-produced, prototypical, experimental PIR laminated boardstock foams blown with five gases: CFC-11, HCFC-123, HCFC-141b, and 50/50 and 65/35 blends of HCFC-123/HCFC-141b. The k-values were determined from 30 to 120°F using the ORNL UTHA and the ORNL Advanced R-Matic Apparatus. The test results on panels with facers provide an independent laboratory check on the increase in k observed for a 241-d field exposure in the RTRA. The observed laboratory increase in k for a 241-d field exposure was between 8 and 11%: CFC-11 (8.6%), HCFC-123 (11.1%), and HCFC-141b (9%).

The laboratory tests show that, prior to the RTRA exposure, the k of the foams blown with the alternate gases were greater than that of the foam blown with CFC-11: HCFC-123 (5.5%) and HCFC-141b (11.7%). After the 241-d RTRA exposure these values were HCFC-123 (7.9%) and HCFC-141b (12.9%); after the 430-d RTRA exposure these values were HCFC-123 (4.5%) and HCFC-141b (9%). The k of foams blown with the blends was about 5.8% greater than that of the CFC-11 blown foam prior to the RTRA exposure. Foams blown with blends after 300 d of RTRA exposure showed an increase in k of about 20% as a result of the RTRA exposure.

The k-values of a set of thin-specimen foam cores planed from these experimental boardstock insulation increase with time after production. The thin specimens were aged at 75 and 150°F for up to 290 d to establish the long-term thermal resistance of each of the gas-filled cellular foams. For each of the foams, the increase in k-values for specimens of three thicknesses can be described as an exponential function of k with time$^{1/2}$/thickness. This dependency shows two distinct linear regions of behavior with an intermediate zone when the results are plotted as a function of time$^{1/2}$/thickness, ($d^{1/2}$/mm). The thinnest specimen reached larger values of time$^{1/2}$/thickness sooner than the thicker specimen for the same time of aging (i.e., aging is accelerated).

The first linear region was associated with the increase in k because of the influx of air components (O_2, N_2), and the second, lower slope, linear region was associated with the loss of blowing agent from the foam. This yielded effective diffusion coefficients (D) for air components into the foam and blowing agent out of the foam. The D (air) values for aging at 75°F were between 1.5×10^{-8} cm^2/s and 2.5×10^{-8} cm^2/s,

and D-values for aging at 150°F were three to seven times larger. The D (blowing agent) values for aging at 75°F were between 1.8×10^{-10} cm^2/s and 12×10^{-10} cm^2/s and increased two to four times for aging at 150°F. Activation energies of 3500 to 9500 cal/mol were obtained for these processes. The accelerated aging test results provided an estimate of 5-year thermal resistivity (1/k) of these experimental foams at 75°F that is within 12% of that obtained for foams blown with CFC-11 under similar conditions.

The MIT computer program that models foam aging was programmed in Fortran (MITB) and used to predict the k of foams for a variety of conditions. These simulations using MITB showed that the D values from the accelerated aging tests are of the correct order of magnitude and may be sufficient for many purposes. The simulations and the aging tests show that the ASTM 180-d-after-manufacture test is an inadequate description of long-term k-values. The MITB program was used to show the effect of changing the permeability of O_2, N_2, and blowing agent; the effect of specimen thickness; and the effect of initial blowing agent gas pressure on the long-term k-value of foams.

9. RECOMMENDATIONS

The cooperative industry-government project provided the opportunity for manufacturers, users, and measurers to bring their combined talents to focus on an initial solution to the global issue of reducing CFC use in PIR foam insulations. ORNL should recommend this type of project to the producers of other types of foams (e.g., polystyrene and phenolic). The cooperative project has raised a number of interesting questions and results that deserve further study, and these are given below.

1. The project test results create a valuable data base for the initial set of industry-produced experimental, prototypical PIR laminated boardstock foams. ORNL should recommend close examination of these by industry to produce and start tests on a cooperative project on the next generation of improved foams blown with alternative agents.
2. A thin-specimen accelerated-aging test procedure was validated by laboratory tests of specimens aging at 75 and 150°F. ORNL should use these results to help draft an ASTM C 16 standard procedure for the determination of the long-term

thermal resistance of gas-filled cellular plastic foams. A scope has been drafted and balloted by ASTM C 16.30, August 31, 1990.

3. The thin-specimen accelerated-aging test has yielded order-of-magnitude effective diffusion coefficients (D) for O_2, N_2, and blowing agents and process activation energies. Since these are influenced by the foam structural properties (i.e., cell size, wall thickness, and fraction of solid in walls), determination of D could guide product evaluation and development. ORNL should work with industry on a cooperative project to obtain D values by this technique on products with significantly different structural characteristics (i.e., thicker walls, smaller cells, and larger fractions of solid in walls).
4. The thin-specimen accelerated-aging procedure should be applied to field tests (e.g., RTRA panels composed of thin specimens) to see how the procedure works and compares to laboratory aging.
5. The thin-specimen accelerated-aging procedure requires planing thick specimens to a known and uniform thickness below 0.4 in. (10 mm). ORNL should obtain planing equipment to produce uniform-thickness specimens and a means to measure this. For example, NIST has a large flat table with a dial gage to measure specimen thickness over the board area.
6. All means to verify and to confirm the thin-specimen procedure should be explored because this provides a rapid means to predict the long-term thermal performance of foam insulations, and the present ASTM 180-d procedure is inadequate. The current initial effort on applying modeling is one such means to justify a description of the process using the experimentally determined derivative of d (ℓn 100 k)/ d $\sqrt{t}$/L. ORNL should extend the development of this model, the Dow model, and the MIT model in cooperation with research at MIT and the National Research Council of Canada.
7. Interesting results obtained by applying the MITB program suggest additional tests of current foams and new foams. For example, calculations show that the 27-year, long-term k is reduced from 0.19 to 0.16 Btu·in./h·ft^2·°F (16%) if the initial blowing-agent pressure is increased from 0.6 to 1.4-atm pressure. ORNL should work with industry on a cooperative project to demonstrate this dramatic improvement in performance. To help support the experimental and modeling

efforts, ORNL should obtain equipment to measure the gas pressure and composition as a function of time after manufacture.

10. ACKNOWLEDGMENTS

The authors thank each of the members of the Steering Committee and their organizations of the Cooperative Industry/Government Research Project for their encouragement, guidance, and support. The authors thank Dr. M. P. Scofield for requesting a draft of this report as a deliverable for the FY 1990 Building Materials Research Program Statement of Work. This gave us the opportunity to document the current activity, to discuss the results in detail with each other, and to obtain the views of our peers. The authors thank T. G. Kollie, R. S. Carlsmith, J. E. Christian, G. E. Courville, D. F. Craig, and R. L. Wendt of ORNL for their review of this report. We also thank F. J. Weaver for preparing the figures and helping record results. Finally, we thank G. L. Burn for preparing the text.

11. REFERENCES

1. *Protocol on Substances that Deplete the Ozone Layer*, United Nations Environment Programme, Final Act, Montreal, September 1987.

2. *Protection of Stratospheric Ozone: Final Rule and Proposed Rule*, 40 CFR Pt. 82, Fed. Regist., Vol. 52, pp. 47486-523, (Dec. 14, 1987).

3. *Protection of Stratospheric Ozone: Final Rule and Proposed Rule*, 40 CFR Pt. 82, Fed. Regist., Vol. 53, pp. 30566-602 (Aug. 12, 1988).

4. D. L. McElroy and M. P. Scofield, *Chlorofluorocarbon Technologies Review of Foamed-Board Insulation for Buildings*, ORNL/TM-11291, Martin Marietta Energy Systems, Inc., March 1990.

5. Environmental Protection Agency, *How Industry is Reducing Dependence on Ozone-Depleting Chemicals*, June 1988.

6. J. P. Millhone, Report to the Secretary of Energy on Ozone Depleting Substances - *An Analysis of the Energy and Economic Effects of Phasing Out Certain Organic Chlorine and Bromine Products*, October 1989.

7. S. K. Fischer and F. A. Creswick, *Energy-Use Impact of Chlorofluorocarbon Alternatives*, ORNL/CON-273, Martin Marietta Energy Systems, Inc., Oak Ridge Natl. Lab., 1989.

8. L. R. Glicksman and M. R. Torpey, *A Study of Radiative Heat Transfer Through Foam Insulation*, ORNL/Sub/86-09099/3, Martin Marietta Energy Systems, Inc., Oak Ridge Natl. Lab., 1988.

9. A. G. Ostrogorsky, *Aging of Polyurethane Foams* Sc.D. thesis, Massachusetts Institute of Technology, Cambridge, Mass., 1985.

10. Press Release, Association of Home Appliance Manufacturers, Chicago, Ill., July 6, 1987.

11. *Appliance Efficiency Standards*, P400-00-029, Calif. Energy Commission, Sacramento, Calif. (amended August 1985).

12. National Appliance Energy Conservation Act of 1987, Publ. L. 100-12, Stat. 83 (March 17, 1987).

13. W. T. Lawrence and F. E. Ruccia, *Development of Advanced Insulation for Appliances, Task I Report*, ORNL/Sub/81-13800/1, Union Carbide Corp., Nuclear Div., Oak Ridge Natl. Lab., June 1981.

14. L. R. Glicksman, "Methods to Enhance the Insulating Values of Closed Cell Foam," pp. 149-56 in *Buildings IV*, American Society of Heating, Refrigeration, and Air Conditioning Engineers, December 1989.

15. J. E. Christian and D. L. McElroy, *Results of Workshop to Develop Alternatives for Insulations Containing CFCs - Research Project Menu*, ORNL/CON-269, Martin Marietta Energy Systems, Inc., Oak Ridge Natl. Lab., December 1989.

16. G. E. Courville et al., *An Apparatus for Thermal Performance Measurements of Insulated Roof Systems. Thermal Insulation: Materials and Systems*, ASTM STP 922, ed. F. J. Powell and S. L. Matthews, American Society for Testing and Materials, Philadelphia, 1987, pp. 449-59.

17. "Standard Test Method for Steady-State Thermal Transmission Properties by Means of the Thin-Heater Apparatus," ASTM C1114-89, pp. 600-606 in *1989 Annual Book of ASTM Standards*, Vol. 04.06, American Society for Testing and Materials, Philadelphia, 1989.

18. "Standard Test Method for Steady-State Heat Flux Measurements and Thermal Transmission Properties by Means of the Heat Flow Meter Apparatus," ASTM C 518-85, pp. 150-62 in *1989 Annual Book of ASTM Standards*, Vol. 04.06, American Society for Testing and Materials, Philadelphia, 1989.

19. Characterization tests and model predictions were done at the Massachusetts Institute of Technology under subcontract to Martin Marietta Energy Systems, Inc.

20. D. L. McElroy et al., *A Flat Insulation Tester that Uses an Unguarded Nichrome Screen Wire Heater, Guarded Hot Plate and Heat Flow Meter Methodology*, ASTM STP 879, American Society for Testing and Materials, Philadelphia, 1985, pp. 121-39.

21. R. S. Graves, D. W. Yarbrough, and D. L. McElroy, "Apparent Thermal Conductivity Measurements by an Unguarded Technique," pp. 339-56 in *Thermal Conductivity 18*, Plenum, New York, 1985.

22. "Standard Specification for Membrane-Faced Rigid Cellular Polyurethane Roof Insulation," ASTM C 1013-85, pp. 498-500 in *1989 Annual Book of ASTM Standards*, Vol. 04.06, American Society for Testing and Materials, Philadelphia, 1989.

23. "Standard Practice for Using the Guarded Hot Plate Apparatus in the One-Sided Mode to Measure Steady-State Heat Flux and Thermal Transmission Properties," ASTM C 1044-85, pp. 528-30 in *1989 Annual Book of ASTM Standards*, Vol. 04.06, American Society for Testing and Materials, Philadelphia, 1989.

24. The Advanced R-Matic Apparatus was produced by Holometrix, Inc., Cambridge, Mass., and delivered to ORNL in March 1989.

25. The boardstock was produced by Atlas Roofing Corporation at their plant in East Moline, Ill.

26. L. R. Glicksman, Massachusetts Institute of Technology, personal communication to D. L. McElroy, Oak Ridge National Laboratory, Feb. 26, 1990.

27. A. E. Lund, R. G. Richard, and I. R. Shankland, "A Performance Evaluation of Environmentally Acceptable Blowing Agents," pp. 290-96 in *SPI Polyurethane '88*, 1988.

28. H. A. Fine et al., *Analysis of Heat Transfer in Building Thermal Insulation*, ORNL/TM-7481, Union Carbide Corp., Nuclear Div., Oak Ridge Natl. Lab., December 1980.

29. R. Siegel and J. R. Howell, *Thermal Radiation Heat Transfer*, McGraw, New York, 1972.

30. R. S. Graves et al., "Thermal Performance of a Closed-Cell Foamboard Insulation Containing HCFC-22," pp. 35-49 in *Proceedings of the Sixth International Conference on Thermal Insulation*, Vol. 6, Product Safety Commission, February 1990.

31. SPI Polyurethane Division k Factor Task Force, "Rigid Polyurethane and Polyisocyanurate Foams: An Assessment of Their Insulating Properties," pp. 323-37 in *SPI Polyurethane '88*, October 1988.

32. L. R. Glicksman, "Models to Predict Aging and R-Values of Foam Insulation," pp. 99-113 in *Proceedings of the Symposium on Mathematical Modeling of Roof Systems, Oak Ridge, Tennessee, September 15-16, 1988.*

33. C. F. Sheffield, "Description and Applications of a Diffusion Model for Rigid Closed-Cell Foams," pp. 113-29 in *Proceedings of the Symposium on Mathematical Modeling of Roof Systems, Oak Ridge, Tennessee, September 15-16, 1988.*

34. M. R. Destephen, *Thermophysical Properties of Two Foam Insulations*, Master of Science thesis, Tennessee Technological University, Cookeville, 1988.

35. H. S. Carslaw and J. C. Jaeger, *Conduction of Heat in Solids*, 2nd ed., Oxford Univ. Press, London, 1959.

36. B. Carhahan, H. A. Luther, and J. O. Wilkes, *Applied Numerical Methods*, Wiley, New York, 1969.

37. pp. 441-42.

38. L. A. Lindsay and L. A. Bromley, "Thermal Conductivity of Gas Mixtures," *Ind. Engr. Chem.* **42**, 1508 (1950).

39. Matpro-Version 11, *A Handbook of Material Properties for Use in the Analysis of Light Water Reactor Fuel Rod Behavior*, NUREG/CR-0497, EG&G, Idaho, February 1979.

40. R. C. Reid et al., *The Properties of Gases and Liquids*, 4th ed., McGraw, New York, 1987.

41. *1989 ASHRAE Handbook of Fundamantals. Refrigerant Tables and Charts*, American Society of Heating, Refrigerating, and Air Conditioning Engineers, Atlanta, 1989.

42. D. W. Yarbrough and R. S. Graves, "The Thermal Performance of Closed-Cell Foamboard Insulations Containing a Gas Other than Air," Paper 344 EN-A08 in *40th Canadian Chemical Engineering Conference, Halifax, Nova Scotia, July 15-21, 1990.*

43. W. J. Batty, S. D. Probert, and P. W. O'Callaghan, "*Apparent Thermal Conductivities of High-Porosity Cellulary Insulants*," *Applied Energy* **18**, 117-35 (1984).

APPENDIX A. k (PANELS) MEASURED IN THE ADVANCED R-MATIC APPARATUS AND THE UNGUARDED THIN-HEATER APPARATUS

Table A1. Advanced R-Matic Apparatus k-results on RTRA panels prior to installation

CFC-11, 2.782 lb/ft^3					
Boards 1 + 2 (66 d)		Board 1 (68 d)		Board 2 (69 d)	
t	k	t	k	t	k
30.20	0.1233	30.13	0.1237	29.17	0.1265
60.98	0.1245	60.71	0.1258	60.71	0.1278
75.65	0.1312	75.49	0.1317	75.50	0.1342
90.23	0.1406	90.18	0.1382	90.15	0.1412
119.84	0.1644	119.73	0.1523	119.73	0.1577
74.62	0.1322				
121.66	0.1582				
$k = 6.957 \times 10^{-2} + 6.371 \times 10^{-4}\ t + 1.0725\ t^{-1}$, ±1.18%[a]					
HCFC-123, 2.778 lb/ft^3					
72 d		73 d		74 d	
30.101	0.1381	30.176	0.1366	30.173	0.1356
60.884	0.1396	60.776	0.1280	60.748	0.1371
75.594	0.1461	75.515	0.1448	75.516	0.1450
90.356	0.1541	90.758	0.1524	90.105	0.1516
119.892	0.1700	119.842	0.1698	119.749	0.1668
74.656	0.1432			74.199	0.1414
121.690	0.1721				
$k = 7.857 \times 10^{-2} + 6.564 \times 10^{-4}\ t + 1.1616\ t^{-1}$, ±1.56%					
HCFC-141b, 2.724 lb/ft^3					
78 d		80 d		81 d	
29.171	0.1521	30.300	0.1518	30.249	0.1463
60.985	0.1463	60.800	0.1472	60.633	0.1445
75.714	0.1536	75.383	0.1537	75.440	0.1515
90.331	0.1613	90.215	0.1622	90.208	0.1596
119.937	0.1801	119.785	0.1796	119.799	0.1764
73.813	0.1594				
121.758	0.1803				
$k = 8.074 \times 10^{-2} + 6.936 \times 10^{-4}, t + 1.4529\ t^{-1}$, ±1.89%					
HCFC-141b, 2.724 lb/ft^3					
83 d		85 d		86 d	
30.032	0.1489	30.300	0.1453	30.200	0.1464
60.158	0.1465	60.800	0.1411	60.620	0.1409
78.474	0.1513	75.290	0.1466	74.300	0.1447
90.302	0.1575	90.171	0.1542	90.072	0.1526
119.893	0.1751	119.740	0.1723	119.817	0.1674
77.352	0.1520				
121.706	0.1795				
$k = 7.082 \times 10^{-2} + 4.323 \times 10^{-4} + 1.6307\ t^{-1}$, ±1.5%					

[a]Average percent deviation.

Table A2. Advanced R-Matic Apparatus results on RTRA panels prior to installation

50/50 blend, 2.892 lb/ft^3 Boards 1 + 2 (15 d)	
t	k
60.54	0.1356
75.51	0.1430
90.34	0.1513
119.95	0.1670
$k = 0.1032 + 5.315 \times 10^{-4}\ t$, ±0.40%	

65/35 blend, 2.778 lb/ft^3 Boards 1 + 2 (21 d)	
t	k
60.57	0.1356
75.42	0.1431
90.35	0.1486
120.00	0.1646
$k = 0.1061 + 4.8347 \times 10^{-4}\ t$, ±0.40%	

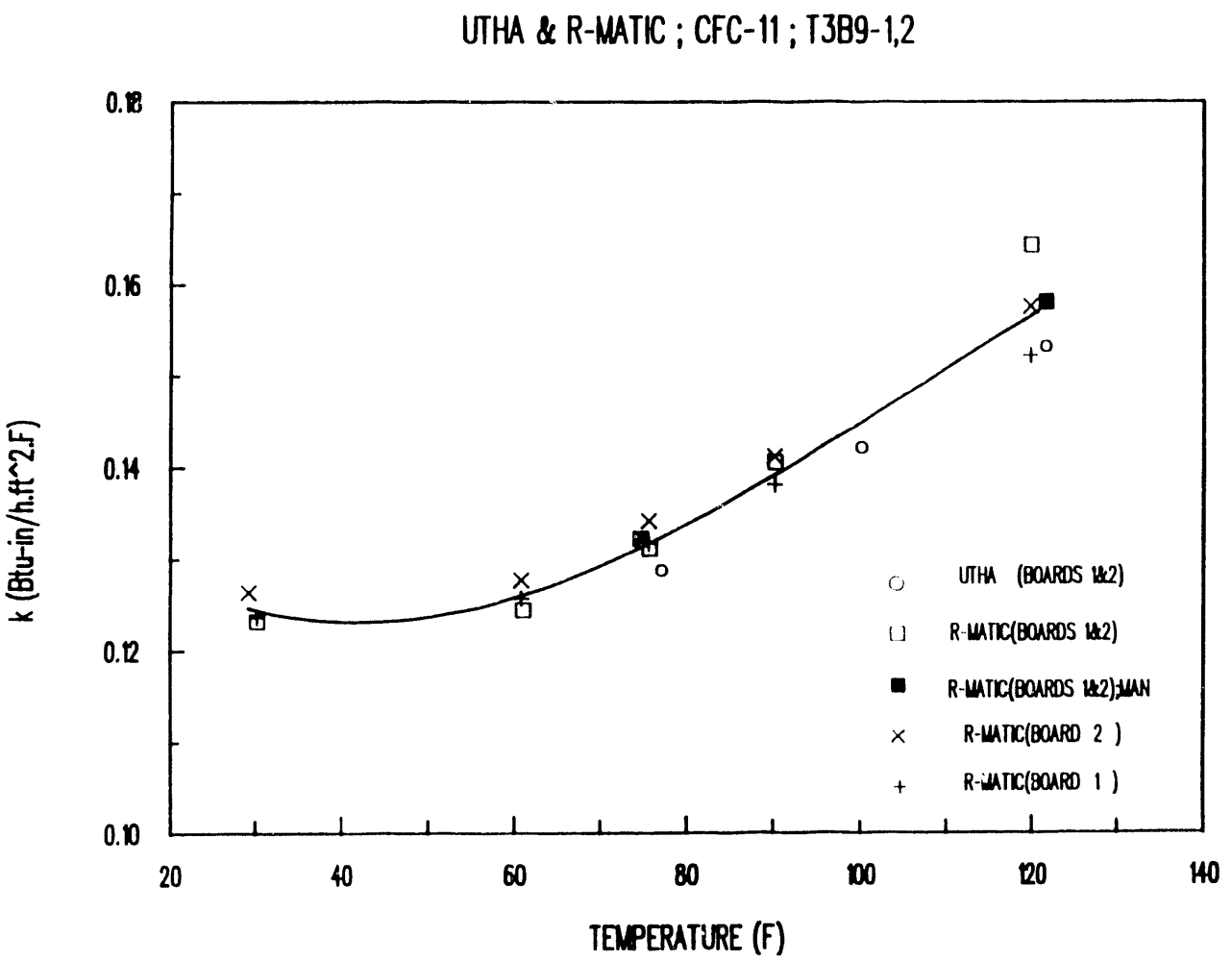

Fig. A1. The temperature dependency of the thermal conductivity of boardstock blown with CFC-11.

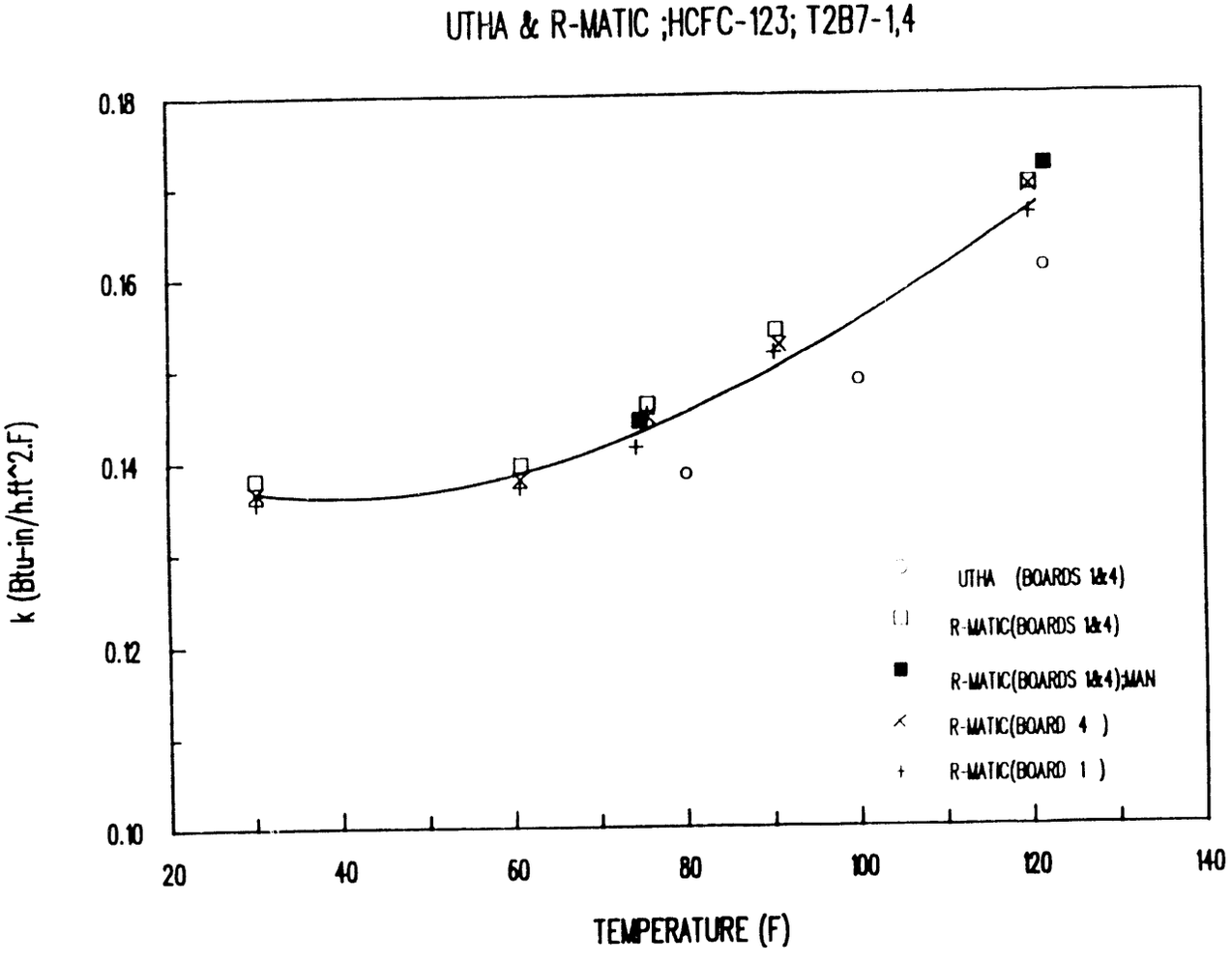

Fig. A2. The temperature dependency of the thermal conductivity of boardstock blown with HCFC-123.

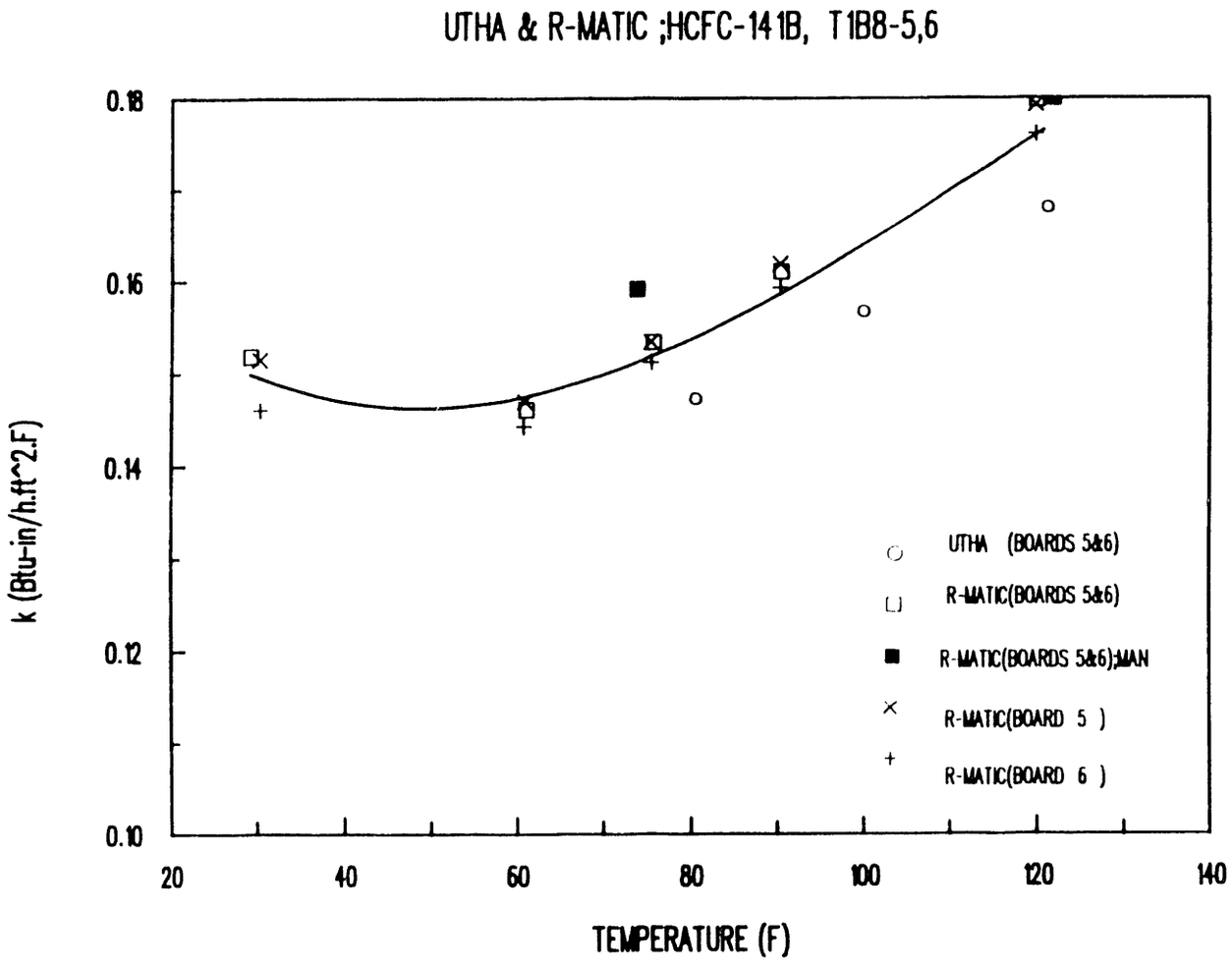

Fig. A3. The temperature dependency of the thermal conductivity of boardstock blown with HCFC-141b (black EPDM).

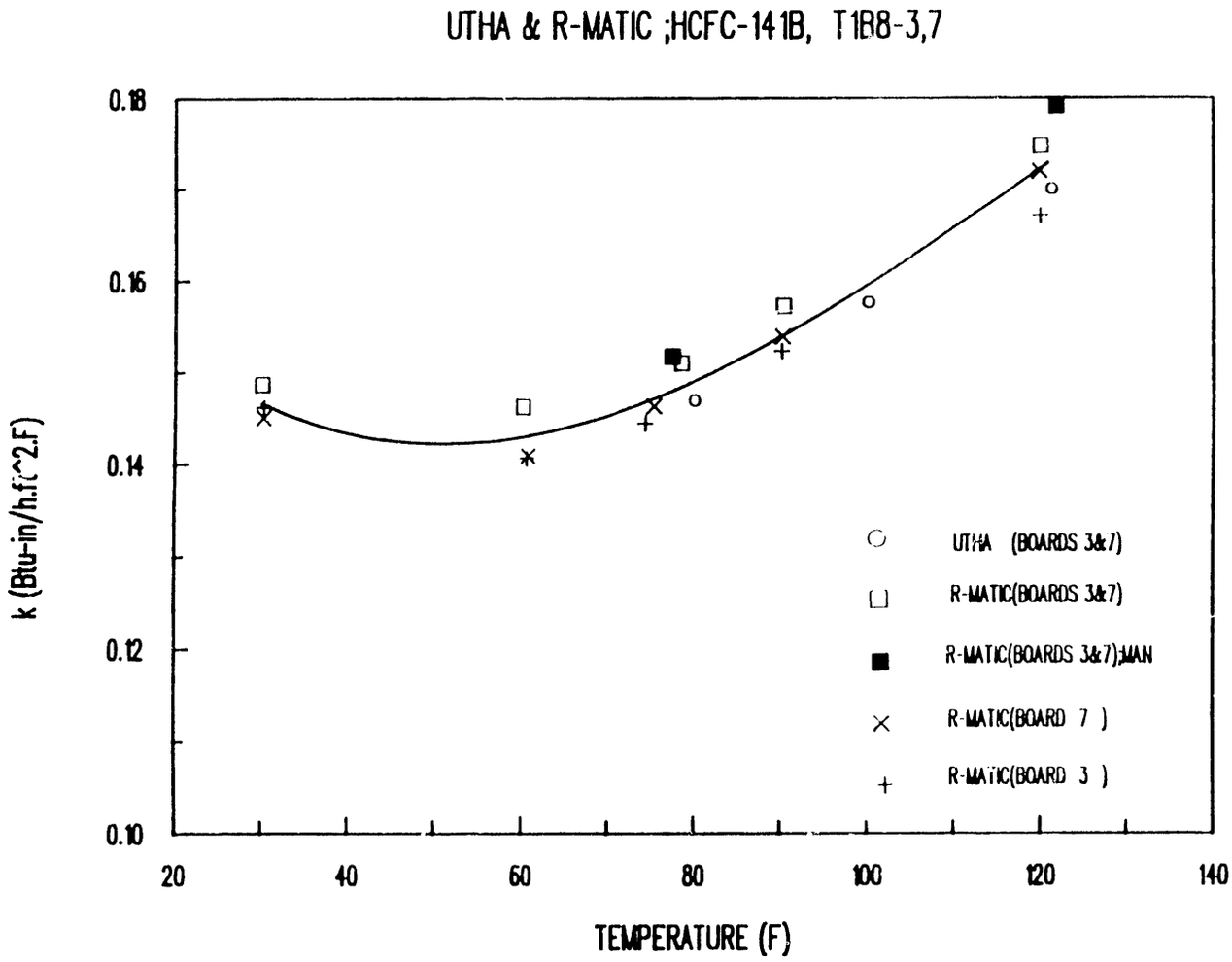

Fig. A4. The temperature dependency of the thermal conductivity of boardstock blown with HCFC-141b (white EPDM).

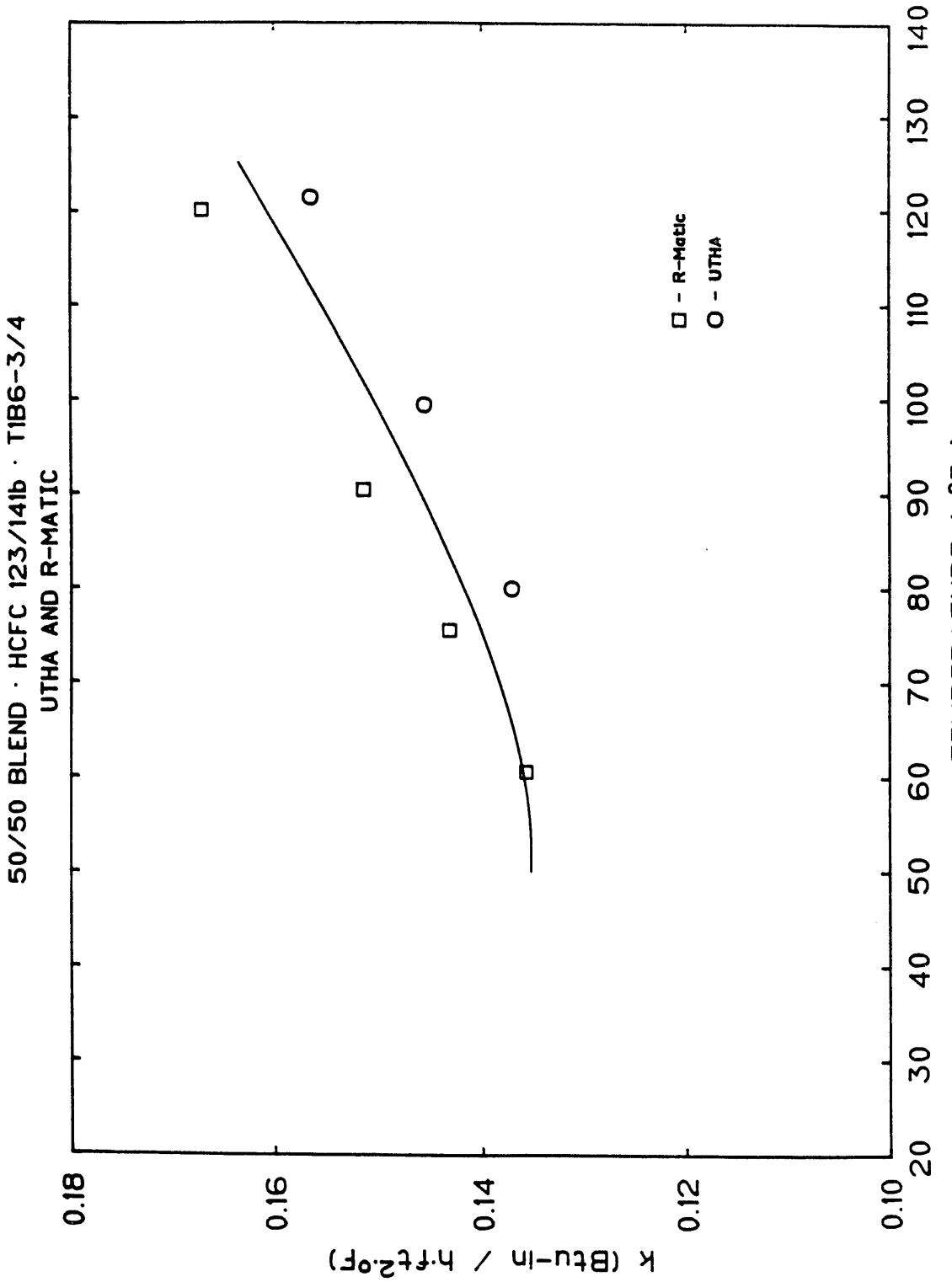

Fig. A5. The temperature dependency of the thermal conductivity of boardstock blown with a 50/50 blend.

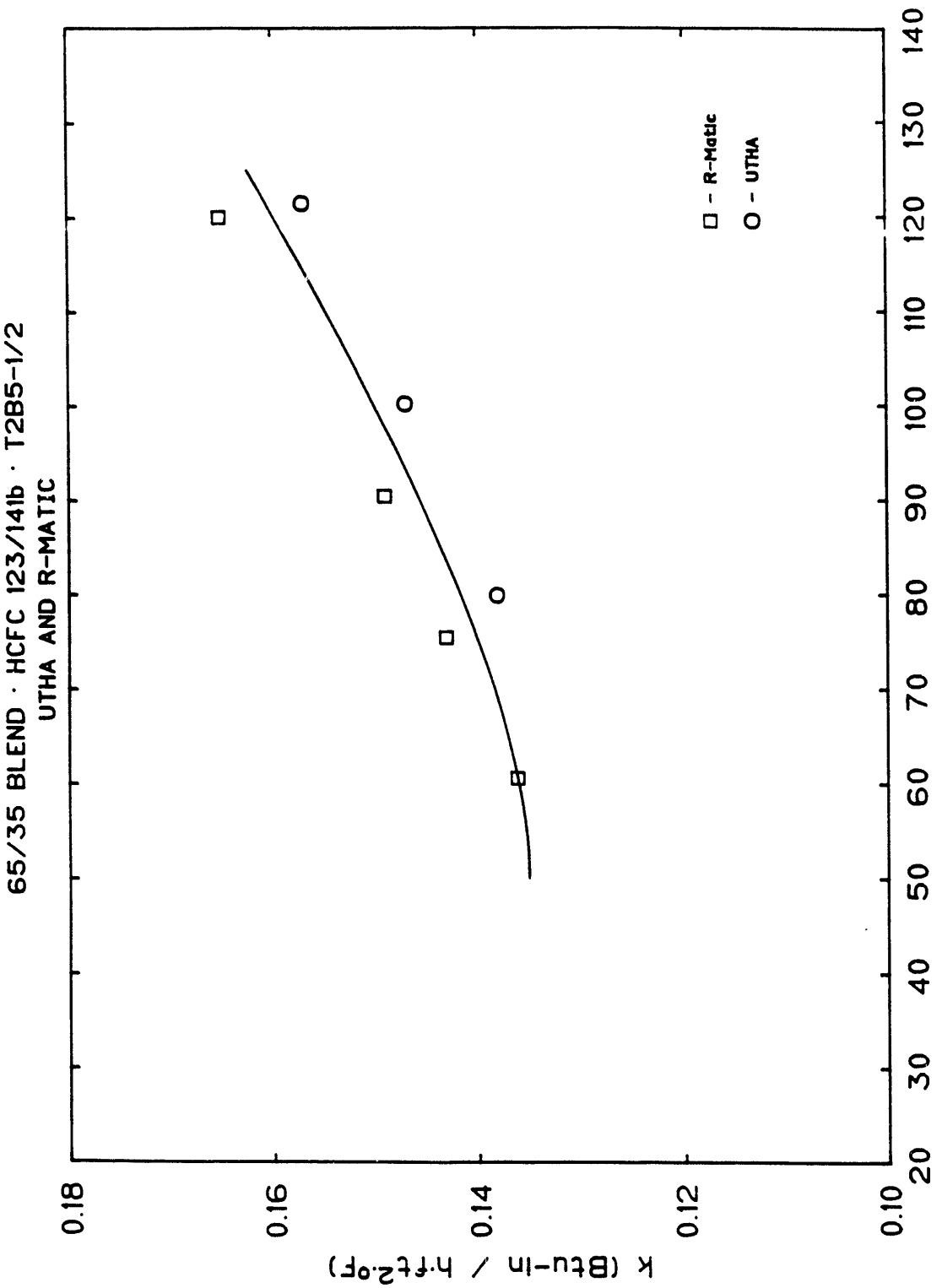

Fig. A6. The temperature dependency of the thermal conductivity of boardstock blown with a 65/35 blend.

Table A3. Thermal conductivity results on RTRA panels after 430-d exposure

1. CFC-11, Boards T3B9 (1 and 2)

Advanced R-Matic Apparatus (532 d)		UTHA (529 d)	
t (°F)	k (Btu·in./h·ft²·°F)	t (°F)	k (Btu·in./h·ft²·°F)
30.37	0.1532	121.53	0.1776
37.76	0.1490	99.64	0.1654
43.05	0.1473	75.38	0.1565
49.26	0.1475		
56.32	0.1494		
75.76	0.1574		
98.70	0.1683		
120.02	0.1787		
		A = 0.3842	

$k = 9.115 \times 10^{-2} + 6.342 \times 10^{-4}\ t + 1.279/t$

2. HCFC-123, Boards T2B7 (1 and 4)

Advanced R-Matic Apparatus (531 d)		UTHA (533 d)	
t (°F)	k (Btu·in./h·ft²·°F)	t (°F)	k (Btu·in./h·ft²·°F)
30.30	0.1555	75.34	0.1642
37.76	0.1529	99.67	0.1738
43.94	0.1527	121.45	0.1838
49.23	0.1528		
56.32	0.1560		
75.65	0.1636		
98.80	0.1740		
119.99	0.1841		
		A = 0.3892	

$k = 1.081 \times 10^{-1} + 5.711 \times 10^{-4}\ t + 8.872 \times 10^{-1}$

Table A3. (continued)

3. HCFC-141b, Boards T1B8 (3 and 7), White EPDM

Advanced R-Matic Apparatus (525 d)		UTHA (519 d)	
t (°F)	k (Btu·in./h·ft²·°F)	t (°F)	k (Btu·in./h·ft²·°F)
37.56	0.1649	121.02	0.1904
43.92	0.1620	99.54	0.1796
49.21	0.1614	75.26	0.1694
56.34	0.1617		
75.67	0.1705		
98.62	0.1831		
120.01	0.1938		
		A = 0.3764	

$k = 9.734 \times 10^{-2} + 6.851 \times 10^{-4}\ t + 1.532/t$

4. HCFC-141b, Boards T1B8 (5 and 6), Black EPDM

Advanced R-Matic Apparatus (519 d)		UTHA (527 d)	
t (°F)	k (Btu·in./h·ft²·°F)	t (°F)	k (Btu·in./h·ft²·°F)
29.26	0.1679	121.01	0.1924
37.70	0.1638	99.62	0.1808
42.97	0.1618	75.30	0.1707
49.30	0.1616		
56.30	0.1630		
75.68	0.1714		
98.61	0.1830		
119.90	0.1933		
		A = 0.3656	

$k = 1.0358 \times 10^{-1} + 6.532 \times 10^{-4}\ t + 1.317/t$

Table A3. (continued)

5. 50/50 Blend, Boards T1B6 (3 and 4)

Advanced R-Matic Apparatus (314 d)		UTHA (309 d)	
t (°F)	k (Btu·in./h·ft²·°F)	t (°F)	k (Btu·in./h·ft²·°F)
30.26	0.1611	121.09	0.1832
37.67	0.1571	99.01	0.1735
43.94	0.1557	75.10	0.1634
49.26	0.1556		
56.29	0.1564		
75.68	0.1645		
98.83	0.1759		
119.89	0.1865		
		A = 0.3873	

$k = 9.910 \times 10^{-2} + 6.267 \times 10^{-4}\, t + 1.2903/t$

6. 65/35 Blend, Boards T2B5 (1 and 2)

Advanced R-Matic Apparatus (310 d)		UTHA (314 d)	
t (°F)	k (Btu·in./h·ft²·°F)	t (°F)	k (Btu·in./h·ft²·°F)
30.25	0.1588	121.09	0.1838
43.85	0.1547	99.98	0.1726
56.40	0.1566	74.98	0.1650
75.62	0.1646		
98.61	0.1760		
119.93	0.1855		
		A = 0.3702	

$k = 1.068 \times 10^{-1} + 5.763 \times 10^{-4}\, t + 1.030/t$

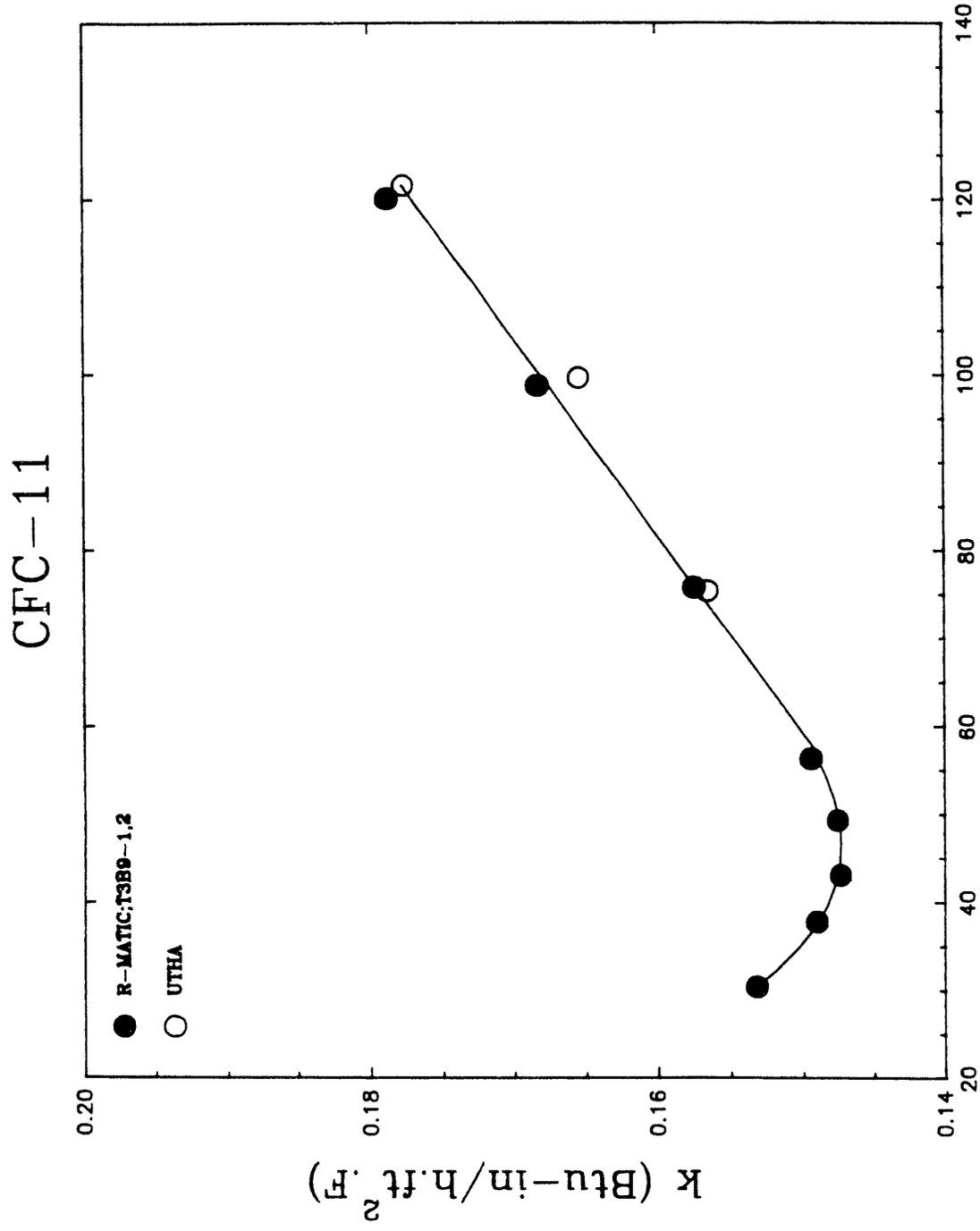

Fig. A7. The temperature dependency of the thermal conductivity of boardstock blown with CFC-11 after 420-d exposure in the RTRA.

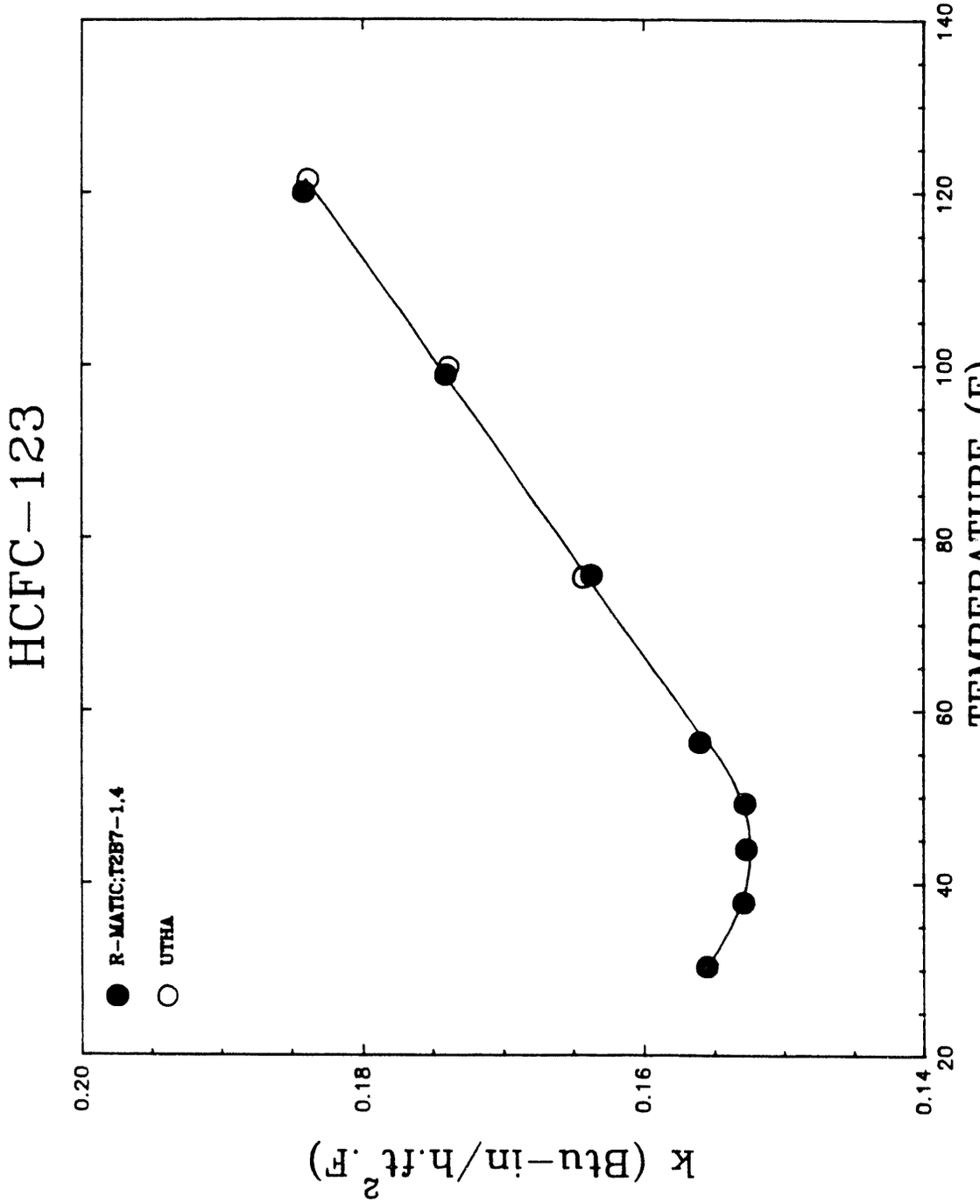

Fig. A8. The temperature dependency of the thermal conductivity of boardstock blown with HCFC-123 after 420-d exposure in the RTRA.

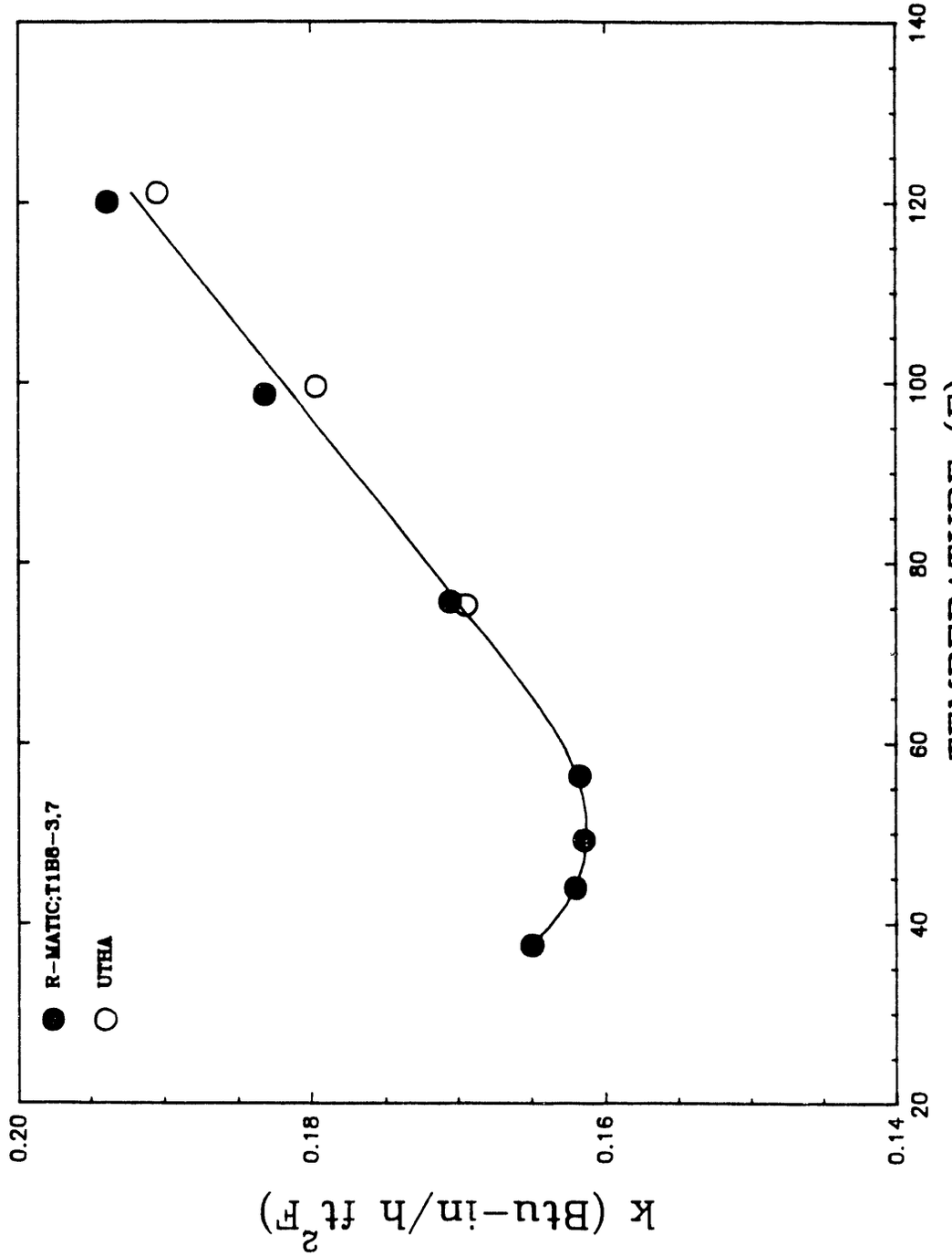

Fig. A9. The temperature dependency of the thermal conductivity of boardstock blown with HCFC-141b (white) after 420-d exposure in the RTRA.

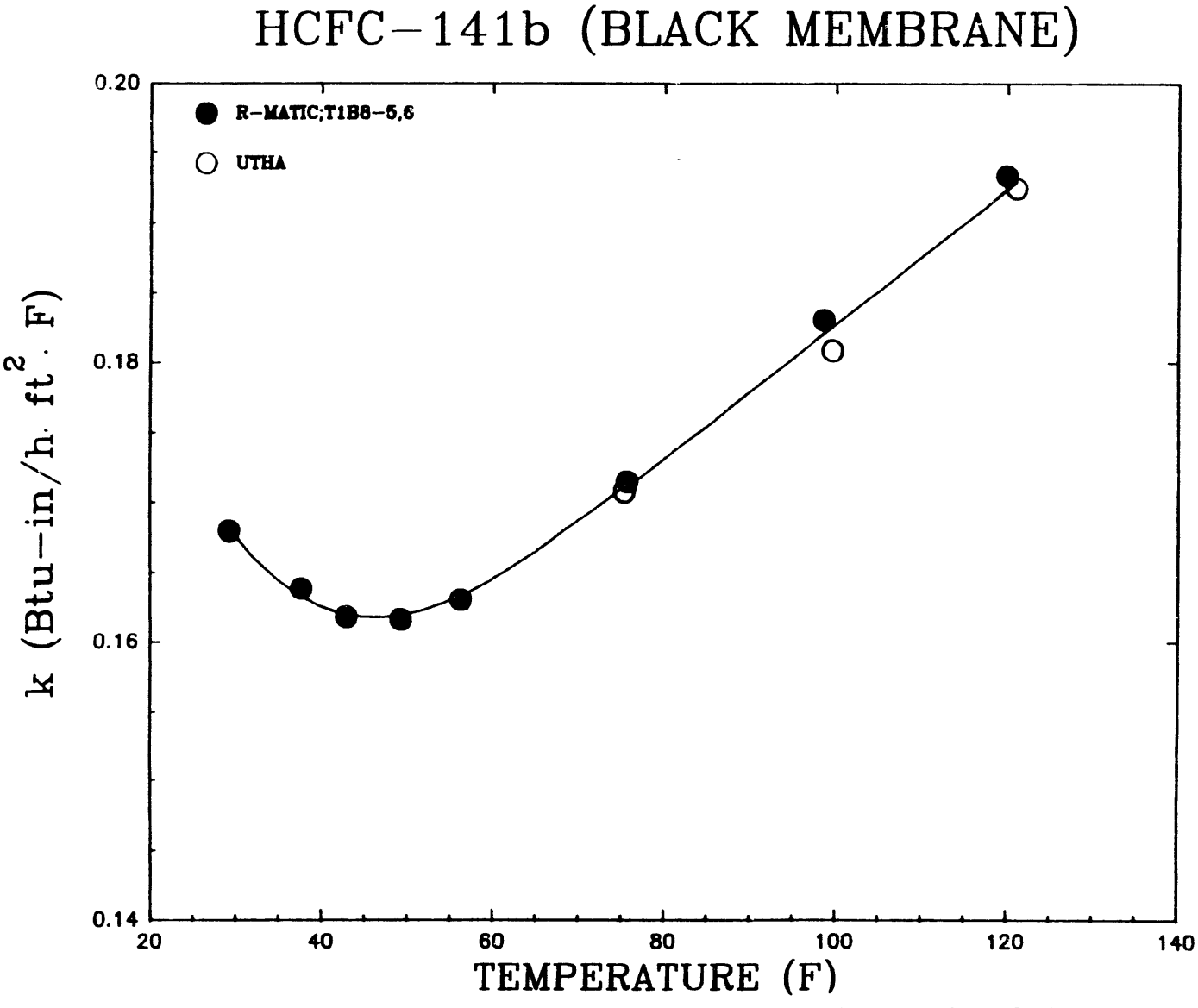

Fig. A10. The temperature dependency of the thermal conductivity of boardstock blown with HCFC-141b (black) after 420-d exposure in the RTRA.

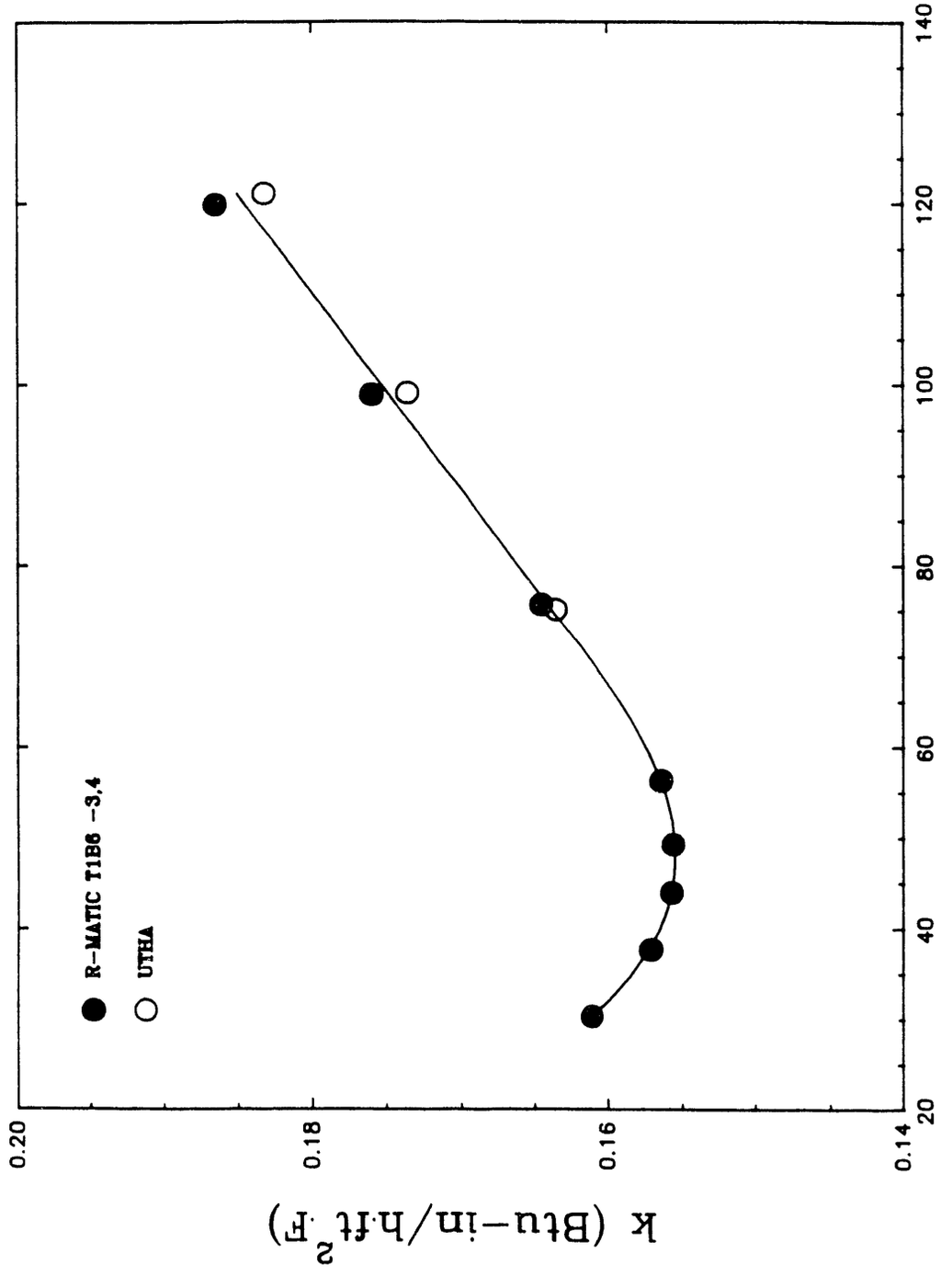

Fig. A11. The temperature dependency of the thermal conductivity of boardstock blown with a 50/50 blend after 420-d exposure in the RTRA.

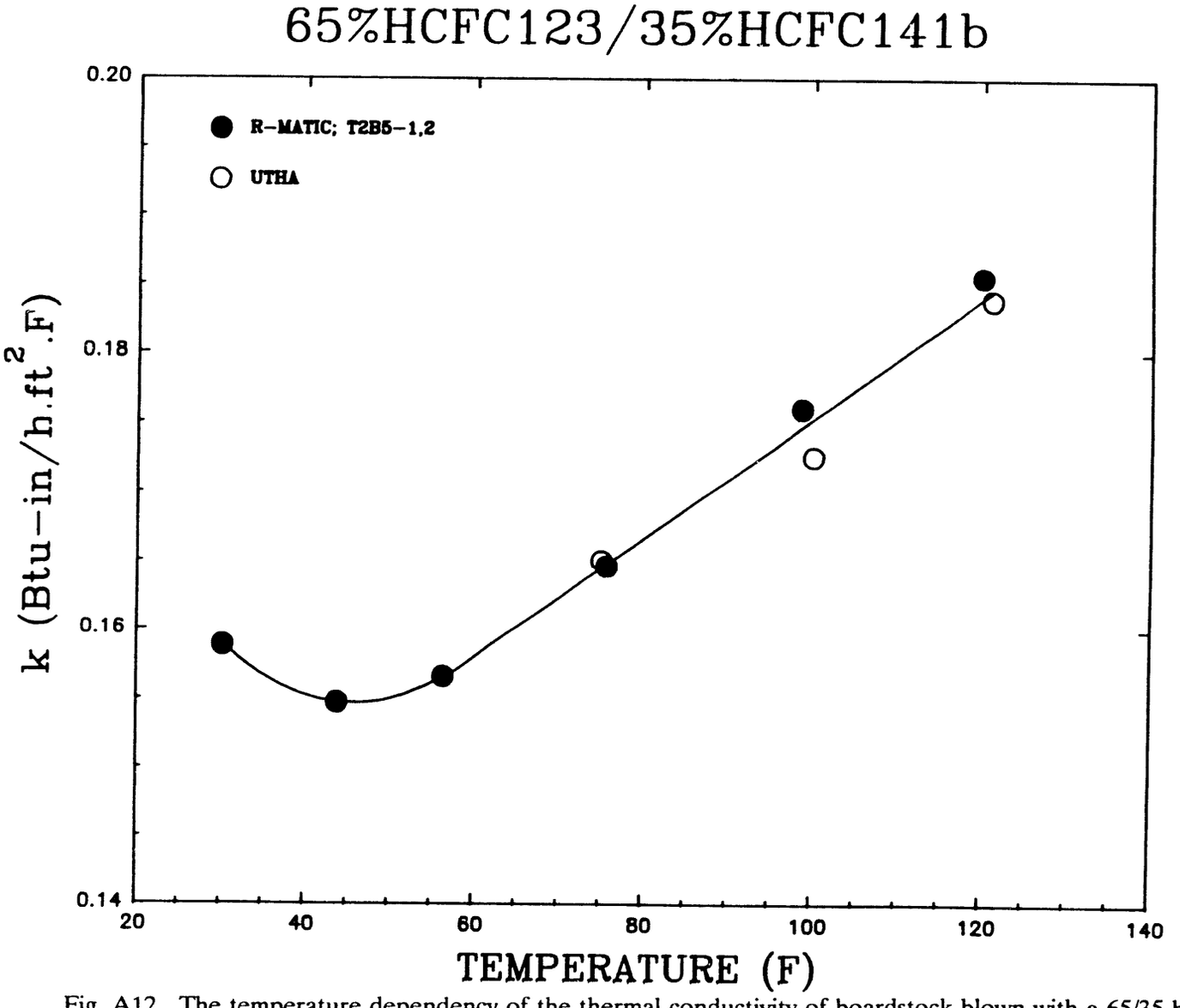

Fig. A12. The temperature dependency of the thermal conductivity of boardstock blown with a 65/35 blend after 420-d exposure in the RTRA.

APPENDIX B. VALUES OF THE QUANTITY t/h^2 FOR THE TEST RESULTS GIVEN IN TABLES 14 AND 15

Table B1. Values of t/h^2 in d/mm^2 for the k-values given in Table 14 (aging at 75° F) for the thicknesses given in Table 7

Age (d)	Board	CFC-11	HCFC-123	HCFC-141b	Age (d)	50/50	65/35
3	1	0.0027	0.0027	0.0027	2	0.0020	0.0022
	2	0.0081	0.0085	0.0082		0.0067	0.0068
	4	0.0294	0.0294	0.0300		0.0217	0.0217
17	1	0.0156	0.0152	0.0156	42.5	0.0423	0.0469
	2	0.0461	0.0481	0.0466		0.1428	0.1453
	4	0.1667	0.1667	0.1700		0.4612	0.4612
51.5	1	0.0473	0.0462	0.0473	74.5	0.0741	0.0822
	2	0.1397	0.1457	0.1412		0.2503	0.2547
	4	0.5048	0.5048	0.5150		0.8082	0.8082
106.5	1	0.0978	0.0955	0.0978	127	0.1264	0.1402
	2	0.2889	0.3013	0.2919		0.4268	0.4343
	4	1.0041	1.0441	1.0650		1.3780	1.3780
190	1	0.1745	0.1703	0.1745			
	2	0.5154	0.5367	0.5208			
	4	1.8627	1.8627	1.9000			
290	1	0.2662	0.2600	0.2662			
	2	0.7865	0.8205	0.7950			
	4	2.8429	2.8429	0.28999			

Table B2. Values of $(t/h^2)^{1/2}$ in $(d/mm^2)^{1/2}$ for the k-values given in Table 14 (aging at 75°F) for the thicknesses given in Table 7

Age (d)	Board	CFC-11	HCFC-123	HCFC-141b	Age (d)	50/50	65/35
3	1	0.0519	0.0519	0.0525	2	0.0446	0.0470
	2	0.0902	0.0921	0.0907		0.0820	0.0827
	4	0.1715	0.1715	0.1732		0.1473	0.1473
17	1	0.1249	0.1234	0.1249	42.5	0.2056	0.2166
	2	0.2147	0.2193	0.2159		0.3779	0.3812
	4	0.4082	0.4083	0.4123		0.6791	0.6791
51.5	1	0.2175	0.2149	0.2175	74.5	0.2723	0.2867
	2	0.3738	0.3817	0.3757		0.5003	0.5047
	4	0.7105	0.7105	0.7176		0.8990	0.8990
106.5	1	0.3127	0.3090	0.3127	127	0.3555	0.3744
	2	0.5375	0.5489	0.5403		0.6533	0.6590
	4	1.0218	1.0218	1.032		1.1739	1.1739
190	1	0.4177	0.4127	0.4177			
	2	0.7179	0.7332	0.7217			
	4	1.3648	1.3648	1.3784			
290	1	0.5160	0.5099	0.5160			
	2	0.8869	0.9058	0.8916			
	4	1.6861	1.6861	1.7029			

Table B3. Values of t/h^2 in d/mm^2 for the k-values given in Table 15 (aging at 75° F) for the thicknesses given in Table 7

Age (d)	Board	CFC-11	HCFC-123	HCFC-141b	Age (d)	50/50	65/35
1.5	1	0.0014	0.0014	0.0015	1.5	0.0015	0.0014
	2	0.0055	0.0056	0.0056		0.0050	0.0049
	4	0.0198	0.0208	0.0198		0.0132	0.130
13.5	1	0.0130	0.0129	0.0131	29.5	0.0293	0.0285
	2	0.0496	0.0502	0.0505		0.0989	0.0969
	4	0.1783	0.1869	0.1783		0.2577	0.2552
43	1	0.0414	0.0412	0.0417	62.5	0.0622	0.0603
	2	0.1579	0.1598	0.1608		0.2077	0.2052
	4	0.5681	0.5952	0.5681		0.5460	0.5408
114.5	1	0.1104	0.1098	0.1111	118.5	0.1179	0.1143
	2	0.4205	0.4257	0.4284		0.3936	0.3891
	4	1.5126	1.5848	1.5127		1.0351	1.0254
185	1	0.1784	0.1773	0.1795			
	2	0.6795	0.6879	0.6921			
	4	2.4442	2.5603	2.4442			

Table B4. Values of $(t/h^2)^{1/2}$ in $(d/mm^2)^{1/2}$ for the k-values given in Table 15 (aging at 150° F) for the thicknesses given in Table 7

Age (d)	Board	CFC-11	HCFC-123	HCFC-141b	Age (d)	50/50	65/35
1.5	1	0.0380	0.0379	0.0382	1.5	0.0386	0.0380
	2	0.0742	0.0747	0.0749		0.0706	0.0702
	4	0.1408	0.1441	0.1408		0.1147	0.1139
13.5	1	0.1141	0.1137	0.1145	29.5	0.1713	0.1687
	2	0.2227	0.2240	0.2247		0.3130	0.3113
	4	0.4223	0.4323	0.4223		0.5076	0.5052
43	1	0.2036	0.2030	0.2043	62.5	0.2494	0.2455
	2	0.3974	0.3998	0.4010		0.4557	0.4530
	4	0.7537	0.7715	0.7537		0.7389	0.7354
114.5	1	0.3323	0.3313	0.3333	118.5	0.3434	0.3381
	2	0.6485	0.6525	0.6545		0.6274	0.6238
	4	1.2299	1.2589	1.2299		1.0174	1.0126
185	1	0.4224	0.4211	0.4237			
	2	0.8243	0.8294	0.8319			
	4	1.5634	1.6001	1.5634			

Table B5. Data excerpted from computer runs by MIT (26)

Specimen thickness: 5.08 mm	
Days	k (Btu·in.·h·ft^2·°F)
0.78	0.1452
1.28	0.1521
2.78	0.1627
5.28	0.1709
7.78	0.1752
10.53	0.1780
14.78	0.1807
Specimen thickness: 50.8 mm	
Days	k (Btu·in.·h·ft^2·°F)
21.0	0.1303
40.0	0.1367
83.0	0.1461
123.0	0.1515
163.0	0.1555
305.0	0.1640
505.0	0.1704
705.0	0.1742
905.0	0.1767
1105	0.1784
1305	0.1798
2605	0.1848
4905	0.1905

APPENDIX C. FORTRAN CODE KMIX.FOR

Equation for KMIX.

$$k_{mix} = \sum_{i=1}^{n} \left(\frac{k_i x_i}{x_i + \sum_{j=1}^{n} \psi_{ij} x_j} \right)$$

$$\psi_{ij} = \phi_{ij} \left(1 + 2.41 (M_i - M_j) (M_i - 0.142 M_j) / (M_i + M_j)^2 \right)$$

$$\phi_{ij} = \left(1 + (k_i / k_j)^{1/2} (M_i / M_j)^{1/4} \right)^2 / 2^{3/2} (1 + M_i / M_j)^{1/2}$$

n = *number of components*

M_i = *molecular weight of component i*

x_i = *mole fraction of component i*

k_i = *thermal conductivity of component i (W/m K)*

Sample input and output for KMIX for a three-component mixture.

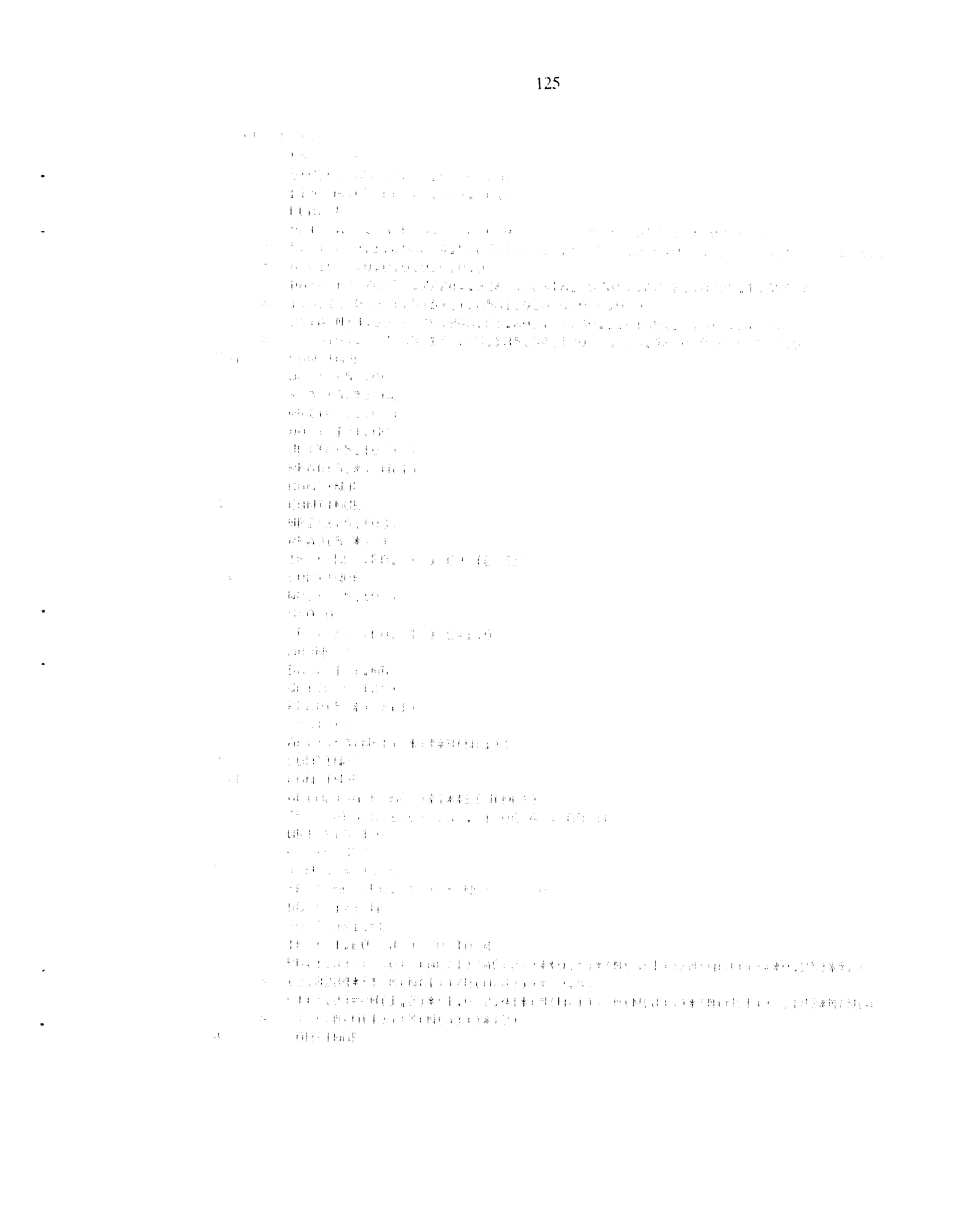

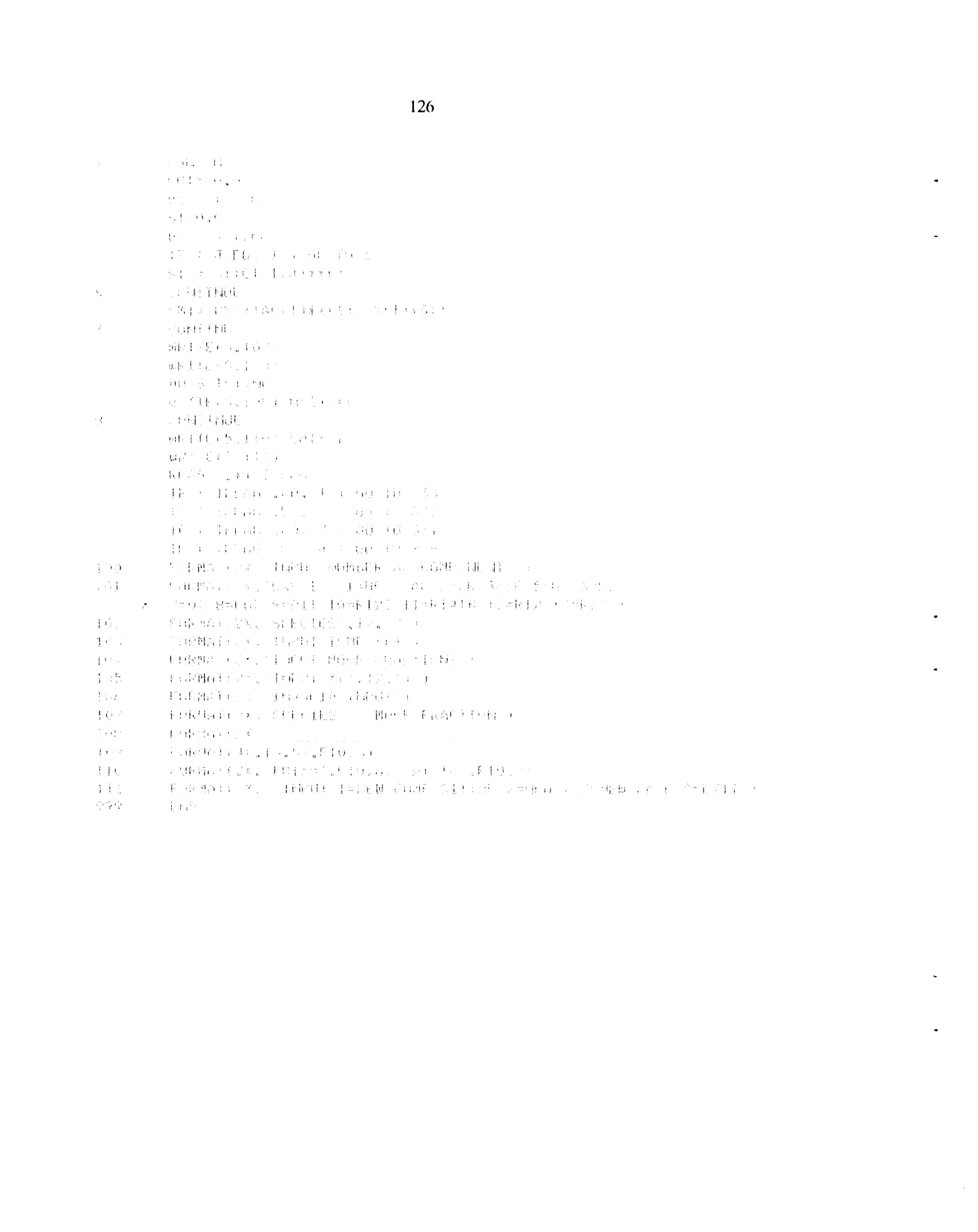

APPENDIX D. FORTRAN PROGRAM TO IMPLEMENT THE CALCULATION OF THE THERMAL CONDUCTIVITY OF GAS MIXTURES USING THE LINDSAY-BROMLEY EQUATION LB.FOR

Lindsay-Bromley

$$k_{mix} = \sum_{i=1}^{n} \frac{k_i}{\frac{1}{x_i} \sum_{j=1}^{n} A_{ij}\, x_j}$$

$$A_{ij} = \frac{1}{4}\left\{1 + \left[\frac{\mu_i}{\mu_j}\left(\frac{M_j}{M_i}\right)^{3/4} \frac{\left(1 + \frac{S_i}{T}\right)}{\left(1 + \frac{S_j}{T}\right)}\right]^{1/2}\right\}^2 \frac{(1 + S_{ij}/T)}{(1 + S_j/T)}$$

$$S_i = 1.5\ T_{Bi}$$

$$S_{ij} = \sqrt{S_i S_j}$$

μ_i = *viscosity for species i*

T_{Bi} = *normal boiling point for component i*

```
C      LB.FOR     DWY   3.90
       IMPLICIT REAL * 8(A-H,K-Z)
       DIMENSION ETA(20),S(20),MA(20,20),MOL(20),AA(20,20),R(20)
       DIMENSION  SS(20,20)
       CO2=1
       O2 =2
       N2 =3
       R22=4
       MOL(CO2) = 44.01
       MOL(O2)  = 31.999
       MOL(N2)  = 28.013
       MOL(R22) = 86.469
       S(CO2)   = 4.82E-01
       S(O2)    = 1.00E+00
       S(N2)    = 1.03E+00
       S(R22)   = 7.65E-01
       DO 20 I=1,4
       DO 20 J=1,4
       SS(I,J) = SQRT(S(I)*S(J))
20     CONTINUE
10     CONTINUE
       ETA(CO2) = 8.345
       ETA(O2)  = 8.504
       ETA(N2)  = 8.332
       ETA(R22) = 8.199
100    CONTINUE
       WRITE(5,100)
       READ(5,*) X(CO2),X(O2),X(N2)
       X(R22) = 1.0-X(CO2) - X(O2) - X(N2)
       WRITE(5,101)
       READ(5,*) TA
C      THERMAL CONDUCTIVITY IN W/MK
       K(CO2) = -6.305E-3+7.651E-5*TA
       K(O2)  =  2.557E-3+8.033E-5*TA
       K(N2)  =  4.302E-3+7.202E-5*TA
       K(R22) = -7.003E-3+6.000E-5*TA
       DO 12 I=1,4
       DO 12 J=1,4
       IF ( I.EQ. J ) AA(I,J) = 1.0
       IF ( I.EQ. J) GO TO 12
       AA(I,J) = 0.25*(1.0+SQRT((ETA(I)/ETA(J))*(MOL(J)/MOL(I)
     &  )**0.75*((TA+S(I))/(TA+S(J))))**2.*(TA+SS(I,J))/
     &  (TA+S(I))
12     CONTINUE
```

```
.TYPE LB.FOR
C          LB.FOR          DWY   8/90
           IMPLICIT REAL (A-H,K-Z)
           DIMENSION ETA(20),S(20),AA(20,20),MOL(20),YA(20),X(20),K(20
           DIMENSION  SS(20,20)
           CO2=1
           O2 =2
           N2 =3
           R22=4
           MOL(CO2)  =  44.01
           MOL(O2)   =  31.999
           MOL(N2)   =  28.018
           MOL(R22)  =  86.469
           S(CO2)    =  292.011
           S(O2)     =  125.282
           S(N2)     =  116.025
           S(R22)    =  340.600
           DO 20 I=1,4
           DO 10 J=1,4
           SS(I,J)  = SQRT(S(I)*S(J))
10         CONTINUE
20         CONTINUE
           ETA(CO2)  =  8.843
           ETA(O2)   =  8.504
           ETA(N2)   =  6.872
           ETA(R22)  =  5.199
333        CONTINUE
           WRITE(5,100)
           READ(5,*)  X(CO2),X(O2),X(N2)
           X(R22)  =  1.0-X(CO2)  -  X(O2)  -  X(N2)
           WRITE(5,101)
           READ(5,*)  TA
C          THERMAL  CONDUCTIVITY  IN  W/MK
           K(CO2)  =  -5.205E-3+7.651E-5*TA
           K(O2)   =   2.557E-3+8.035E-5*TA
           K(N2)   =   4.302E-3+7.202E-5*TA
           K(R22)  =  -7.001E-3+6.000E-5*TA
```

```
      DO 15 I=1,4
      DO 12 J=1,4
      IF ( I.EQ. J ) AA(I,J) = 1.0
      IF ( I.EQ. J) GO TO 12
      AA(I,J) = 0.25*(1.0+SQRT(( TA(I)/TA(J))*(MU(J)/MU(I))
    & )**0.75*((TA+S(I))/(TA+S(J))))**2.*(TA+SS(I,J))/
    & (TA+S(I))
      CONTINUE
      YA(I) = X(CO2)*AA(I,CO2)+X(O2)*AA(I,O2)+X(N2)*
    & AA(I,N2)+X(R22)*AA(I,R22)
      CONTINUE
      KGAS = K(CO2)*X(CO2)/YA(1)
    & +K(O2)*X(O2)/YA(2)
    & +K(N2)*X(N2)/YA(3)
    & +K(R22)*X(R22)/YA(4)
      WRITE(5,102) X(CO2),X(O2),X(N2),X(R22)
      WRITE(5,103) KGAS,TA
0     FORMAT(2X,'INPUT COMPOSITION CO2,O2,N2')
1     FORMAT(2X,'INPUT TEMPERATURE (K)')
2     FORMAT(2X,'XCO2=',F8.3,' XO2=',F8.3,'  XN2=',F8.3,'  XR22=',F8.3)
3     FORMAT(2X,'KGAS =',F12.5,'  AT T(K)=',F8.2)
      WRITE(5,104)
4     FORMAT(2X,'TYPE 1 TO INPUT NEW DATA')
      READ(5,*) FLAG1
      IF ( FLAG1 .EQ. 1 ) GO TO 333
      END
```

APPENDIX E. FORTRAN CODE MARIO.FOR WITH SAMPLE INPUT

```
.TYPE FOR40.DAT
5.08.400..10..0,0.0.0.e.300
```

```
..TYPE MARIO.FOR
00100   C         CAL OF KA OF POLYSTYRENE WITH TIME
00200             IMPLICIT REAL (A-H,K-Z)
00300             EXTERNAL F
00400             EXTERNAL FF
00500             COMMON/BLK1/P(4,500)
00600             COMMON/BLK2/MOL(4),S(4),SS(4,4),TOTP(500),DF(4)
00700             COMMON/BLK3/CO2,O2,N2,FR
00800             COMMON/BLK4/TH,TA
00900             COMMON PI
01200             CO2=1
01300             O2=2
01400             N2=3
01500             FR=4
01510             CW=0.1
01600             MOL(CO2)=44.01
01700             MOL(O2)=31.999
01800             MOL(N2)=28.018
01900             MOL(FR)=86.469
02000             EB=5.6693E-10
02100             E=0.9
02200             EC=0.8
02300             KS=0.157
02400             DS=1050.0
02500             DG=4.72
02600             DEF=32.04
02700             PI=(DS-DEF)/(DS-DG)
02800             READ(40,*)TH,MAXT,DT,P(CO2,2),P(O2,2),
02900            &  P(N2,2),P(FR,2),TA
02910             WRITE(5,*) TH,MAXT,DT,P(CO2,2),P(O2,2),P(N2,2),P(FR,2),TA
03000             CALL NEWTON(X)
03100             A=SINH(X)
03200             RS1=X/KS
03300             RS2=(COSH(1.)-COSH(X))/(A*KS)
03400             AA=(A*A+1)**0.5
03500             B=EXP(1.)-EXP(X)
03600             N=2*TH/CW-1
03700             RTE=(2/E-N)+(2*(N-1)/EC)
03800             KR=8*EB*TH*TA**3/RTE
03900             MAXT=MAXT*3600*24
04000             DT=DT*3600*24
04100             IT=1
04200             TIME=0.0
```

```
04300            WRITE(5,23)
04400    23      FORMAT(       TIME          KA',/)
04500    111     IT=IT+1
04600            CALL CONMIX(IT,TIME,KGAS)
04700            KG=KGAS
04800            KG=(1.-X-A*ALOG((B-A-AA)/(B-A+AA))/AA)/KG
04900            RT=RS1+1/(1/RS2+1/KG)
05000            KC=1/RT
05100            KFOAM=KC+KR
05199            TPR=TIME/3600/24
05200            WRITE(5,22)TPR,KFOAM
05300    22      FORMAT(5X,F8.1,15X,F7.5/)
05400            TIME=TIME+DT
05500            IF(TIME.LE.MAXT) GO TO 111
05600            STOP
05700            END
05800            SUBROUTINE NEWTON(XROOT)
05900            IMPLICIT REAL (A-H,K-Z)
05905            COMMON PI
05906            TOL=0.00001
05907            X0=0.01
05908    10      FX0=F(X0,PI)
05909            DFX0=FF(X0)
05911            X1=X0-FX0/DFX0
05912            FX1=F(X1,PI)
05913            IF(ABS(FX1).LT.TOL) GO TO 20
05914            X0=X1
05915            GO TO 10
05916    20      XROOT=X1
06300            RETURN
06400            END
06500            FUNCTION FF(X)
06600            IMPLICIT REAL (A-H,K-Z)
06700            A=ALOG(TANH(0.5))
06800            B=ALOG(TANH(0.5*X))
06900            C=SINH(X)*SINH(X)-COSH(X)*SINH(X)-SINH(X)
07000            FF=COSH(X)*(A-B)-0.5*SINH(X)/(B*COSH(X/2.)**2)+1.0
07100            RETURN
07200            END
07300            FUNCTION F(X,PI)
07400            IMPLICIT REAL (A-H,K-Z)
07500            A=TANH(1/2.)
07600            B=TANH(X/2.)
07700            F=SINH(X)*(ALOG(A)-ALOG(B))+1-PI
07800            RETURN
07900            END
```

```
08000            SUBROUTINE CONMIX(I,TIME,KGAS)
08100            IMPLICIT REAL*8(A-H,K-Z)
08200            COMMON/BLK1/P(4,500)
08300            COMMON/BLK2/MOL(4),S(4),SS(4,4),TOTP(500),DF(4)
08400            COMMON/BLK3/     CO2,O2,N2,FR
08500            COMMON/BLK4/TH,TA
08600            DIMENSION ETA(4),AA(4,4),YA(4),K(4),X(4)
08700            S(CO2)=1.5*(273.-78.4760)
08800            S(O2)=1.5*(273-182.962)
08900            S(N2)=1.5*(273.-195.8)
09000            S(FR)=1.5*(273.-40.75)
09100            DO 20 I=1,4
09200            DO 10 J=1,4
09300            SS(I,J)=SQRT(S(I)*S(J))
09400     10     CONTINUE
09500     20     CONTINUE
09600            PPP=1.0132E+5
09700            P(CO2,1)=0.000314*PPP
09800            P(O2,1)=0.2095*PPP
09900            P(N2,1)=0.78084*PPP
10000            P(FR,1)=0.000*PPP
10100            DF(1)=7.0566E-5
10200            DF(2)=2.0582E-5
10300            DF(3)=2.8423E-6
10400            DF(4)=4.055E-8
10500            IF (IT.EQ.2) GO TO 61
10600            FI=3.14159
10700            DO 70 I=1,4
10800            SUM=0.0
10900            SDS=0.0
11000            CC=FI*FI*DF(I)*TIME/TH/TH/4.
11100            SF=FI*FI*DF(I)*TIME/29.845/29.845/4.
11200            DO 65 Z=1,21,2
11300            IF(CC*Z*Z.GT.80) GO TO 65
11400            SUM=SUM+EXP(-CC*Z*Z)/Z/Z
11500            SD       S=       SD       S+EXP(- SF*Z*Z)/Z/Z
11600     65     CONTINUE
11700            SDS=SDS*8/FI/FI
11800            P(I,IT)=SDS*SDS*SUM*8*( P(I,2)- P(I,1))/FI/FI+  P(I,1)
11900     70     CONTINUE
12000     61     CONTINUE
12100            TOTP(IT)=0.0
12200            TOTP(IT)=TOTP(IT)+P(1,IT)+P(2,IT)+P(3,IT)+P(4,IT)
12300            DO 11 I=1,4
12400            X(I)=P(I,IT)/TOTP(IT)
12500     11     CONTINUE
```

```
12600            ETA(CO2)=4.643
12700            ETA(O2)=3.504
12800            ETA(N2)=3.632
12900            ETA(FR)=3.199
13000            DO 13 I=1,4
13100            DO 12 J=1,4
13200            IF(I.EQ.J) AA(I,J)=1.0
13300            IF(I.EQ.J) GO TO 12
13400            AA(I,J)=0.25*(1.+SQRT(2)*ETA(I)*ETA(J))**4*MOL(J)/MOL(I)
13500           &  **.75*(1.+SQRT(MOL(I)/MOL(J))*(ETA(J)-1)**2.+TA+SS/I,J))/
13600           &  (TA+S(I))
13700    12      CONTINUE
13800            YA(I)=X(CO2)*AA(I,CO2)+X(O2)*AA(I,O2)+X(N2)*
13900           &  AA(I,N2)+X(FR)*AA(I,FR)
14000    13      CONTINUE
14100            K(CO2)=-5.305E-3+7.651E-5*TA
14200            K(O2)=2.557E-3+8.033E-5*TA
14300            K(N2)=4.302E-3+7.202E-5*TA
14400            K(FR)=-7.003E-3+6.000E-5*TA
14500            KGAS=K(CO2)*X(CO2)/YA(1)
14600           &  +K(O2)*X(O2)/YA(2)
14700           &  +K(N2)*X(N2)/YA(3)
14800           &  +K(FR)*X(FR)/YA(4)
14900            RETURN
15000            END
```

APPENDIX F. FORTRAN CODE MITB.FOR

```
TYPE AGE.FOR


C  WRITTEN BY: A. OSTROGORSKY, M.I.T., FEB. 1985
C  MODIFIED BY: F. BREH M.  M.I.T., AUG. 1987
C  MODIFIED BY : L. GLICKSMAN M.I.T. DECEMBER 20, 1989
C  MODIFIED BY D.W.YARBROUGH  ORNL    JUNE 1990
   THIS IS THE AGE PROGRAM.
C AGE COMPUTES THE 1-D TIME CHANGE OF THE GAS
C COMPOSITION AND GAS CONDUCTIVITIY INSIE OF
C AN INFINITE CLOSED CELL FOAM SLAB. AND ADDS
C IT TO  THE CONDUCTIVITY OF SOLID AND CONDUCTANCE
C DUE TO RADIATION TO PRODUCE A PLOT OF EFFECTIVE
C FOAM CONDUCTANCE AS A FUNCTION OF TIME.
C

      COMMON/BLK1/  PP(4,5,51),PTOT(51),TT(5,51)
      COMMON/BLK2/  DF(4,51),PEO(4),E(4)
      COMMON/BLK3/  GASK(51),WMOL(4),S(4),SS(4,4)
      COMMON/BLK4/  NZ,DZ,NT,DT
      COMMON/BLK5/  CO2,O2,N2,FR

      REAL  PATM(4),THICK,MAXTTM,DTI,PDIFF,PRATIO
      REAL  KSOL,KRAD,KGAVG,KGSUM,KFOAM,KNODE,TIME
      REAL  QFLUX,RV,RVT,TPRINT
      INTEGER  I,IZ,NIN,NOU

        WRITE(5,2700)
2700    FORMAT(2X,'INITIALIZING')


C SET UP INPUT AND OUTPUT FILES
C       WRITE(5,3500)
3500    FORMAT(2X,'ENTER 1 TO SUPRESS PARTIAL PRESSURE OUTPUT')
C      READ(5,*) PFLAG
        PFLAG=1
C SYMBOLIC ARRAY INDICES
      CO2=1
      O2=2
      N2=3
      FR=4

C MOLECULAR WEIGHTS:
      WMOL(CO2)=44.0
      WMOL(O2)=32.0
      WMOL(N2)=28.0
      WMOL(FR)=137.4
```

```
04700
04800   C CONSTANTS FOR KG MIXTURE
04900         S(CO2)=1.5*(273.-78.476)
05000         S(O2)=1.5*(273.-182.962)
05100         S(N2)=1.5*(273.-195.8)
05200         S(FR)=1.5*(273.+10.)
05300         DO 20 I=1,4
05400            DO 10 J=1,4
05500               SS(I,J)=SQRT(S(I)*S(J))
05600   10       CONTINUE
05700   20    CONTINUE
05800
05900   C READ THE INPUT FILE
06000            WRITE(5,6200)
06100   6200     FORMAT(2X,'INPUT FILE NUMBER')
06200            READ(5,*) NIN
06300            NOU = NIN + 10
06400            WRITE(5,6204) NOU
06500   6204     FORMAT(2X,'OUTPUT FILE',I5)
06600         READ(NIN,*)THICK,
06700        1           MAXTIM,TPRINT,
06800        1           PEO(CO2),E(CO2),PP(CO2,1,2),
06900        1           PEO(O2),E(O2),PP(O2,1,2),
07000        1           PEO(N2),E(N2),PP(N2,1,2),
07100        1           PEO(FR),E(FR),PP(FR,1,2),
07200        1           KSOL,KRAD
07300   C                THICKNESS (CM), NUMBER OF NODES= NUMBER OF DIV'S +1
07400   C                MAXIMUM TIME DAYS, TIME INTERVAL (DAYS), PRINT TIME INTE
RVAL
07500   C                PP: PARTIAL PRESSURE (PASCALS),
07600   C                PP(COMPONENT,TIME INDEX,SPACE INDEX)
07700   C                TT: TEMP (K)  TT(TIME INDEX,SPACE INDEX)
07800   C                KSOL,KRAD: SOLID AND RADIATION K (W/M C)
07900   1111     CONTINUE
08000   C        WRITE(5,6207)
08100   6207     FORMAT(2X,' HOW MANY NODES ? MAX = 51')
08200   C        READ(5,*) NZ
08210            NZ=11
08300   C        WRITE(5,6210)
08400   6210     FORMAT(2X,' INPUT TIME STEP, DAYS')
08500   C        READ(5,*) DTI
08510            DTI=5.0
08600            WRITE(5,3709)
08700   3709     FORMAT(2X,'INPUT BOUNDARY TEMPS')
08800   C        READ(5,*) TT(1,1),TT(1,NZ)
08900            TT(1,1) = 298.0
09000            TT(1,NZ) = 298.0
09100   C CONVERT INPUT DATA TO USEABLE FORM
09200         IF(NZ.GT.51)NZ=51
09300         DZ=THICK/(NZ-1)
09400         NT=MAXTIM/DTI
09500         DTI=3600.*24.*DTI
09600         MAXTIM=3600.*24.*MAXTIM
09700         TPRINT=TPRINT*3600.*24.
```

```
09800
09900   C SET INTIAL FOAM TO STANDARD TEMP
10000         DO 51 IZ=2,NZ-1
10100            TT(1,IZ)=298
10200   51    CONTINUE
10300
10400   C CALCULATE IMPOSED TEMPERATURE PROFILE
10500         TT(2,1)=TT(1,1)
10600         DO 50 IZ=2,NZ-1
10700            TT(2,IZ)=TT(1,1)+(IZ-1)*(TT(1,NZ)-TT(1,1))/(NZ-1)
10800   50    CONTINUE
10900         TT(2,NZ)=TT(1,NZ)
11000
11100   C SET PARTIAL PRESSURES OUTSIDE THE FOAM
11200         PPP=1.0132E+5
11300         PATM(CO2)=.000314
11400         PATM(O2)=.2095
11500         PATM(N2)=.78084
11600         PATM(FR)=0.0
11700         DO 25 I=1,4
11800            PP(I,1,1)=PATM(I)*PPP
11900            PP(I,1,NZ)=PATM(I)*PPP
12000   25    CONTINUE
12100
12200   C SET INITIAL PARTIAL PRESSURES INSIDE THE FOAM
12300         DO 40 IZ=2,NZ-1
12400            DO 30 I=1,4
12500               PP(I,1,IZ)=PP(I,1,2)
12600   30       CONTINUE
12700   40    CONTINUE
12800
12900   C WRITE INITIAL HEADER TO OUTPUT FILE
13000           WRITE(NOU,11800)
13100   11800   FORMAT(2X,'THICKNESS(CM),NUMBER OF NODES,D(THICK) (CM) ')
13200         WRITE(NOU,*)THICK,NZ,DZ
13300           WRITE(NOU,12000)
13400   12000   FORMAT(2X,'MAX TIME (DAYS) , D(TIME) (DAYS)')
13500           OMAX=MAXTIM/3600.0/24.0
13600           ODTI=DTI/3600./24.
13700           WRITE(NOU,*) OMAX,ODTI
13800           WRITE(NOU,12200)
13900   12200   FORMAT(2X,'P     EO                E         INIT PART. PRESS. ')
14000         DO 41 I=1,4
14100            WRITE(NOU,*)PEO(I),E(I),PP(I,1,2)
14200   41    CONTINUE
14300   C       DO 42 IZ=1,NZ
14400   C       WRITE(NOU,*) TT(2,IZ)
14500   42    CONTINUE
```

```
14600           WRITE(NOU,12900)
14700   12900   FORMAT(2X,'SOLID CONDUCTION    K - RADIATION  (W/M K)')
14800         WRITE(NOU,14600)KSOL,KRAD
14900   14600   FORMAT(2X,E12.4,5X,E12.4,//)
15000           WRITE(NOU,14602)
15100   14602   FORMAT(2X,'DAYS      K-GAS    K-FOAM  K(BTU-IN)    T/H**2      T**
15200        &.5/H    LN (100K)',/)
15300   C SET LOOP VARIABLES TO BEGIN TIME ITERATIONS
15400         DT=DTI
15500         IT=0
15600         TIME=0
15700           WRITE(5,13600)
15800   13600   FORMAT(2X,'STARTING TIME ITERATIONS')
15900
16000   C UPDATE LOOP VARIABLES FOR THIS TIME THROUGH
16100   1000  CONTINUE
16200         IT=IT+1
16300         IF(IT .LT. 4) GOTO 1006
16400          IT = IT - 1
16500          DO 1005 NIT=IT-1,IT
16600           DO 1005 NONZ=1,NZ
16700            DO 1005 I=1,4
16800             PP(I,NIT,NONZ) = PP(I,NIT+1,NONZ)
16900   1005     CONTINUE
17000   1006     TIME=TIME+DT
17100   C        TIME IN SECONDS
17200         IF(TIME.GT.MAXTIM) GOTO 2000
17300
17400
17500   C SET THE B.C.'S
17600   C   PRESSURE:
17700           DO 55 I=1,4
17800              PP(I,IT+1,1)=PP(I,1,1)
17900              PP(I,IT+1,NZ)=PP(I,1,1)
18000   55      CONTINUE
18100   C   TEMPERATURE:
18200           TT(IT+1,1)=TT(1,1
18300           TT(IT+1,NZ)=TT(1,NZ)
18400
18500   C COMPUTE PRESSURE CHANGE DUE TO TEMPERATURE CHANGE
18600           DO 70 IZ=2,NZ-1
18700              DO 60 I=1,4
18800                 PP(I,IT,IZ)=PP(I,IT,IZ)*TT(IT+1,IZ)/TT(IT,IZ)
18900   60         CONTINUE
19000   70      CONTINUE
```

```
19100
19200   C COMPUTE THE PRESSURE CHANGE DUE TO DIFFUSION
19300         CALL PPRES(IT)
19400
19500   C COMPUTE THE CONDUCTIVITY OF THE GAS MIXTURE
19600         CALL KMIX(IT)
19700         KGSUM=0.0
19800         DO 80 IZ=2,NZ-1
19900            KGSUM=KGSUM+GASK(IZ)
20000   80    CONTINUE
20100         KGAVG=KGSUM/(NZ-2)
20200         KFOAM=KSOL+KRAD+KGAVG
20300
20400   C COMPUTE THE FOAM RESISTANCE, HEAT FLUX, AND NEW TEMP PROFILE
20500         RV=0.0
20600         DO 90 IZ=2,NZ-1
20700            RV=RV+DZ/GASK(IZ)
20800   90    CONTINUE
20900         RVT=1/(1/RV+(KSOL+KRAD)/THICK)
21000         QFLUX=(TT(IT+1,NZ)-TT(IT+1,1))/RVT
21100         DO 100 IZ=2,NZ-1
21200            KNODE=(GASK(IZ-1)+GASK(IZ))/2.+(KSOL+KRAD)/NZ
21300            TT(IT+2,IZ)=TT(IT+1,IZ-1)+QFLUX*DZ/KNODE
21400   100   CONTINUE
21500
21600   C       PTIME = PTIME + DT
21700   C       IF(PTIME .LT. TPRINT .AND. TIME .GT. DT) GOTO 111
21800   C       PTIME = 0
21900           IF ( TIME - DT .EQ. 0 )  GOTO 3333
22000           IF ( AINT(TIME/TPRINT) .EQ. AINT ((TIME-DT)/TPRINT)) GOTO 111
22100   C       IF (TIME .LE. DT) PTIME=DTI
22200            OTIM=TIME/3600./24.
22300            OK=KFOAM/1.7307*12
22400   3333     WRITE(5,1001)OTIM,OK
22500   1001     FORMAT('+','TIME (DAYS)=',F8.1,' K (BTU-IN UNITS)=',F10.4)
22600   C WRITE LOOP RESULTS TO OUTPUT FILE
22700         IF ( PFLAG .EQ. 1 .OR. ILOOP .NE. 0 ) GO TO 3334
22800         ILOOP = 1
22900            WRITE(NOU,21000)
23000    1000    FORMAT(2X,'TIME(DAYS0 GAS(W/MK)  FOAM(W/MK)
23100        '  FOAM(BTU IN)   R
23200       &  GAS  K (W/MK)
23300       1 FT2 F) TIME/THCK2')
23400   C        TIME/THCK2  (DAYS/CM2)
23500   3334     CONTINUE
```

```
         OTIM=TIME/3600/24.0
         OKFOAM=KFOAM/1.7307*12
         XTIME=(OTIM**.5)/THICK
         XLOG=ALOG(100*OKFOAM)
         OTTH=TIME/3600/24/THICK**2
         WRITE(NOU,3001)OTIM,KGAVG,KFOAM,OKFOAM,OTTH,XTIME,XLOG
 3001  FORMAT(7G10.4)
       IF (PFLAG .EQ. 1) GOTO 111
         WRITE(NOU,21800)
 21800   FORMAT(2X,'T (C) P(CO2) (PASCALS) P(O2)  P(N2)    P(R-11)
      1 K (W/M C)')
       DO 110 IZ=1,NZ
         OTT=TT(IT+1,IZ)-273
         WRITE(NOU,3002) OTT,PP(CO2,IT,IZ),PP(O2,IT,IZ),
      1                  PP(N2,IT,IZ),PP(FR,IT,IZ),GASK(IZ)
 3002  FORMAT(1X,6G10.3)
 110   CONTINUE
 111   CONTINUE

C EVALUATE LOOP VARIABLES FOR EXIT CONDITION
       IF(DT.GT.8.6E+6)GOTO 200
       PDIFF=ABS(PP(N2,IT+1,NZ/2)-PP(N2,IT,NZ/2))
       IF(PDIFF.NE.0)PRATIO=PP(N2,IT,NZ/2)/PDIFF
       IF(PDIFF.EQ.0)PRATIO=9
       IF(PRATIO .LT. 4) PRATIO=0
         PRATIO = 0
C        PRATIO = 4
       DT=(1+PRATIO)*DTI
 200   IF(DT.GT.8.64E+6)DT=8.64E+6
       IF(IT.LT.200)GO TO 2002
         OTIM=TIME/3600/24.0
         WRITE(5,2001) OTIM
 2001    FORMAT(2X,'MEMORY FULL ',F10.2,' DAYS')
          GOTO 2000
 2002    CONTINUE
       GO TO 1000
 2000  CONTINUE

C MARK END OF OUTPUT FILE

C END OF MAIN PROGRAM
         MAXTIM=MAXTIM/3600/24
         TPRINT=TPRINT/3600/24
         WRITE(5,26804)
 26804   FORMAT(2X,'INPUT 1 FOR MORE CALC')
         READ(5,*) NFLAG
         IF ( NFLAG .EQ. 1 ) GO TO 1111
       STOP
       END


CCCCCCCCCCCCCCCCCCCCCCCCCCCCCCCCCCCCCCCCCCCCCCCCCCCCCCCCCCCCCCCCCCCCCCC
CCCCCCC
```

```
C
C
C      SUBROUTINE T SE(I)
C
C  THIS SUBROUTINE COMPUTES THE CHANGE OF GAS PARTIAL PRESSURE
C  WITH TIME
C
      REAL   PP(51),U(51),A(51),B(51),C(51),L(51)
      REAL   D(51),DF(51),Q(51)
C
      COMMON/BLK1/  PP(4,3,51),TOT(51),T(5,51)
      COMMON/BLK2/  DF(4,51),PEO(4),E(4)
      COMMON/BLK4/  NZ,DZ,NT,DT
      COMMON/BLK5/  CO2,O2,N2,PP
C
C SET CONSTANT MATRIX COEFFICIENTS
      DO 15 IZ=1,NZ
         B(IZ)=1
         C(IZ)=1
15    CONTINUE
C
C COMPUTE DIFFUSION COEFFICIENTS AS FUNCTION OF TEMPERATURE
      DO 20 IZ=2,NZ-1
         DO 10 I=1,4
            DF(I,IZ)=PEO(I)*EXP(-E(I)/(T(IT+1,IZ))*TT(IT+1,IZ)/298.
10       CONTINUE
20    CONTINUE
C
C COMPUTE THE PRESSURE CHANGES
      DO 50 I=1,4
         AP(2)=DZ*DZ/(DT*DF(I,2)*.5)
         A(2)=-(2.+AP(2))
         AP(NZ-1)=DZ*DZ/(DT*DF(I,NZ-1)*.5)
         A(NZ-1)=-(2.+AP(NZ-1))
         Q(2)=-2.*PP(I,IT,1)+PP(I,IT,2)*(2.-AP(2))-PP(I,IT,3)
         Q(NZ-1)=-PP(I,IT,NZ-2)+PP(I,IT,NZ-1)*(2.-AP(NZ-1))
     1             -2.*PP(I,IT,NZ)
         DO 30 IZ=3,NZ-2
            AP(IZ)=DZ*DZ/(DT*DF(I,IZ)*.5)
            A(IZ)=-(2.+AP(IZ))
            Q(IZ)=-PP(I,IT,IZ-1)+PP(I,IT,IZ)*(2.-AP(IZ))
     1              -PP(I,IT,IZ+1)
30       CONTINUE
         CALL LUDE(A,B,C,L,D,U,NZ)
         CALL  FBACK(L,D,U,Q,X,NZ)
         DO 40 IZ=2,NZ-1
            PP(I,IT+1,IZ)=X(IZ)
40       CONTINUE
50    CONTINUE
```

```
C COMPUTE THE TOTAL PRESSURE
      DO 70 IZ=1,NZ
         PTOT(IZ)=0.0
         DO 60 I=1,4
            PTOT(IZ)=PTOT(IZ)+PP(I,IT+1,IZ)
60       CONTINUE
70    CONTINUE

      RETURN
      END


CCCCCCCCCCCCCCCCCCCCCCCCCCCCCCCCCCCCCCCCCCCCCCCCCCCCCCCCCCCCCCCCCCCCCCCCCC
CCCCCC
C
      SUBROUTINE KMIX(IT)
C
C THE SUBROUTINE COMPUTES THE CONDUCTIVITY OF THE GAS MIXTURE
C INSIDE THE CLOSED FOAM CELLS AS A FUNCTION OF GAS COMPOSITION
C AT EACH NODE.
C
      REAL ETA(4),TA(4),X(4,51),K(4),AA(4,4)
      INTEGER  IT,IZ,I,J

      COMMON/BLK1/  PP(4,5,51),PTOT(51),TT(5,51)
      COMMON/BLK3/  GASK(51),WMOL(4),S(4),SS(4,4)
      COMMON/BLK4/  NZ,DZ,NT,DT
      COMMON/BLK5/  CO2,O2,N2,FF

C COMPUTE MOL FRACTIONS:
      DO 15 IZ=1,NZ
         DO 10 I=1,4
            X(I,IZ)=PP(I,IT+1,IZ)/PTOT(IZ)
10       CONTINUE
15    CONTINUE

C MIXTURE CONDUCTIVITY GASK(IZ):
      DO 40 IZ=1,NZ
         ETA(CO2)=(14.958+(TT(IT,IZ)-300.)/50.*2.247)*1.E-6
         ETA(O2)=(20.63+(TT(IT,IZ)-300.)/50.*2.53)*1.E-6
         ETA(N2)=(17.84+(TT(IT,IZ)-300.)/100.*4.14)*1.E-6
         ETA(FR)=20.000E-6
         DO 20 I=1,4
            DO 20 J=1,4
               IF(I.EQ.J)AA(I,J)=0.0
               IF(I.EQ.J)GOTO 20
               AA(I,J)=.25*(1.+SQRT(ETA(I)/ETA(J))*
     1                     (WMOL(J)/WMOL(I))**.25*
     1                     (TT(IT,IZ)+S(I))/(TT(IT,IZ)+S(J)))**2.*
     1                     (TT(IT,IZ)+SS(I,J))/(TT(IT,IZ)+S(I))
20          CONTINUE
```

```
          YA(I)=X(CO2,IZ)*AA(I,CO2)+X(O2,IZ)*AA(I,O2)
     1               +X(N2,IZ)*AA(I,N2)+X(FR,IZ)*AA(I,FR)
 30   CONTINUE
      K(CO2)=.016572+(TT(IT,IZ)-300.)/50.*.003898
      K(O2)=.02676+(TT(IT,IZ)-300.)/50.*.00394
      K(N2)=.02620+(TT(IT,IZ)-300.)/100.*.00715
      K(FR)=8.3022E-3+(9.426E-3-8.3022E-3)/27.8*(TT(IT,IZ)-310.93)
      GASK(IZ)=K(CO2)*X(CO2,IZ)/(X(CO2,IZ)+YA(1))
     1         +K(O2)*X(O2,IZ)/(X(O2,IZ)+YA(2))
     1         +K(N2)*X(N2,IZ)/(X(N2,IZ)+YA(3))
     1         +K(FR)*X(FR,IZ)/(X(FR,IZ)+YA(4))
 40   CONTINUE

C      WRITE(5,*)GASK(1)

      RETURN
      END


CCCCCCCCCCCCCCCCCCCCCCCCCCCCCCCCCCCCCCCCCCCCCCCCCCCCCCCCCCCCCCCCCCCCCCCCCCCCCCCC
C
      SUBROUTINE LUDE(A,B,C,L,D,U,N)
C
C THIS ROUTINE DECOMPOSES A TRIDIAGONAL MATRIX [ABC] INTO LOWER AND UPPER
C DIAGONAL MATRICES [L] AND [DU].
C
      REAL A(N),B(N),C(N),L(N),D(N),U(N)
      INTEGER  I

      D(2)=A(2)
      U(2)=C(2)
      DO 10 I=3,N-1
         L(I)=B(I)/D(I-1)
         D(I)=A(I)-L(I)*U(I-1)
         U(I)=C(I)
 10   CONTINUE

      RETURN
      END
```

```
CCCCCCCCCCCCCCCCCCCCCCCCCCCCCCCCCCCCCCCCCCCCCCCCCCCCCCCCCCCCCCCCCCCCCCCCC
CCCCCCC
C
      SUBROUTINE FBACK(L,D,U,Q,X,N)
C
C THIS ROUTINE PERFORMS FORWRD/BACKWARD SOLVE OF MATRIX SYSTEM
C [L][U][X]=[Q].
C
      REAL L(N),D(N),U(N),Q(N),X(N)
      INTEGER  I

      X(2)=Q(2)
      DO 10 I=3,N-1
         X(I)=Q(I)-L(I)*X(I-1)
10    CONTINUE
      X(N-1)=X(N-1)/D(N-1)
      DO 20 I=N-2,2,-1
         X(I)=(X(I)-U(I)*X(I+1))/D(I)
20    CONTINUE

      RETURN
      END
```

INTERNAL DISTRIBUTION

1-2. Central Research Library
3. Document Reference Section
4-5. Laboratory Records Department
6. Laboratory Records, ORNL RC
7. ORNL Patent Section
8-10. M&C Records Office
11-20. C. L. Brown
21-30. G. L. Burn
31. R. S. Carlsmith
32. J. E. Christian
33. J. W. Cooke
34. D. F. Craig
35-39. R. S. Graves
40. T. G. Kollie
41. M. A. Kuliasha
42-46. D. L. McElroy
47. K. E. Wilkes
48-52. D. W. Yarbrough
53. A. D. Brailsford (Consultant)
54. Y. A. Chang (Consultant)
55. H. W. Foglesong (Consultant)
56. J. J. Hren (Consultant)
57. M. L. Savitz (Consultant)
58. J. B. Wachtman, Jr. (Consultant)

EXTERNAL DISTRIBUTION

59. Abrey, D. R., New York State Energy Office, Albany, NY 12223
60. Alumbaugh, R. L., Naval Civil Engineering Lab, Port Hueneme, CA 73043
61. Anderson, J., Foam Enterprises, Minneapolis, MN 55441
62. Aresteh, D., Lawrence Berkeley Laboratory, Berkeley, CA 94720
63. Bales, E., New Jersey Institute of Technology, Newark, NJ 07102
64. Bankvall, C., SP, P.O. Box 857, S-501 15 Boras, Sweden
65. Bassi, M., Mobay Corp., Pittsburgh, PA 15205
66. Baumgardner, R. L., Stroudsburg, PA 18360
67. Beck, J. V., Michigan State University, East Lansing, MI 48824
68. Boissy, K., Factory Mutual Research Corp., Norwood, MA 02062
69. Bomberg, M., National Research Council of Canada, Ontario K1A OR6, Canada
70. Braun, S., MIMA, Alexandria, VA 22314
71. Brod, B., Barrier Systems, Canastota, NY 13032-0346
72. Clinton, J. L., NRG Barriers, Inc., Saco, ME 04072-1859
73. Desjarlais, A. O., Holometrix, Inc., Cambridge, MA 02139
74. Durkin, G., National Center for Appropriate Technology, Butte, MT 59702
75. Ellis, W. P., Harleysville, PA 19438
76. Emmert, D. E., Thermal Products International, Pittsburgh, PA 15238
77. Fine, H. A., EPA, Washington, DC 20460
78. Floyd, S., Weyerhauser, WA 98477
79. Flynn, D. R., NIST, Gaithersburg, MD 20899
80. Freeman, T., Dow Chemical, Granville, OH 43023
81. French, W. R., French Engineering, Inc., Spring, TX 77388
82. Funk, S. A., The Celotex Corp., Tampa, FL 33607

83. Gillenwater, R. J., Carlisle Syntec, Carlisle, PA 17013
84. Glicksman, L. R., MIT, Cambridge, MA 02139
85. Goss, W. P., Amherst, MA 01003
86. Hagan, J. R., Jim Walter Research Corp., St. Petersburg, FL 33716
87. Harris, T., BASF Canada, Inc., Toronto, Ontario M9W 6N9, Canada
88. Haynes, R., Charleston, SC 29411
89. Hendricks, R. V., EPA, Research Triangle Park, NC 27711
90. Howard, B. D., The Alliance to Save Energy, Washington, DC 20006-1401
91. Howerton, K., Federal Trade Commission, Washington, DC 20580
92. Huempfner, R., Marne Industries, Inc., Grand Rapids, MI 49588-8465
93. Hyma, B., Energy Saver Imports, Inc., Broomfield, CO 80038
94. Kifer, E. W., Thermal Products International, Pittsburgh, PA 15238
95. Lacher, M. B., CertainTeed Corp., Valley Forge, PA 19482
96. LaCosse, R. A., Mt. Prospect, IL 60056
97. Leger, G., Leger Designs, New Boston, NH 03020
98. Lichtenberg, F. W., The Society of the Plastics Industry, New York, NY 10017
99. Martin, R., Roof Maintenance Systems, Farmingdale, NJ 07727
100. Martin, W. F., Roof Design Works, Inc., Knoxville, TN 37919
101. McBride, M., Owens-Corning Fiberglas, Granville, OH 43023-1200
102. McCaa, D. J., CertainTeed Corp., Blue Bell, PA 19422
103. McGuire, D., Regal Industries, Crothersville, IN 47229
104. Miller, R. G., Jim Walters Reserach Corp., St. Petersburg, FL 33716
105. Minsker, J. H., Dow Chemical USA, Granville, OH 43023
106. Mumaw, J. R., Owens-Corning Fiberglas, Granville, OH 43023-1200
107. Ober, D. G., Manville Sales Corp., Denver, CO 80217
108. Poppendiek, H. F., Geoscience, Ltd., Solana Beach, CA 92075
109. Portfolio, D. C., Tremco, Inc., Cleveland, OH 44104
110. Powell, F. J., Jacksonville, FL 32223
111. Richards, D. E., DER, Inc., Sylvania, OH 43560-3715
112. Riley, E. G., Northampton, MA 01060
113. Roberts, H. J., RMAX, Inc., Dallas, TX 75244-5291
114. Roberts, V., Plymouth Foam Products, Plymouth, WI 53073
115. Roodvoets, D. L., Dow Chemical, USA, Granville, OH 43023
116. Roofing Services, Inc., Springfield, VA 22152-1621
117. Roux, J. A., University of Mississippi, University, MS 38677
118. Sherman, M., St. Petersburg, FL 33710-5405
119. Shern, R. M., Owens-Corning Fiberglas Corp, Toledo, OH 43659
120. Shirtliffe, C. J., NRC, Ottawa K1A OR6, Canada
121. Sievert, G. H., SPI/PFCD, Washington, DC 20005
122. Sikand, R. S., NAHB National Research Center, Upper Marlboro, MD 20772
123. Slavik, S., Rockford, MN 55373
124. Smith, D. R., NIST, Boulder, CO 80303-3328
125. Smith, J. A., National Association of Home Builders, Washington, DC 20005
126. Sterling, R. L., Underground Space Center, Minneapolis, MN 55455
127. Stern, E., Montreal, Quebec H4V 2A4, Canada
128. Stumpf, P., Major Industries, Morristown, NJ 07960
129. Tewes, S., Small Homes Council, Champaign, IL 62820
130. Tong, T. W., Arizona State University, Tempe, AZ 85287

131. Tseng, P., Montgomery County Government, Rockville, MD 20850
132. Tsongas, G., Portland State University, Portland, OR 97207
133. Tuluca, A., Steven Winter Associates, Inc., Norwalk, CT 06854
134. Tye, R. P., Cohasset, MA 02025
135. Vander Linden, C. R., Vander Linden and Associates, Littleton, CO 80123
136. Van Geem, M. G., CTL, Skokie, IL 60077
137. Wells, J. R., Owens-Corning Fiberglas, Granville, OH 43023
138. Wojtechko, B., U. C. Industries, Tallmadge, OH 44278
139. Wolfgram, K., Dow Chemical USA, Granville, OH 43023
140. Wysocki, D. C., Mobay Corp., Pittsburgh, PA 15205-9741
141. Zarr, R. R., NIST, Gaithersburg, MD 20899
142. DOE Field Office, P.O. Box 2008, Oak Ridge, TN 37831-8600
143-152. Department of Energy, Office of Scientific and Technical Information, P.O. Box 62, Oak Ridge, TN 37831
For distribution by microfiche as shown in DOE/OSTI-4500, Distribution Category UC-350 (Energy Conservation in Buildings and Community Systems)

END

DATE FILMED

12/23/91